The Dynamic Behavior of Rain Attenuation on Satellite Communication Links

by

David Wendell Lee

thesis submitted to the Faculty of the

Virginia Polytechnic Institute and State University

in partial fulfillment of the requirements for the degree of

MASTER OF SCIENCE

in

Electrical Engineering

APPROVED:

Charles W. Bostian

Timothy Pratt

Ioannis M. Besieris

June, 1983
Blacksburg, Virginia

'THE DYNAMIC BEHAVIOR OF RAIN ATTENUATION ON SATELLITE COMMUNICATION LINKS'

by

David W. Lee

(ABSTRACT)

The proposed use of communication satellites operating above 10 GHz has stimulated research into the effects of atmospheric rain and ice on the reception of these signals. This thesis examines the statistics of faderate, fade duration, and interfade intervals on 19 and 28 GHz communication links, at an elevation angle of 45 degrees. The study uses 2 years of data collected from the COMSTAR-D2 experimental propagation beacons at Blacksburg, Virginia. The results are shown to depend on frequency, elevation angle, time of year, rainrate, rainfall amount, and the signal polarization. The results are also shown to depend on the receiver time constants, the data acquisition system sampling rate, and the signal-to-noise ratio. The number of fade events and interfade intervals was found to vary slightly when hysteresis was added to the data reduction program.

ACKNOWLEDGEMENTS

The author wishes to express his deep gratitude to all members of the Virginia Tech Satellite Communications Group. This remarkable group of dedicated people has spent untold hours develping hardware and software, collecting and reducing data, and overseeing the day-to-day operations of the satellite tracking station. The author has, in many ways, stood on the shoulders of these people, and has benefitted from their freindship and support over the past two years. Without them, this thesis truly could not have been done. The author wishes to specifically thank the following people: Mr. Robert Porter, for his help with the computer programming, and for writing the fade duration program; Dr. Louis Beex, Dr. David DeWolf, Dr. Ioannis Besieris, and Dr. Douglas Lindner, for their advice on signal processing; Dr. P.H. Wiley for his help with receiver time constant study; Mr. Pete Santago, for his help with the data processing; Ms. Alexia Teleki, and other members of the Blacksburg community too numerous to mention, for all their friendship and support over the past few years, which has made the author's academic experience so pleasureable and rewarding.

Most of all, the author wishes to thank his advisor, Dr. Charles Bostian, for all of his patience, encouragement, ad-

vice, and guidance, and for enabling the author to continue his education at the master's level. The financial support of NASA, the Jet Propulsion Laboratory, and the Intelsat Organization, who funded the contracts under which this research was performed, is also gratefully acknowledged.

TABLE OF CONTENTS

Appendix

Chapter I

INTRODUCTION

The use of geosynchronous communication satellites operating in the 4 and 6 Gigahertz (GHz) bands has grown enormously in recent years, and saturation of this band has led to the development of systems operating at higher frequencies. The use of higher frequencies has the advantages of greater bandwidth availability and narrower antenna beamwidths for closer orbital spacing, but radiowave propagation at these frequencies can be severely impaired by rain and ice crystals in the lower atmosphere. These impairments consist primarily of signal attenuation caused by the absorptive properties of rain, and depolarization caused by the scattering of electromagnetic fields by rain and ice. On dual polarized links, this causes cross-talk interference between the orthogonal channels.

Below 10 GHz, these two processes have negligible impact, and system power margins of only a few decibels are adequate to overcome most random propagation losses (Weather-related signal losses are considered to be random losses since they can only be accounted for in terms of their statistical properties.). However, above 10 GHz, attenuation losses routinely exceed 10 decibels (dB); power margins of this

size are expensive and, in many cases, impractical to implement. For these reasons, recent research efforts have concentrated on accurate methods of modelling and predicting attenuation and depolarization phenomena, and on developing measures for counteracting these effects at the system level.

Such countermeasures include variable earth terminal transmitting power, adaptive control of satellite transmitting power, and adaptive cancellation of cross-polariztion interference on dual polarized links. Obviously, long-term statistics on the percentage of time that rainfall and attenuation levels are exceeded are important criteria in the design and implementation of these systems. However, the "real time" nature of these techniques requires that information be known about the dynamic behavior of attenuation and depolarization, that is, the rate of change and the duration of these phenomena. The design of satellite power supplies and transponders, earth terminal network control and data acquisition systems, and channel bandwidth, power allocation, and coding schemes will require that such information be available. In systems which employ adaptive control of transmitting power to overcome rain attenuation, it must also be possible to measure these dynamic processes accurately in real time so that timely corrective measures can be taken.

This thesis presents the statistics of fade duration and the rate of change of attenuation (faderate) at 19 and 28 GHz using propagation data recorded between June, 1977, and December, 1979. The data were collected by the Satellite Communications Group of the Virginia Polytechnic Institute and State University (VPI&SU) using the signal levels of the 19 GHz (nominally vertically polarized) and 28 GHz experimental propagation beacons from the COMSTAR-D2 satellite. The elevation angle was 45 degrees. The earth terminal was located at Blacksburg, Virginia, approximately 2000 feet above sea level. The area usually experiences mild summers with moderate thunderstorm activity, and moderately cold winters with several feet of snowfall. Annual precipitation averages about 40 inches per year, and is distributed almost uniformly throughout the year. All earth terminal equipment was developed and operated by members of the Satellite Communications Group. After being screened for missing and invalid values, the data were recorded on magnetic tape for permanent storage.

This thesis will also discuss the problems involved in obtaining accurate measurements of faderates and fade durations using sampled data, and will present methods for overcoming these difficulties. Among the problems addressed are:

1. The effect of post-detection filters with long time constants on the measurement of fading signals.
2. The effect of the data acquisition system sampling rate on faderate statistics.
3. The effects of receiver and data acquisition system noise on faderate measurement.
4. The calculation of bounds on the required sampling rate and the measurement error of faderates.

Where possible, the thesis will attempt to relate the results obtained to actual system parameters and requirements, and to the physical processes which cause attenuation and depolarization.

Chapter II

REVIEW OF THE LITERATURE

While the measurement, prediction, and modelling of attenuation has reached a highly developed state in recent years, the study of faderates and fade durations (on a per-event basis) has yet to receive significant attention in the technical literature. The amount of reference material available on faderates is rather limited, and consists primarily of the three papers which will now be reviewed.

E. Matricciani (1981) analyzed approximately 68 hours of attenuation event data using the 11 GHz SIRIO experimental beacon at an earth terminal in Lario, Italy. The signal was sampled at intervals of 0.1 sec, and ten consecutive samples were then averaged together for an effective sampling rate of 1 sec. Samples were retained when the signal level had changed by some predesignated amount (Increments of 1.5, 2.0, 2.5, and 3.0 dB were used.). Matricciani found that the distribution of mean faderates with respect to the attenuation threshold at which they occurred was approximately lognormal. He also found that the statistics were somewhat sensitive to the sampling rate and to the sampling increment (see figures 2.1 and 2.2).

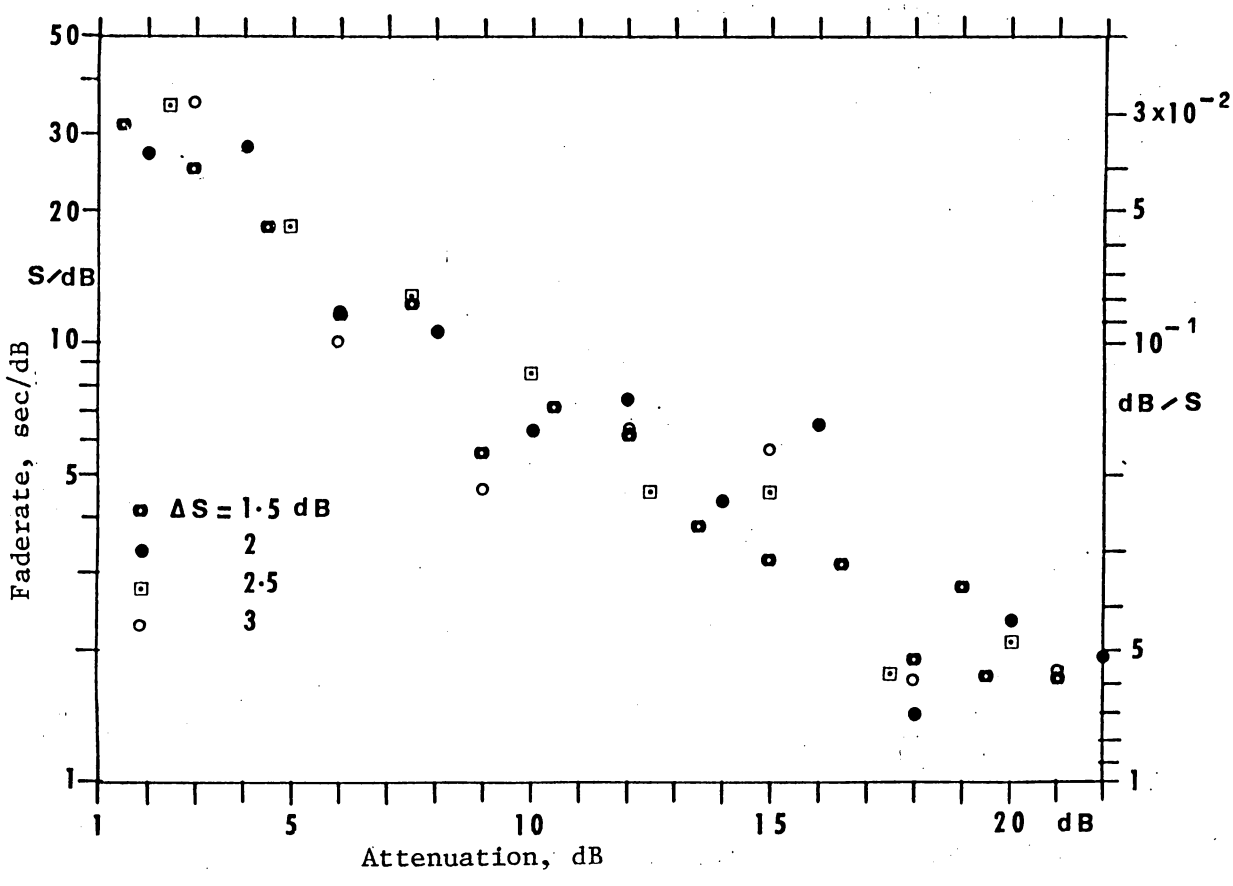

Figure 2.1. Faderate vs. attenuation; 11.6 GHz SIRIO, Lario, Italy (From Matricciani [1]).

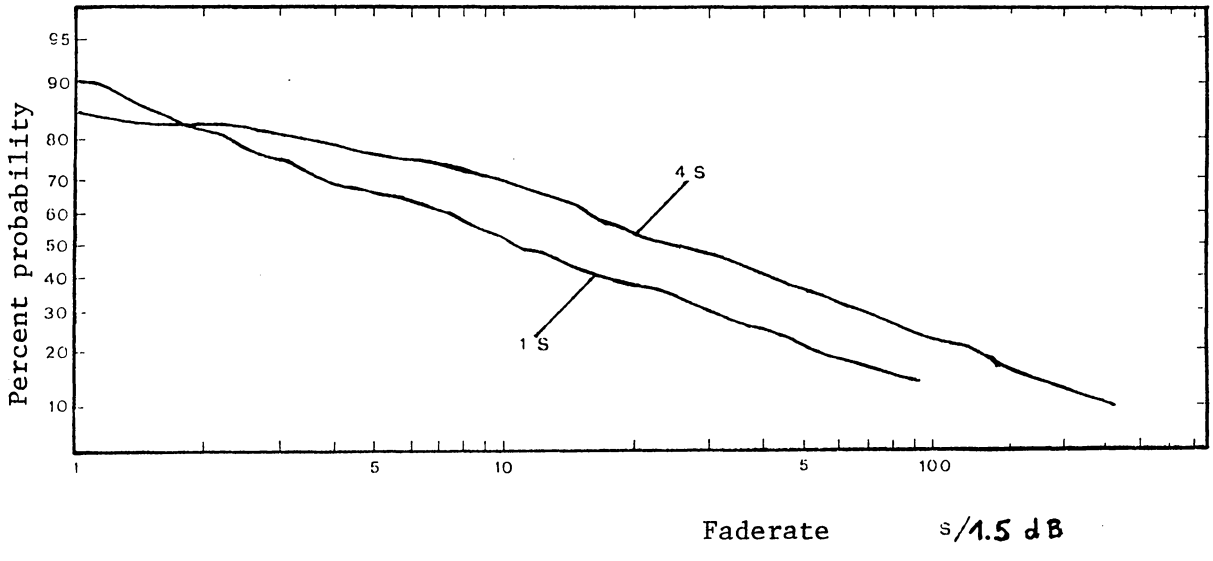

Figure 2.2. Percent probability vs. faderate; 11.6 GHz SIRIO, Lario, Italy (From Matricciani [2]).

There are three possible criticisms of Matricciani's results. First, the data are plotted on a log-log scale; this is equivalent to taking the logarithm of a quantity which has already been expressed in decibels. This causes the data at the higher faderates and attenuations to be severely compressed. A curve which appears to be nearly a straight line when plotted on such a scale may in fact be quite nonlinear when plotted on a non-logarithmic set of axes. Thus the relationship between faderate and attenuation may actually be nearly random at the higher attenuation values.

Secondly, Matricciani's sampling increments may be too large to adequately resolve the signal. Even at the finest sampling increment, changes in signal level of as much as 3 dB could be overlooked, which would produce an exaggerrated smoothing effect on the data. Changes in signal power of 3 dB are quite serious on most communication links.

The third possible criticism of Matricciani's work is his use of high sampling rates. In the analysis of the VPI&SU data it was found that for sampling rates faster than 5 sec, the noise which occurs with the signal significantly distorts the faderate statistics, particularly at the higher attenuation thresholds, where the signal- to-noise ratio (SNR) is poor. The sampling time must be long enough so

that the high-frequency noise present in the signal is "overlooked", but short enough so that the Nyquist sampling theorem is satisfied. (It should be noted that it is the attenuation "envelope" of the beacon signal which is being sampled, not the radio- frequency component.). If the noise spectrum is uncolored, then the mean value of the noise is zero, and the decimation algorithm used by Matricciani would be an acceptable technique for filtering out the noise and obtaining unbiased statistics.

Lin, et al. (1981), analyzed one month of data using the 19 GHz COMSTAR-D2 experimental beacon and an earth terminal in Palmetto, Georgia. This study also reported a lognormal relationship between mean faderate and attenuation, but this conclusion should be regarded as tentative due to the limited size of the data set (see figure 2.3). Another possible criticism of this report is the manner in which mean faderates were calculated. The attenuation spread was divided into six bins, each bin being 5 dB wide; all faderate samples in a given bin were then averaged together to yield a mean faderate, and the corresponding attenuation value was taken as the midpoint of the given bin. This procedure would have a pronounced smoothing effect on the data (see figure 2.4).

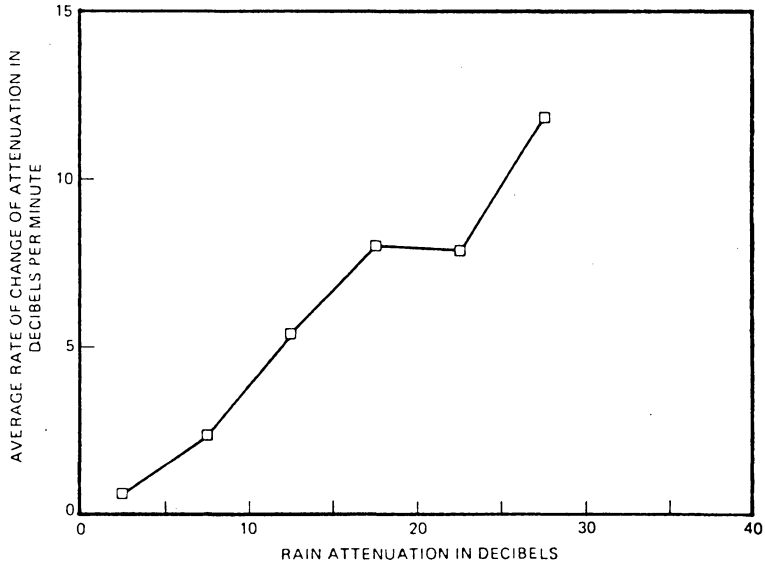

Figure 2.3. Faderate vs. attenuation; 19 GHz COMSTAR, Palmetto, GA (From Lin, et. al. [3]).

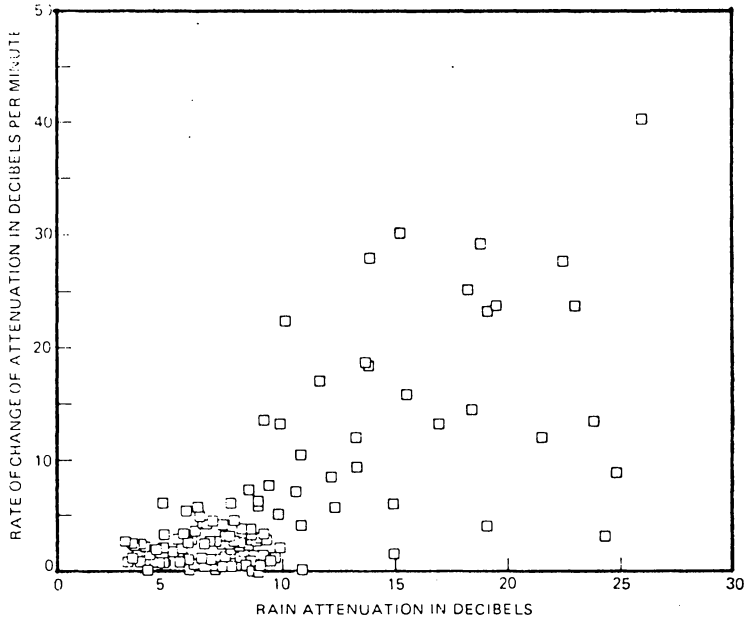

Figure 2.4. Faderate vs. attenuation scatter plot of figure 2.3. (From Lin, et. al. [3]).

F. Dintelman (1981) analyzed 148 attenuation events on 11 GHz earth-to-space links at several locations in Europe. The faderate amplitude probability distribution was found to be nearly Gaussian, and the event duration probability distribution was found to be lognormal (see figures 2.5 and 2.6). This study examined only the 5 dB fade threshold, so the results may not be representative of other fade thresholds. That data from a number of different earth terminals were combined into one set may also have had a biasing effect on the statistics.

H. W. Arnold, et al. (1982), analyzed two years of data at 19 GHz using the COMSTAR-D2 experimental beacon at an earth terminal in northern New Jersey, with a path elevation angle of 43 degrees. This study found that the yearly average number of fades observed tended to decrease with increasing fade depth and increasing fade duration (See figure 2.7.). The statistics of time intervals between fades showed similar behavior (See figure 2.8.). The study also found that the number and depth of fades observed had a strong seasonal dependence; during July and August, fades occurred with nearly twice the frequency of the yearly rate, and the durations tended to be longer, as shown in figure 2.9.

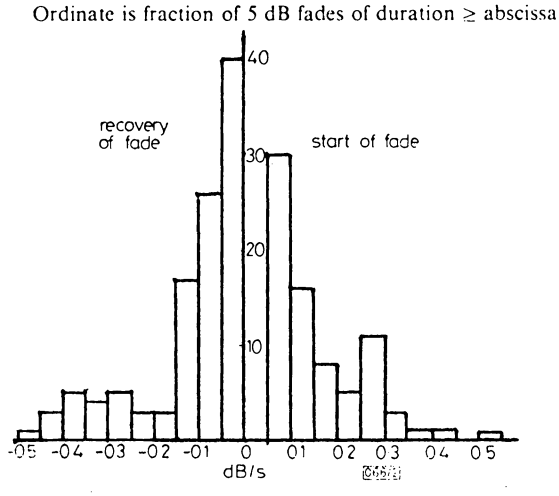

Figure 2.5. Percent probability vs. faderate; 11.6 GHz OTS, several European locations (From Dintelman [4]).

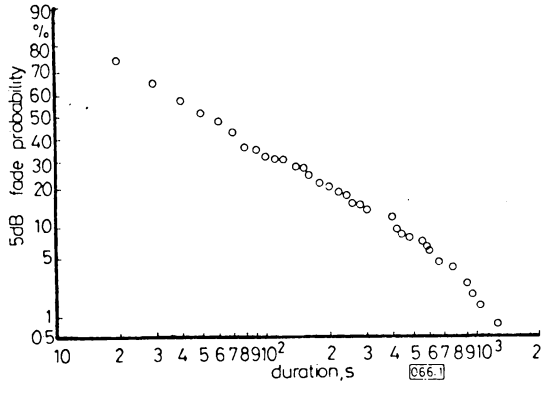

Figure 2.6. Percent probability vs. fade duration; 11.6 GHz OTS, several European locations (From Dintelman [4]).

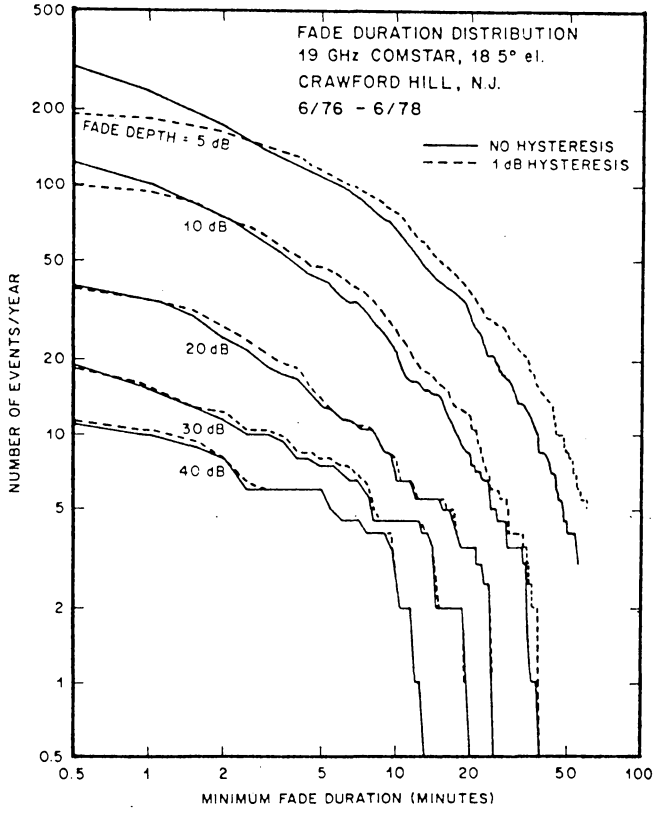

Figure 2.7. Number of fades per year with given duration; 19 GHz Crawford Hill, NJ (From Arnold, et. al. [5]).

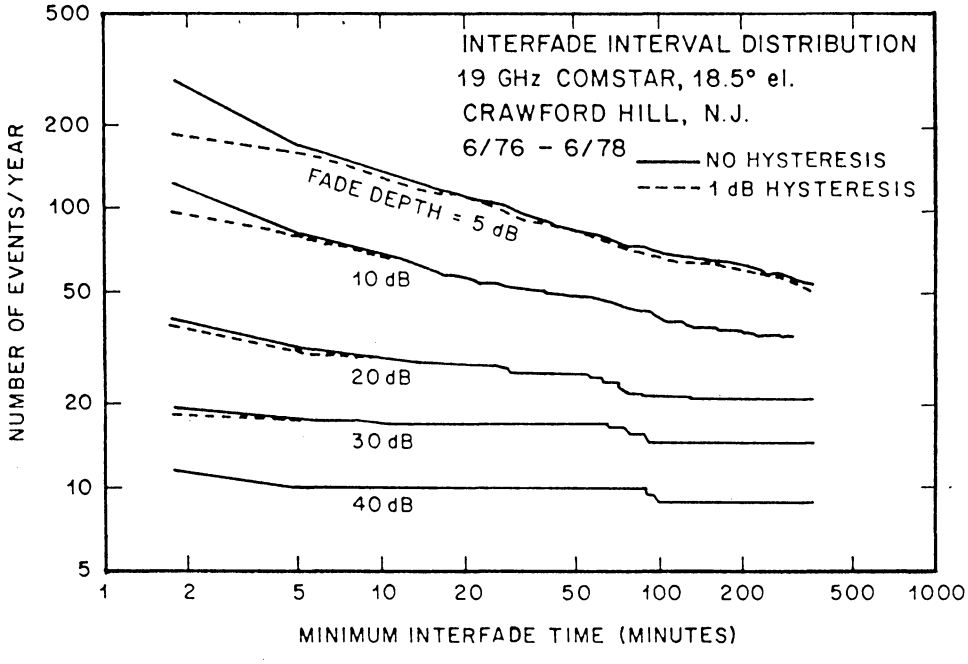

Figure 2.8. Number of interfade intervals per year with given duration; 19 GHz, Crawford Hill, NJ (From Arnold, et. al. [5]).

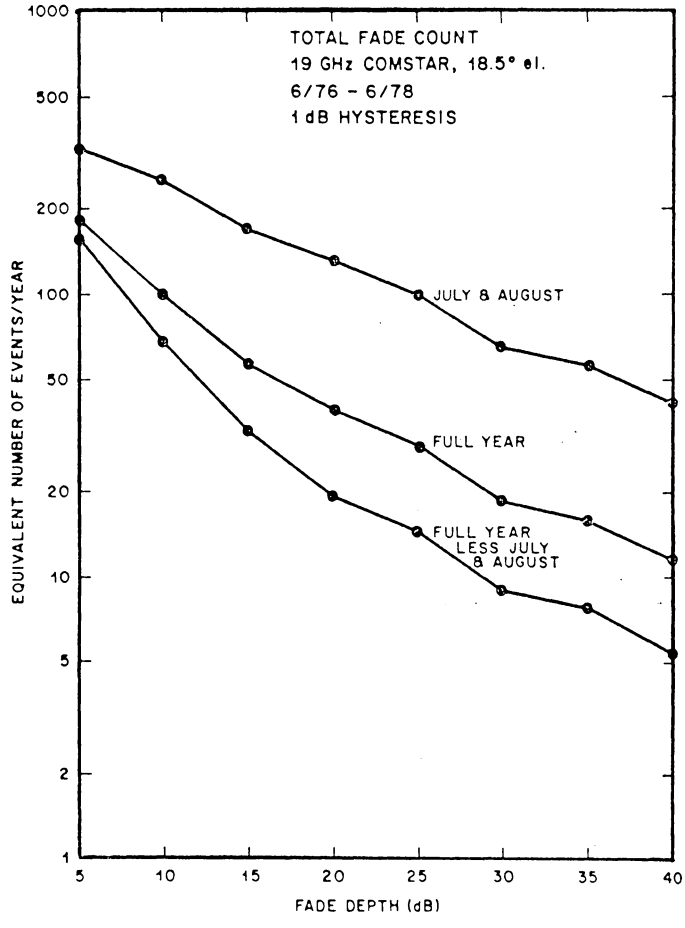

Figure 2.9. Seasonal variation of rain fades; 19 GHz, Crawford Hill, NJ (From Arnold, et. al. [5]).

E. Matricciani (1982) studied the effects of digital filtering on the statistics of fade duration and found that at equal time percentages, longer sampling times resulted in slightly longer fade durations. He also found that the cumulative distribution of fade events was approximately log-log distributed with respect to event duration (See figures 2.10, 2.11, and 2.12.).

P. Khumar (1982) examined both the diurnal and yearly distributions of rain fades at 12, 19, and 28 GHz using the COMSTAR-D1 beacon and a 12 GHz radiometer. The most severe fades were found to occur during the early afternoon and late evening hours (See figures 2.13, 2.14, and 2.15). The yearly distributions of fade events with respect to duration were similar to those reported by Arnold, et al. She also found that the number and duration of fades increased with frequency, in a ratio approximately equal to the square of the frequency ratio; a slight polarization dependence was also found, as shown in figures 2.16 through 2.19.

The previously cited review article by Lin, et al., also reported statistics of fade duration. The exceedence probability of fade events was found to be lognormally distributed with respect to duration, and the average fade duration was found to decrease slightly with fade depth and increase slightly with frequency (See figures 2.20 and

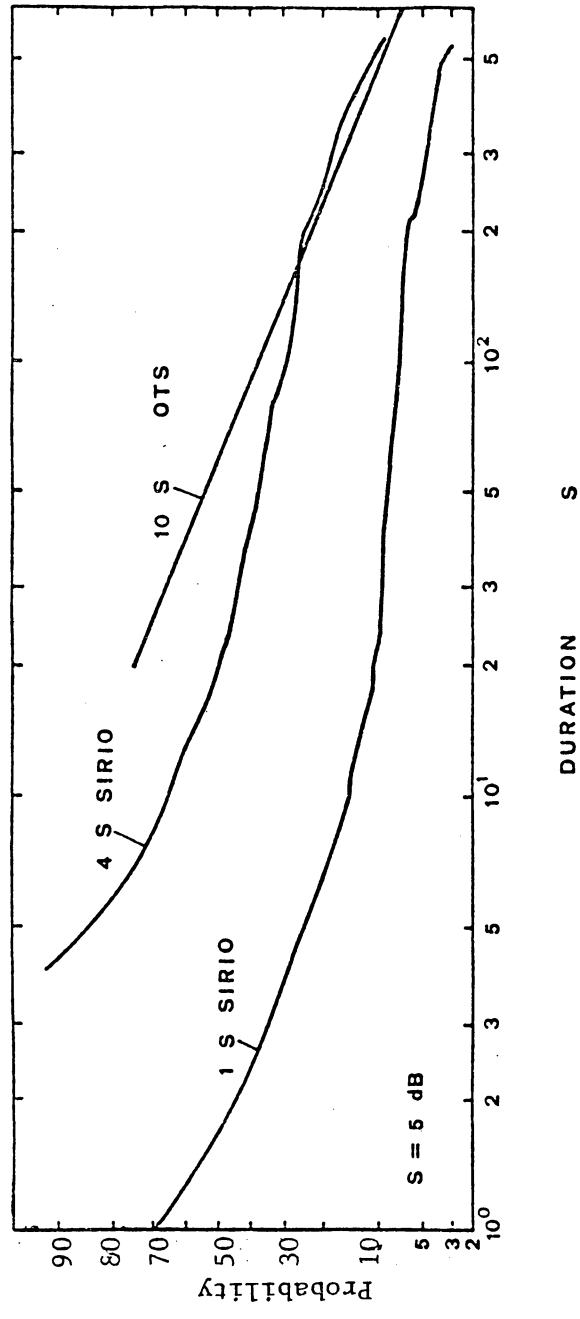

Figure 2.10. Percent probability vs. fade duration; 11 GHz SIRIO, Lario, Italy (From Matricciani [6]).

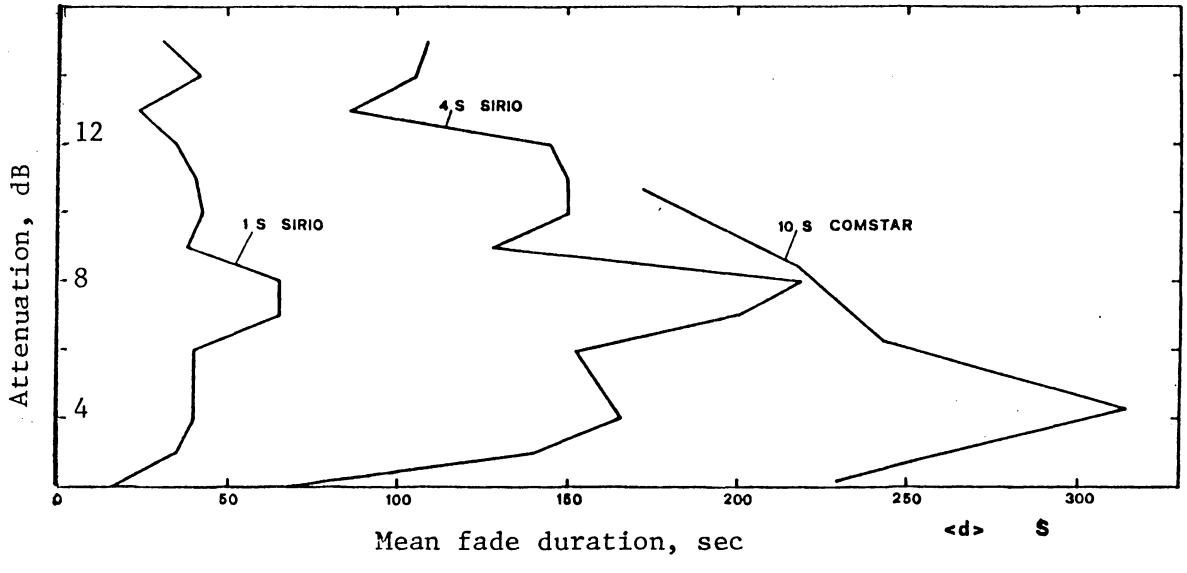

Figure 2.11. Percent probability vs. fade depth, different sampling rates; 11 GHz SIRIO, Lario, Italy (From Matricciani [6]).

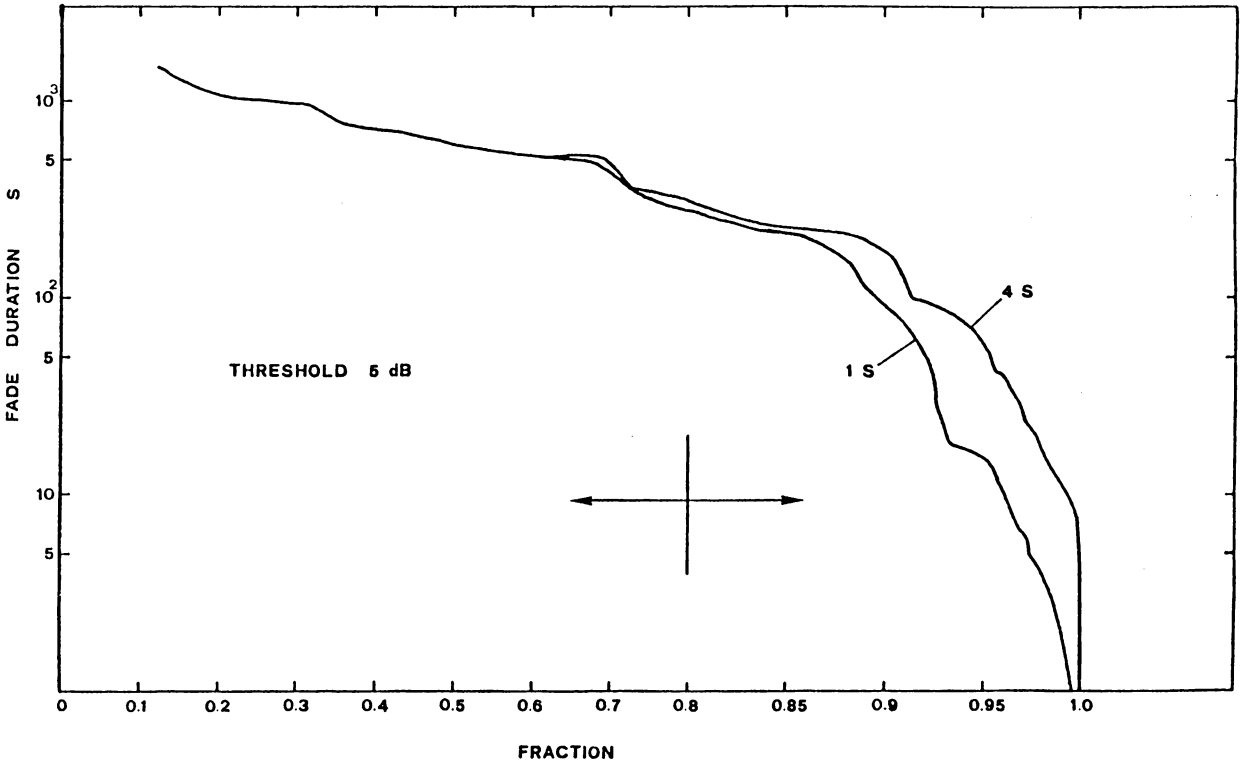

Figure 2.12. Percent probability vs. fade duration, different sampling rates; 11 GHz SIRIO, Lario, Italy (From Matricciani [6]).

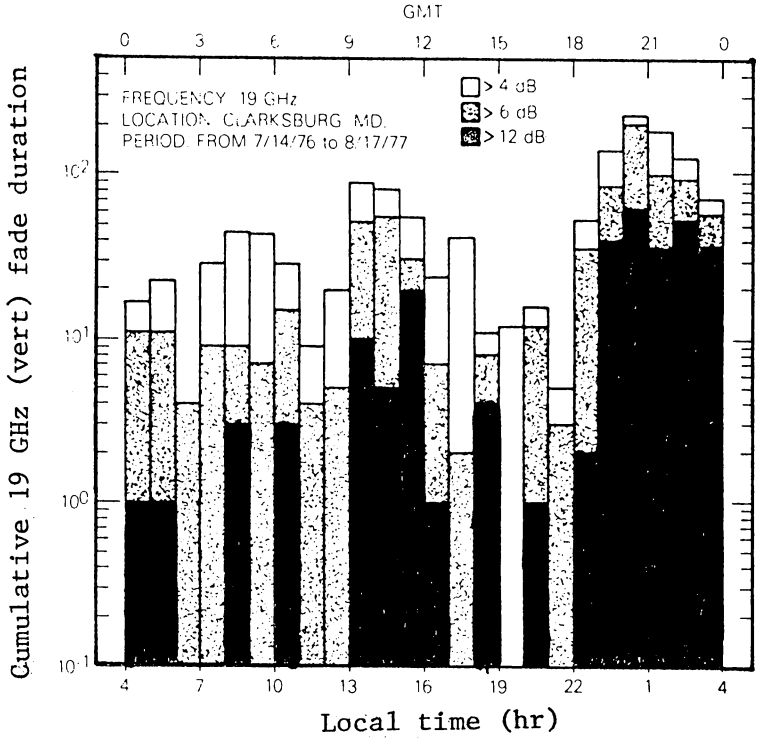

Figure 2.13. Diurnal distribution of fades; 19 GHz vertical COMSTAR, Clarksburg, MD (From Khumar [7]).

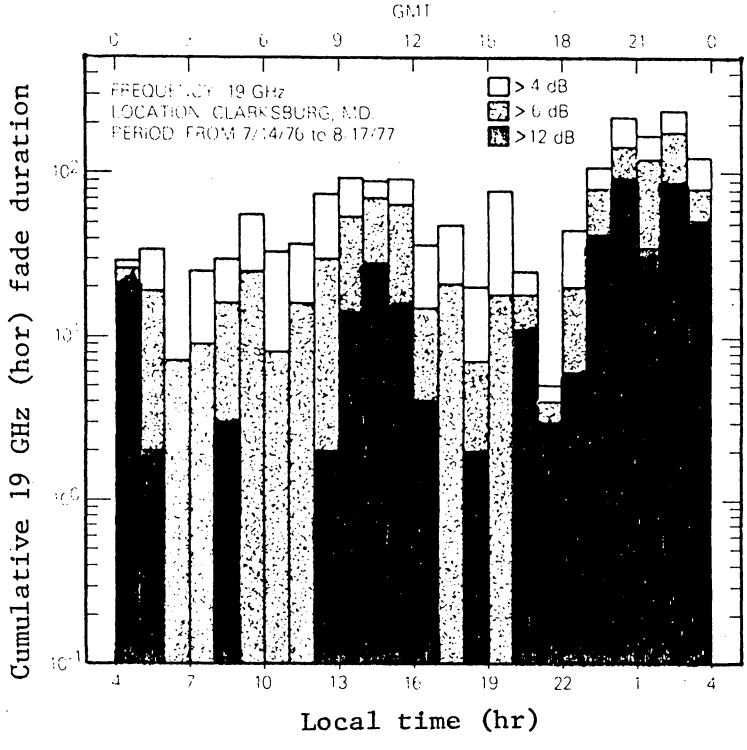

Figure 2.14. Diurnal distribution of fades; 19 GHz horizontal COMSTAR, Clarksburg, MD (From Khumar [7]).

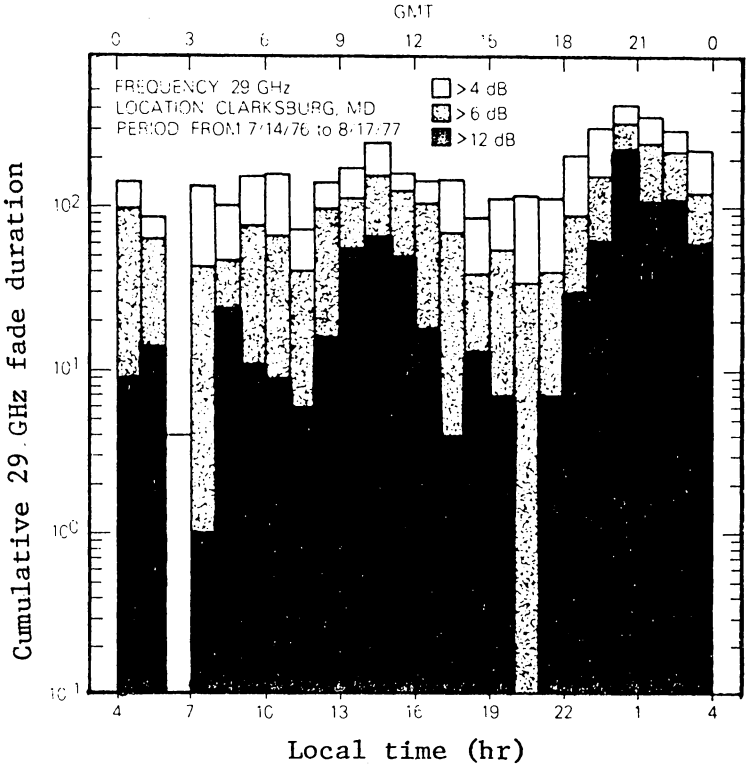

Figure 2.15. Diurnal distribution of fades; 29 GHz COMSTAR, Clarksburg, MD (From Khumar [7]).

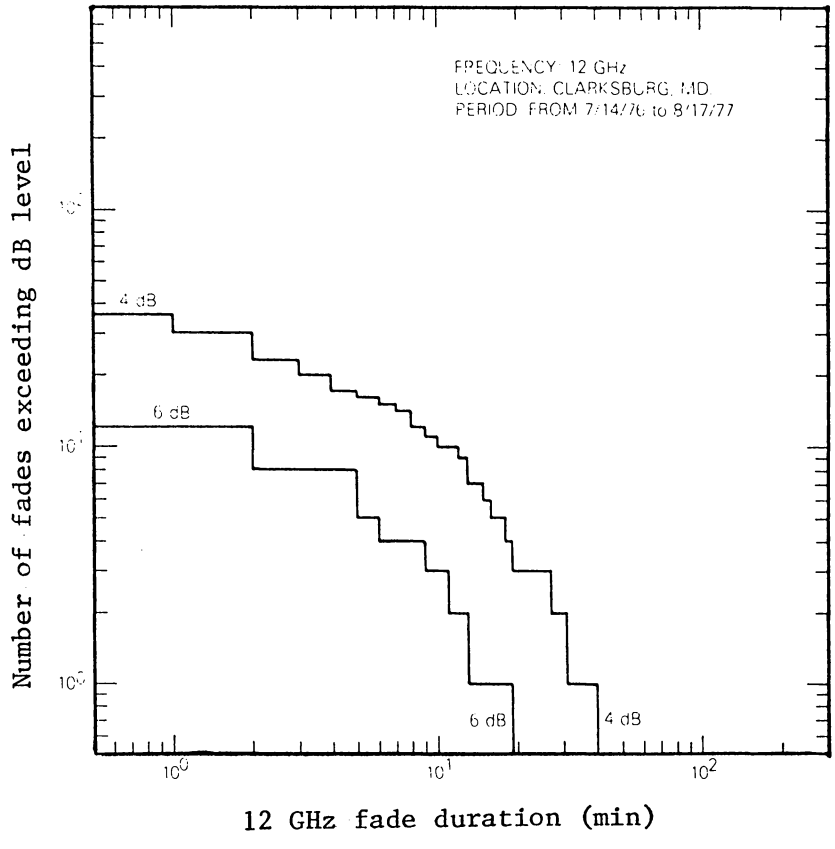

Figure 2.16. Number of events per year with given duration; 12 GHz COMSTAR, Clarksburg, MD (From Khumar [7]).

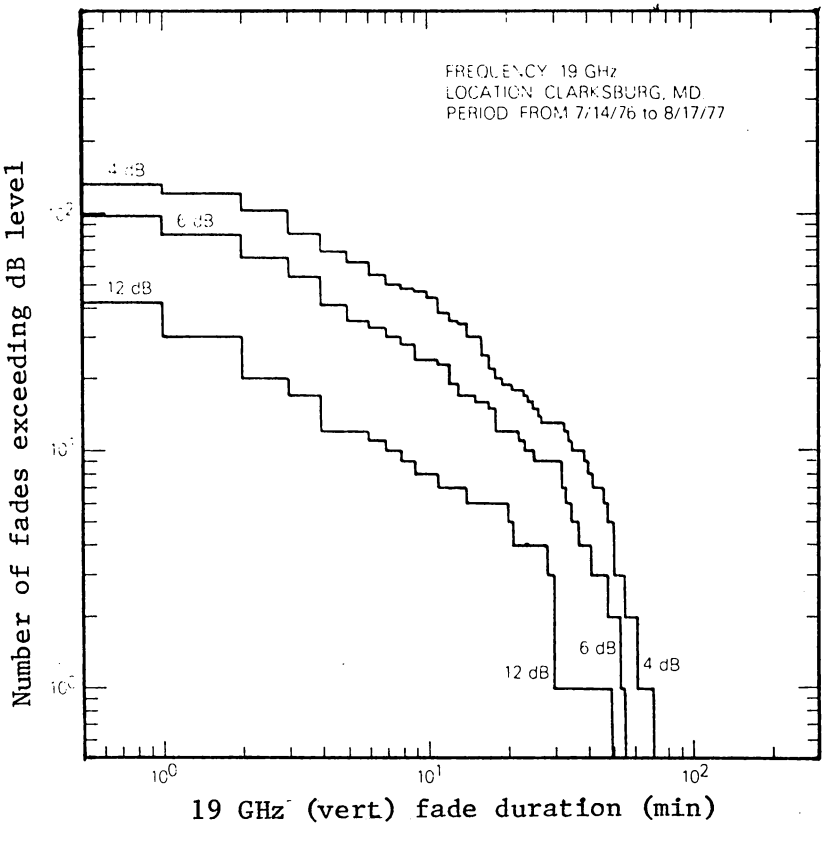

Figure 2.17. Number of events per year with given duration; 19 GHz vertical COMSTAR, Clarksburg, MD (From Khumar).

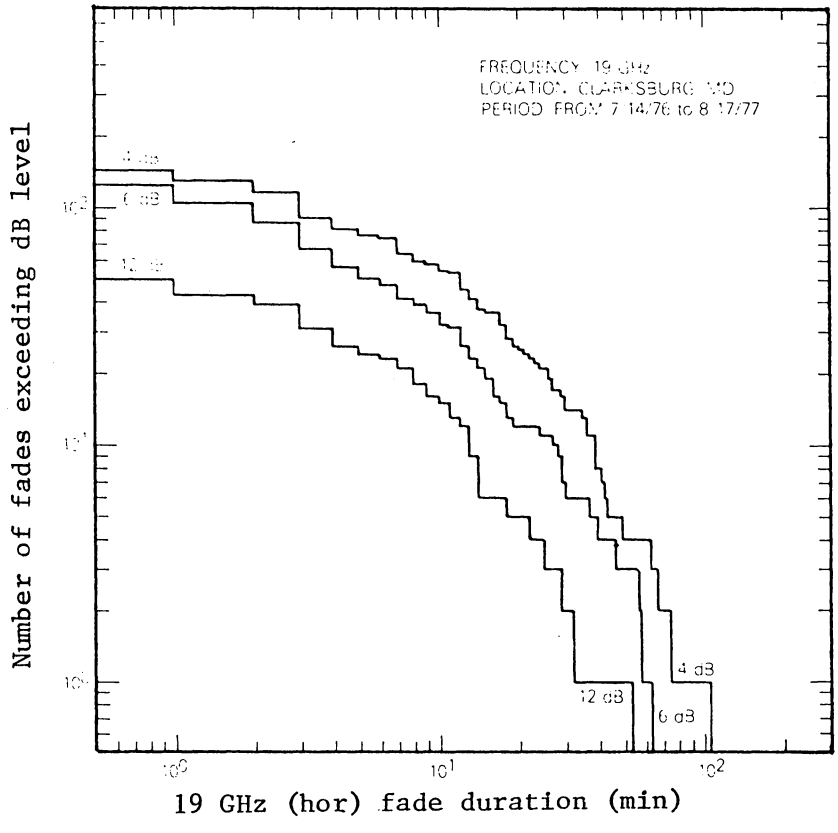

Figure 2.18. Number of events per year with given duration; 19 GHz horizontal COMSTAR, Clarksburg, MD (From Khumar).

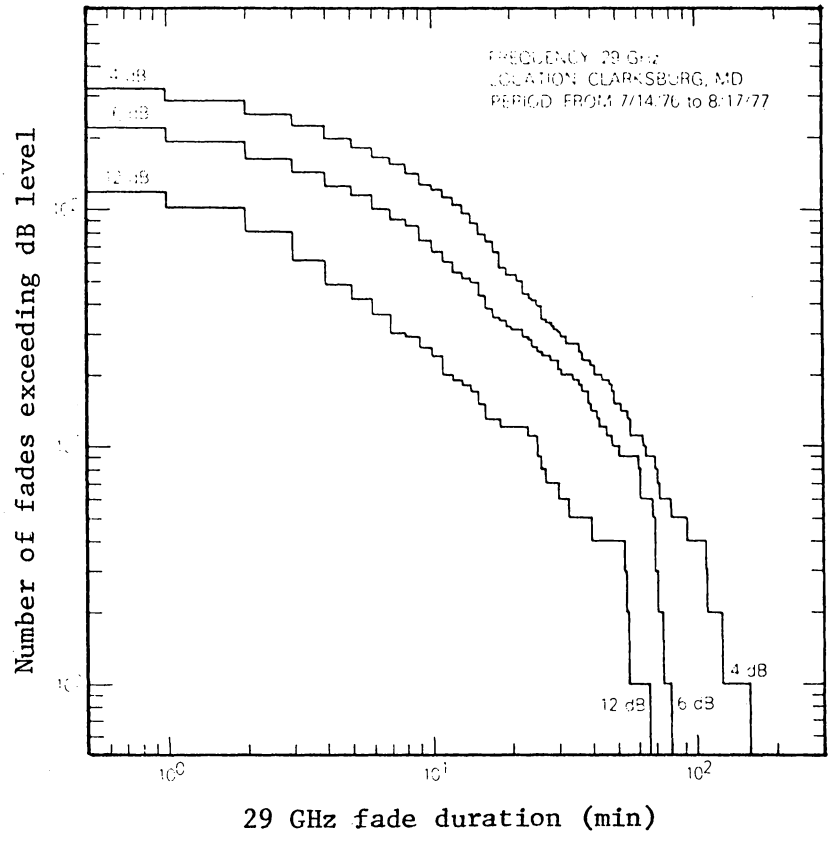

Figure 2.19. Number of events per year with given duration; 29 GHz COMSTAR, Clarksburg, MD (From Khumar).

2.21). This weak dependence on frequency suggests that traditional frequency scaling techniques cannot be used to predict fade duration. It was also found that the probability of a fade duration exceeding its mean was an approximate lognormal distribution (see figure 2.22).

W. Vogel (1982) reported on the statistics of fade duration and intermission duration at Austin, Texas, using the 19 and 28 GHz COMSTAR D3 beacons. The results are shown in table 2-1, and are similar to those reported in [5] and [7].

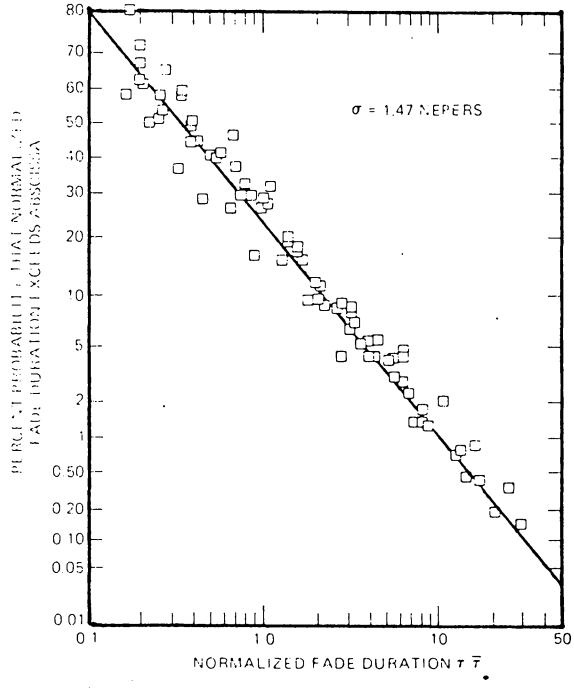

Figure 2.20. Distributions of normalized fade durations; 19 and 28 GHz COMSTAR, Palmetto, GA (From Lin, et. al. [3]).

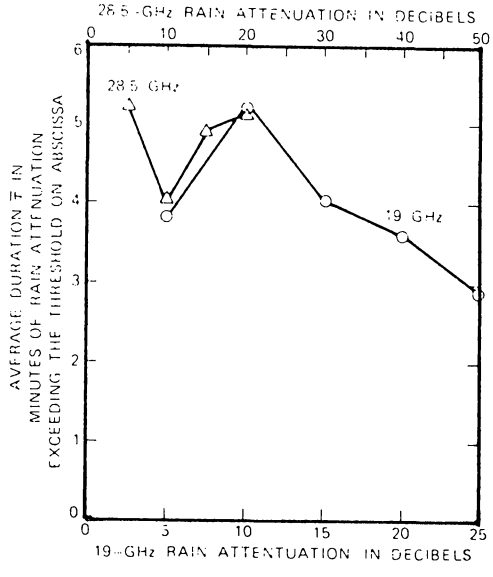

Figure 2.21. Average fade duration vs. fade depth; 19 and 28 GHz COMSTAR, Palmetto, GA (From Lin, et. al. [3])

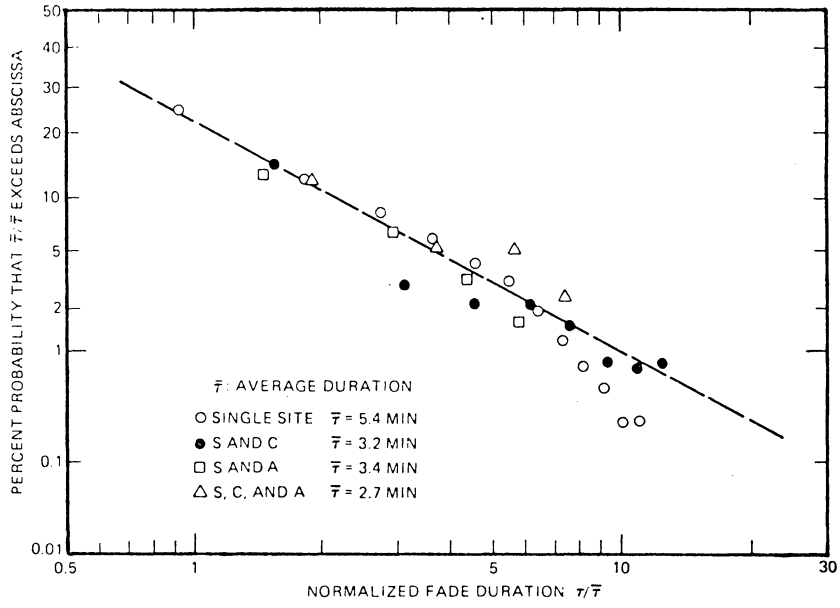

Figure 2.22. Distribution of normalized fade durations; 15.5 GHz radiometer, Holmdel, NJ (From Lin, et. al. [3]).

Table 2-1. Duration percentages for fades and intermissions at the 10 dB level (from Vogel [8]).

Univ of Texas 19.04 GHz — COMSTAR D-3 >10 dB Fades — 10/78-11/80 124 Events

INTERMISSION DURATION - MINUTES	1	2	4	8	16	32	64	128
128	18.5	8.9	8.1	6.4	3.2	0.0	0.0	0.0
64	2.4	0.8	0.8	2.4	0.8	0.0	0.0	0.0
32	4.0	0.8	1.6	0.0	0.0	1.6	0.0	0.0
16	0.8	0.8	0.0	1.6	0.0	0.0	0.0	0.0
8	3.2	1.6	0.0	0.0	0.0	0.0	0.0	0.0
4	3.2	2.4	1.6	2.4	0.0	0.0	0.0	0.0
2	0.8	1.6	1.6	1.6	0.8	0.0	0.0	0.0
1	5.6	4.0	3.2	2.4	0.0	0.0	0.0	0.0

FADE DURATION - MINUTES

Univ of Texas 28.56 GHz — COMSTAR D-3 >10 dB Fades — 10/78-11/80 286 Events

INTERMISSION DURATION - MINUTES	1	2	4	8	16	32	64	128
128	14.3	4.9	6.3	3.1	3.1	0.3	0.0	0.0
64	2.1	1.4	1.4	0.3	1.0	0.0	0.0	0.0
32	2.1	0.7	2.1	1.0	0.7	0.0	0.0	0.0
16	3.8	2.8	0.0	0.7	1.0	1.0	0.0	0.0
8	3.8	1.4	0.0	0.3	0.0	0.0	0.0	0.0
4	5.6	0.3	0.7	1.4	0.3	0.0	0.0	0.0
2	5.6	0.7	0.7	1.0	0.7	0.0	0.0	0.0
1	10.8	3.1	3.8	2.8	1.7	0.3	0.0	0.0

FADE DURATION - MINUTES

Chapter III

THE MEASUREMENT PROBLEM

3.1 RECEIVER TIME CONSTANT EFFECTS

Demodulating the beacon signal from geostationary communication satellites by synchronous detection often requires post-detection filtering to improve the signal-to-noise ratio and to enable fading signals to be tracked adequately. This implies the use of extremely narrow filter bandwidths, and consequently of long filter time constants. While this arrangement is an effective method for detecting weak and noisy signals, it has the disadvantage that during severe fade events, the rate of change of the received signal power is often of the same order as the rate of decay of the time-domain impulse response of the filter. This interaction can cause information about the time derivative of the signal to be lost.

Obviously, then, if accurate faderate and fade duration statistics are to be computed using such a system, some algorithm must be developed which reconstructs the filter input using information from the filter output. Furthermore, this reconstruction process must not cause further corruption of the signal by noise.

The receivers used at Virginia Tech employ synchronous detection with post-detection filtering of the type discussed above, with time constants on the order of 14 seconds (see table A1-1). For such time constants, faderates exceeding approximately 20 decibels per minute cannot be accurately tracked, and some form of reconstruction algorithm must be used.

3.2 MODELLING THE IF PROCESSOR

The filtering operation of the Virginia Tech receivers is actually carried out by a rather sophisticated phase-locked loop circuit, but the response of this loop can be accurately modelled by a first- order differential equation, in a manner developed by P.H. Wiley, as follows (See Appendix A for a more detailed analysis.):

A simple first-order low pass filter is shown in figure 3.1. Using elementary circuit analysis, the describing equation can be readily derived:

$$\frac{dv_o}{dt} + \frac{1}{RC} = -\frac{1}{R_i C} v_i \qquad (1)$$

If the input voltage v_i is fading linearly in dB with a time constant τ_1, then v_i can be written as

$$v_i = Ke^{-\tau_1 t}$$

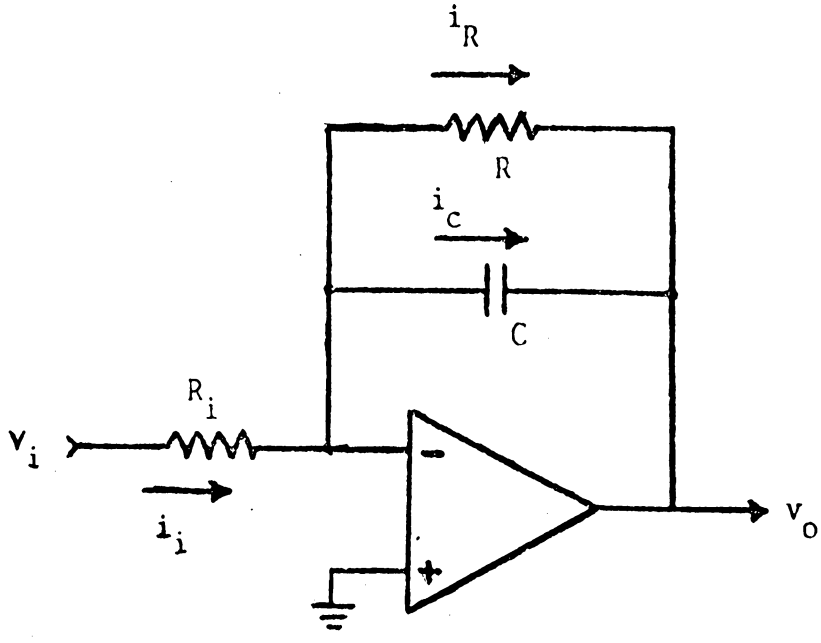

Figure 3.1. Equivalent lowpass filter of IF processor.

where K is the amplitude of v_i at the onset of the fade. Equation (1) may then be written un the form

$$\frac{dv_o}{dt} + \frac{1}{RC} v_o = -\frac{K}{R_i C} e^{-\tau_1 t} \qquad (2)$$

By inspection, the solution is quickly found to be

$$v_o = C_1 e^{-\tau_2 t} + C_2 e^{-\tau_1 t} \qquad \text{where}$$

$$C_2 = -\frac{K}{(\tau_2 - \tau_1) R_i C} \qquad \text{and}$$

$$C_1 = \tau_2 C_2 \qquad \text{with}$$

$$\tau_2 = \frac{1}{RC} \quad . \qquad \text{Then}$$

$$v_o = \frac{K}{R_i C(\tau_2 - \tau_1)} \left(\frac{\tau_1}{\tau_2} e^{-\tau_2 t} - e^{-\tau_1 t}\right)$$

Multiplying this by R/R_i and with $\tau_2 = 1/RC$, we have

$$v_o = K \frac{R}{R_i}\left(\frac{\tau_2}{\tau_2-\tau_1}\right)\left(\frac{\tau_1}{\tau_2} e^{-\tau_2 t} - e^{-\tau_1 t}\right) \qquad (3a)$$

Ideally, we wish the measured output voltage to match the actual input voltage. Thus

$$v_o = Ke^{-\tau_1 t} \qquad (3b)$$

By inspection, (3a) and (3b) will match only if $\tau_2 >> \tau_1$, that is, if the time constant of the fade is much longer than the time constant of the filter. But, since the time constants of the Virginia Tech receivers are approximately 14 seconds, this is not generally the case. In fact, during severe thunderstorms, the two time constants may be nearly equal.

Table A1-2 shows the results of the experiment which was performed to determine the effects of narrow band filtering on the measurement of rapidly fading signals using the Virginia Tech receivers. As can be seen by comparing the figures in the first and last columns, the filter output does not "catch up" to the input voltage until approximately 10 filter time constants have elapsed. Furthermore, this effect is essentially independent of the input faderate.

For the Virginia Tech receivers, whose time constants are approximately 14 seconds, this means that faderates as small as a few dB in 2.5 minutes cannot be measured accurately using uncorrected samples of the receiver output. Analysis of strip chart recordings of attenuation events from other experiments indicates that faderates of this magnitude are routinely exceeded, even during periods of relatively light precipitation. In order to obtain an accurate measurement of faderates, one must either use receivers with shorter filter time constants, or develop an algorithm which reconstructs the receiver input. In terms of using the already available data base at Virginia Tech, the latter approach is more practical.

3.3 THE RECONSTRUCTION ALGORITHM

While the process of reconstructing the input waveform to a system from its measured output and its impulse reponse is, in general, an involved signal processing problem involving deconvolution, some simplifying assumptions can be made which make the algorithm straightforward. Basically, the algorithm involves solving equation (1) for v_i as follows:

$$\frac{dv_o}{dt} + \frac{1}{RC} v_o = - \frac{1}{R_i C} v_i$$

$$v_i = -\frac{R_i}{R}\left(v_o + RC\frac{dv_o}{dt}\right)$$

Since we are only interested in discrete values of v_i, and the differential equation is first order, we can approximate the derivative dv_o/dt using finite differences, and calculate discrete values of v_i. We shall assume that the sampling interval Δt and the voltage increment Δv_o are sufficiently small such that the approximation

$$\frac{\Delta v_o}{\Delta t} \cong \frac{dv_o}{dt}$$

is valid. We will also assume that the value of v_i calculated by this method corresponds to the average value of v_i over the arbitrary time interval (t_i, t_{i+1}). Then

$$v_i\left(t_1 + \frac{\Delta t}{2}\right) = \frac{-R_i}{R}\left(\frac{v_o(t_2) + v_o(t_1)}{2} + RC\,\frac{v_o(t_2) - v_o(t_1)}{\Delta t}\right) \tag{4}$$

where the average value of v_o over the corresponding time interval was used.

Equation (4) was verified by applying exponentially fading signals with various time constants to equation (3a).

The resulting calculated values of v_o were then inserted into equation (4), together with the appropriate sampling interval (See appendix A.). The values of v_i calculated in this manner show good agreement with actual values of v_i, with less than 2% error for all values tested (See table A1-3.).

The time constants of the Virginia Tech COMSTAR receivers were determined by removing the input signal to the receiver while continuing to sample the output. The rate of decay of the output voltage could then be used to determine the time constant of the channel under consideration. Using these time constants in equation (3a) and a known input voltage, the values of v_o predicted by (3a) were compared to the actual measured values of v_o (See table A1-4.). The results again show good agreement.

As long as the signal is sampled at a rate which preserves the desired amount of detail in v_i, equation (4) then gives an accurate method for eliminating the effects of long receiver time constants from the faderate statistics. This is the method which will be used in this thesis.

Chapter IV

MEASUREMENT OF FADERATE

4.1 SAMPLING METHODS

The manner in which data are collected and faderate and attenuation calculated will now be discussed. The Virginia Tech receivers are designed such that the control voltage of the post detection phase-locked loop is proportional to the signal power received from the satellite beacon. After the system was calibrated and reference signal levels determined, a curve which relates the loop control voltage to the received signal power was derived and included in the software of the computer-controlled data acquisition system. It is this control voltage which is sampled, digitized, converted to a received power level, and stored on tape for subsequent analysis.

In this type of data acquistion system, there are basically two methods which can be used to collect data. One approach is to sample the signal at a uniform rate, but only retain the sample when some measurement parameter has changed by a predetermined amount. This method has the advantage that the amount of variation between samples of the parameter being measured is bracketed, and this bracket can be made arbitrarily small. A signal could then be accurate-

ly reconstructed from its samples without any further signal processing, an attractive feature when large sets of data are being stored for later analysis. Another practical consequence of this sampling method is that, in general, considerably fewer samples need to be retained for permanent storage. This is true because little or no data are recorded during periods when the signal is changing very slowly, such as clear weather intervals. This is the type of sampling employed at Virginia Tech.

Alternatively, sampling can be done at a uniform rate. This approach is somewhat simpler and provides some flexibility if any subsequent signal processing is required. This is an important concern since digital signal processing algorithms usually require a uniform sampling rate. If it were desired to filter the signal digitally, or perform a spectral estimation or sampling rate conversion, a uniform sampling rate should be used. The major drawback to this method is that it usually results in extremely large and unmanageable data sets, a considerable problem when data is to be collected over an extended period of time, such as several years. For this reason, this sampling method was not used at Virginia Tech.

4.2 THE MEASUREMENT ALGORITHM

We now wish to find the instantaneous value of the derivative of S(t), where S(t) represents the amplitude of the continuous wave beacon signal. S(t) thus represents a low frequency attenuation envelope, i.e., amplitude modulation, of the satellite beacon. During clear weather, the received signal power remains nearly constant, so the derivative of S(t) is zero. During an attenuation event, S(t) begins to vary slowly. The data acquisition system used in this study stores samples of S(t) when its amplitude changes by 0.7 dB or more. From these samples, a piece-wise linear approximation of the derivative of S(t) is then computed in the following manner. Using the algorithm described in the previous section, the receiver input samples are reconstructed. The faderate is then computed as (See figure 4.1.)

$$F = \frac{\Delta S}{\Delta t} \quad , \qquad \text{where}$$

$$\Delta S = S_2 - S_1 \qquad \text{and}$$

$$\Delta t = t_2 - t_1$$

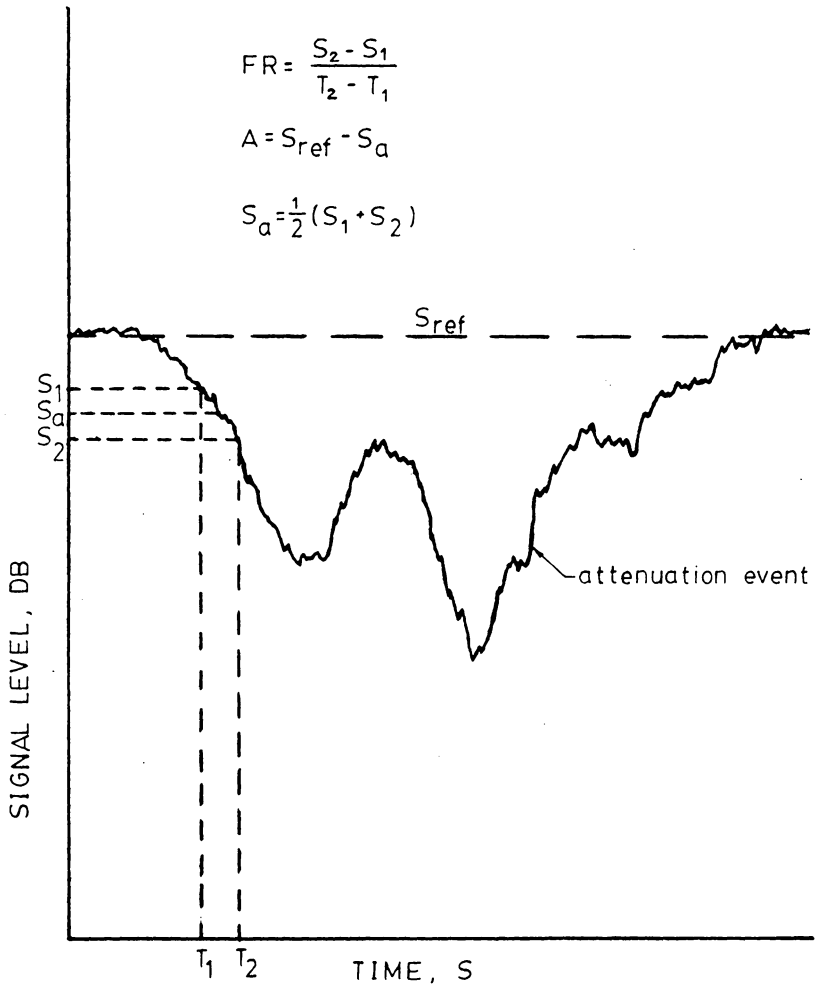

Figure 4.1. Illustration of faderate and attenuation measurement.

Corresponding to each faderate value computed is an attenuation value, given by

$$A = S_{ref} - S_{av}$$

where S_{av} is the average signal power over the interval $[t_1, t_2]$. Since it was assumed that S(t) is piecewise linear over this interval, S_{av} is given by

$$S_{av} = \frac{1}{2}(S_1 + S_2)$$

Data are collected into sets covering a time period of one month, and the mean clear weather signal level S_{ref} is determined for each data set. S_{av} is then subtracted from S_{ref} to determine attenuation. Values of attenuation exceeding 19 dB (and their corresponding faderate values) were not included in the study; at this threshold, the phase-locked loops in the Virginia Tech receivers begin to slip cycles, and the faderate data become unreliable. Since this threshold represents approximately the 0.003% yearly attenuation time exceeded for the 19 GHz data (or about 0.3% of actual attenuation event time), exclusion of these data should not seriously affect the faderate statistics.

The attenuation continuum is then divided into bins, each bin having a width of 1 dB. All faderate values in a given bin are then averaged together to yield a data set containing mean values of faderate, together with their corresponding integerized value of attenuation. Since sampling was done for uniform changes in signal amplitude, all samples were given equal weight. Preliminary analysis showed that the statistics of faderate vs. attenuation for negative rates (fade onset) were nearly identical to the statistics for positive rates (fade recovery), as can be seen in figure 4.2. For this reason, subsequent analyses did not distinguish between positive and negative rates; only the faderate magnitudes were used.

Since the clear weather signal level may vary by a few dB during a given month, there will be some ambiguity in the faderate statistics with respect to the proper attenuation bin. For this reason, adjacent data points on the faderate vs. attenuation curves were averaged together using a N=3 triangular window, with 1-2-1 weighting. This procedure has a slight smoothing effect on the data, and should produce more realistic results.

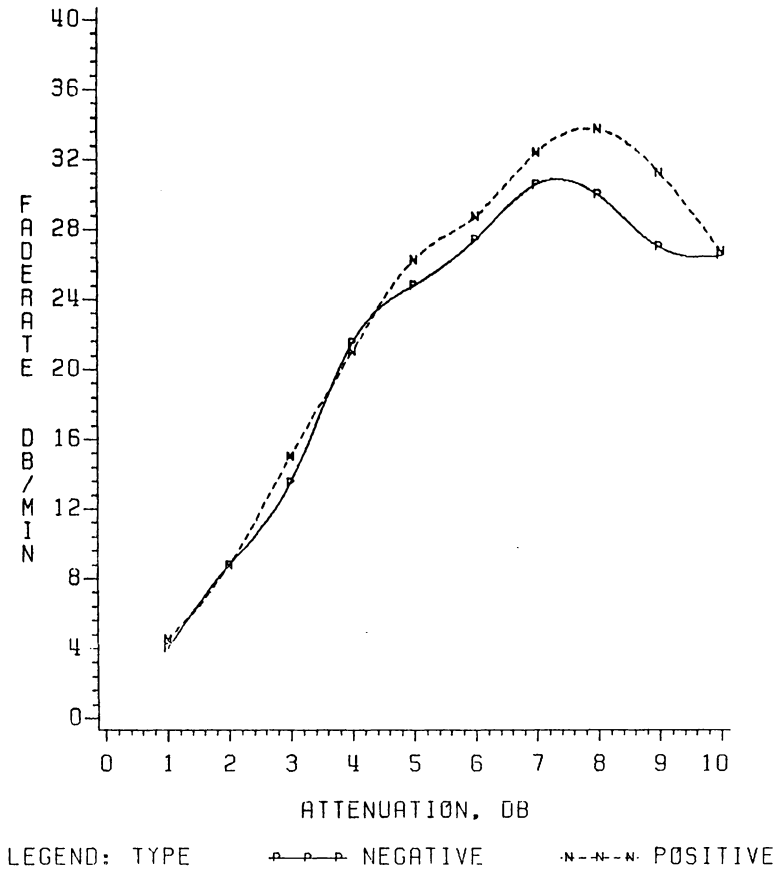

Figure 4.2. Faderate vs. attenuation, positive and negative rates, 19 GHz input, June-August 1977.

Chapter V

STATISTICS OF FADERATE AND ATTENUATION

5.1 MEAN FADERATE VS. ATTENUATION

In this chapter, faderate statistics for the reconstructed receiver input will be presented and compared to the statistics of the uncorrected output. Results for separate years and for each three month season will be shown.

Care must be taken in the computation procedure to screen out invalid or improperly recorded data. This would include data which were recorded while the phase-locked loop was slipping cycles, or while the receivers were in the test mode, or data which were corrupted by equipment malfunctions in the satellite or the earth terminal. Such invalid data was found to comprise less than 2% of event time data during any given month and should not significantly affect the results. The statistics shown apply only to attenuation events; periods of clear weather have been excluded.

Curves of mean faderate vs. attenuation are shown in figures 5.1 through 5.4. No data are shown for fade depths greater than 10 dB since it was found that beyond this threshold, the relationship between faderate and attenuation is essentially random. Up to this threshold, the relationship is nearly lognormal, as suggested by Matricciani and

Lin, et al. This phenomenon will be discussed in more detail later.

Perhaps the first feature to note about these curves is the rather large difference between the receiver input and output data. While the basic curve geometry is preserved, the mean faderates calculated from the receiver input have been scaled upward by a factor of approximately 3.5. This illustrates the severity of the errors which may be encountered when the rate of change of a signal is measured using a device whose time constant is not significantly shorter than that of the signal. On an instantaneous basis, the amount of error may be much greater than the factor of 3.5, and if higher order filtering is used, it may not be practical or even possible to develop an accurate reconstruction algorithm.

The restoration of high frequency components to the input waveform can be seen graphically in figure 5.5, which shows typical signal behavior during an event. Since the "area" under both the input and output waveforms is nearly equal, attenuation cumulative distributions would not be significantly affected by the reconstruction process.

Another salient feature of figures 5.1 and 5.3 is the rather large difference between the 1977-1978 statistics and the 1978-1979 statistics. This difference can be explained

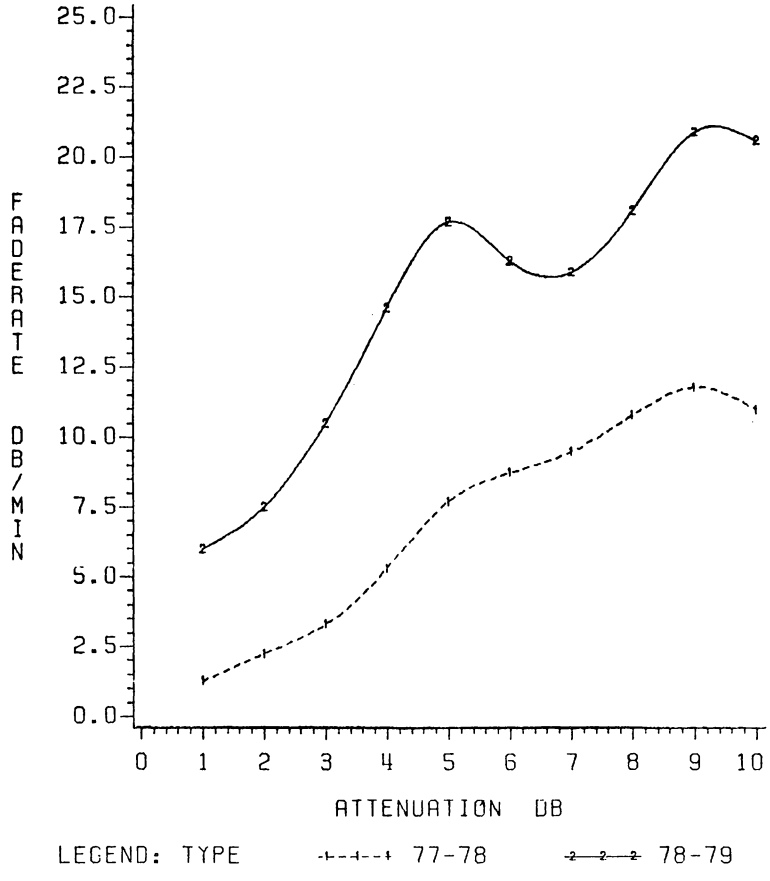

Figure 5.1. Faderate vs. attenuation; 19 GHz input, June 1977- May 1979.

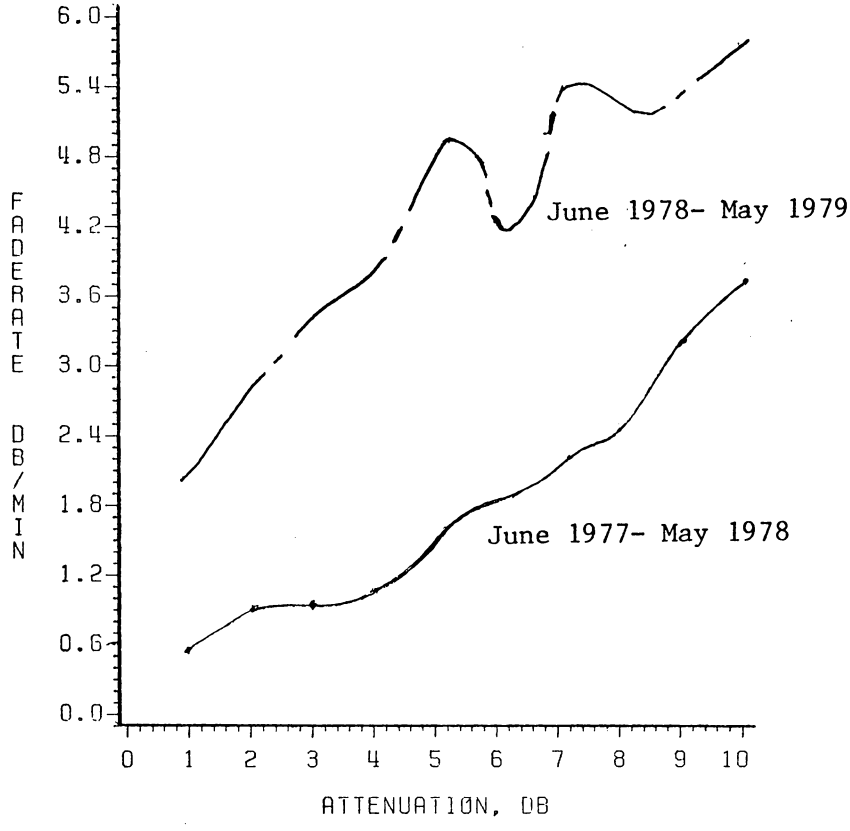

Figure 5.2. Faderate vs. attenuation; 19 GHz output, June 1977- May 1979.

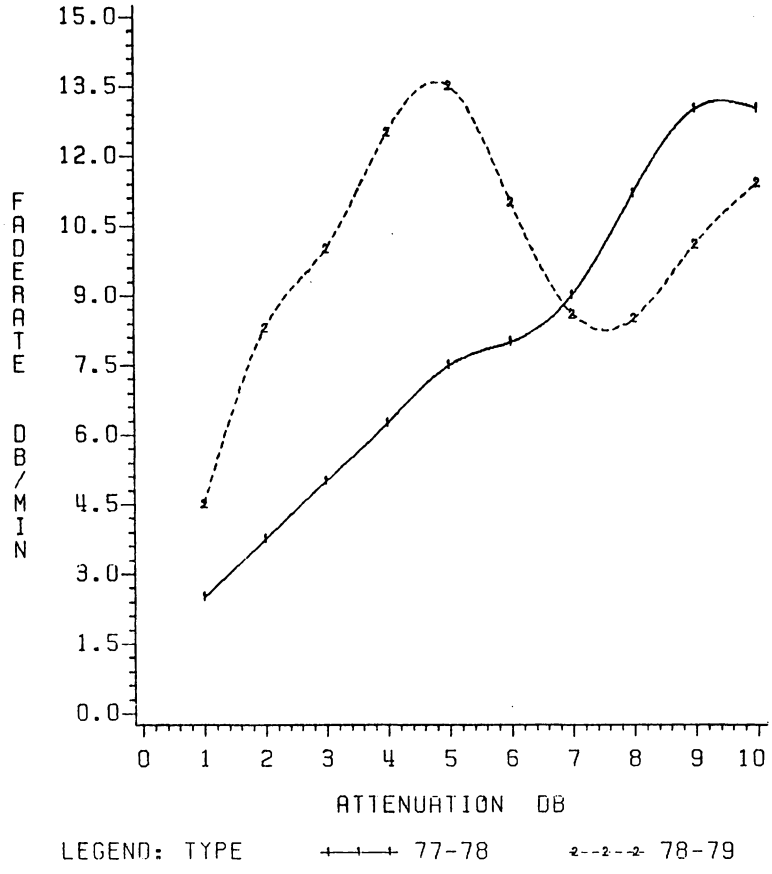

Figure 5.3. Faderate vs. attenuation; 28 GHz input, June 1977- May 1979.

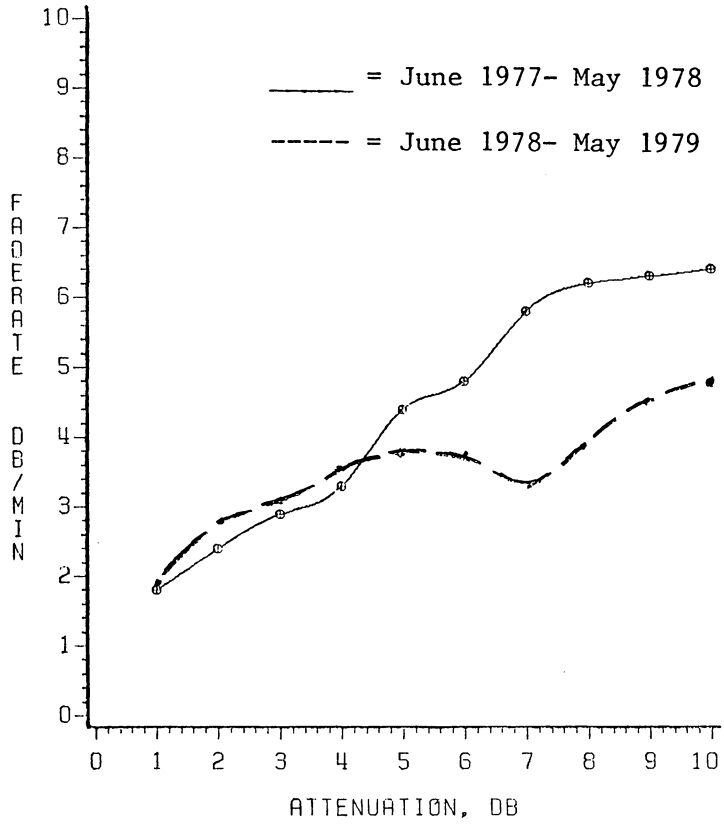

Figure 5.4. Faderate vs. attenuation; 28 GHz output, June 1977- May 1979.

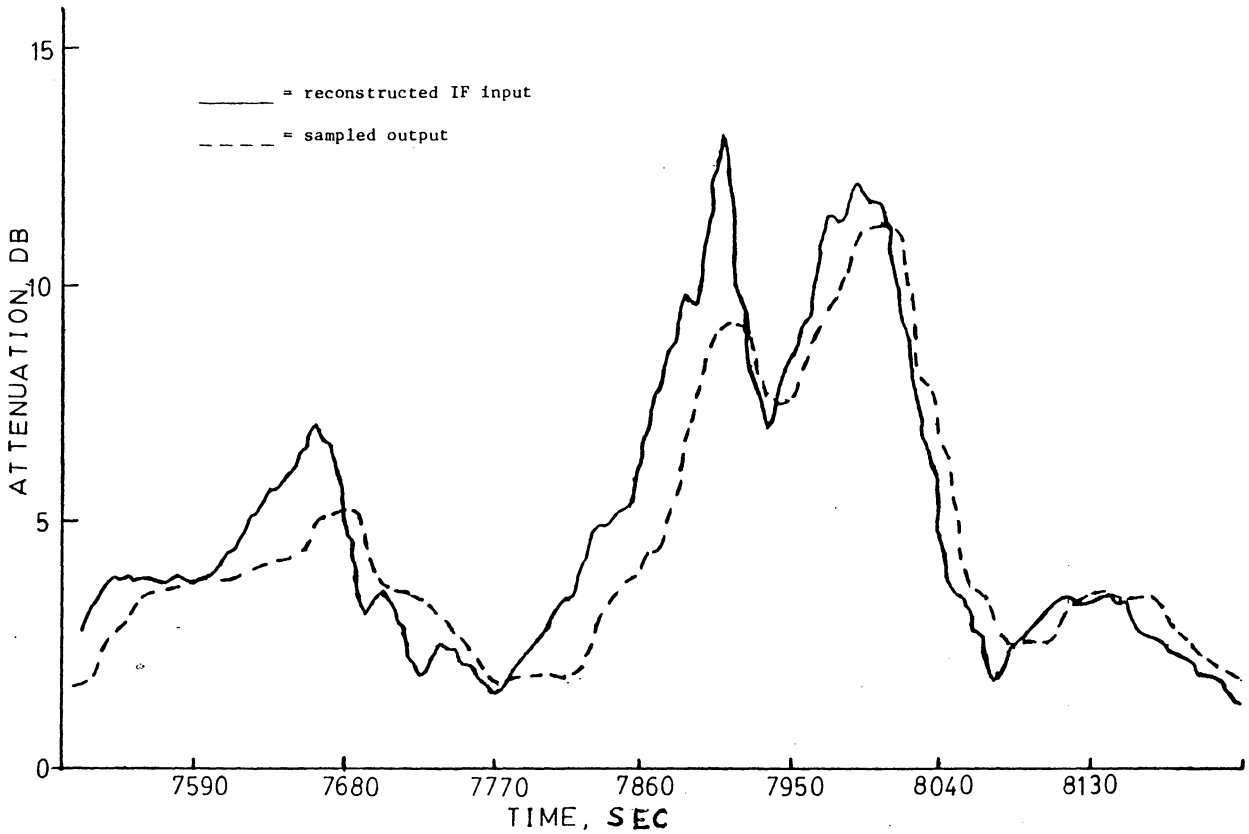

Figure 5.5. Comparison of input and output waveforms for event of June 19, 1977.

by examining the quarterly statistics shown in figures 5.6 through 5.9. While the total number of data points for the two years is nearly identical, the seasonal distribution of the data differs markedly for the two years. The data set for 1977-1978 contains a larger number of points which were collected during periods of prolonged, light rainfall, which corresponds to lower attenuation and faderate values. While nearly equal amounts of rain fell during the two years, the rate and duration characteristics of the rainfall differed markedly between the two years. Figure 5.10 shows the quarterly distributions of fades at 19 and 28 GHz, along with the hours of rainfall and 0.1% rainrate levels for these time intervals. Note that the seasonal rainfall characteristics differ markedly between the two years, while the net rainfall statistics do not. The fall of 1977 was unusually wet, and the spring of 1978 abnormally dry. The period June 1978-May 1979 experienced a dry summer and fall, and a wet summer and spring. These results indicate that rainrate and rainfall amounts are major determinants of faderate; however, the practical difficulties involved in determing these parameters quickly enough for the information to be utilized limit the usefulness of this method. Figures 5.1 and 5.3 also show that the yearly statistics of faderate may vary by as much as a two-to-one margin. Variations from season to season may be even larger.

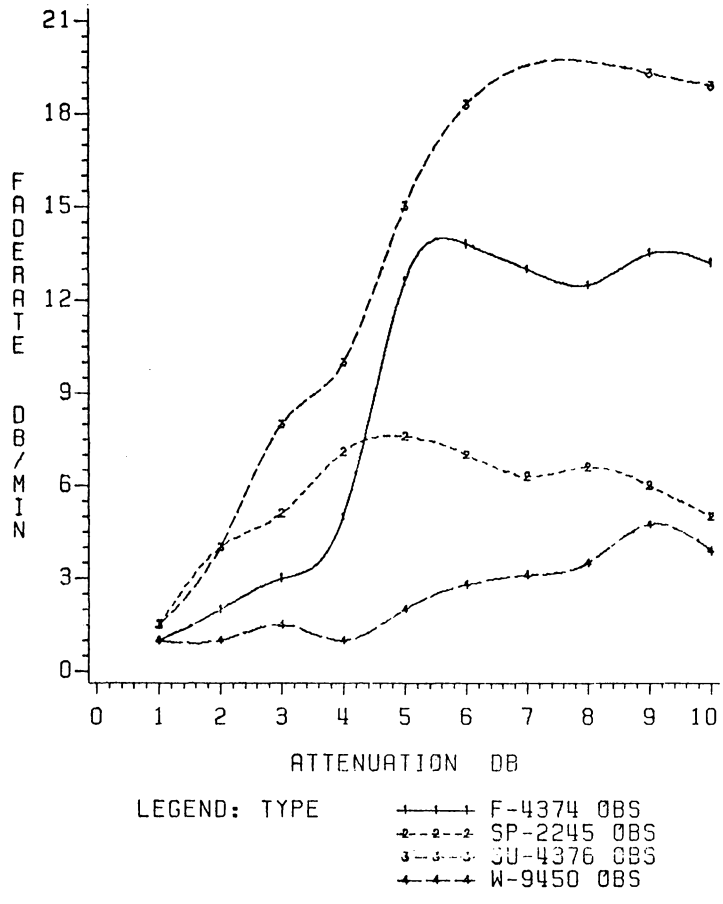

Figure 5.6. Quarterly faderate vs. attenuation, 19 GHz input, June 1977- May 1978; 22,395 observations.

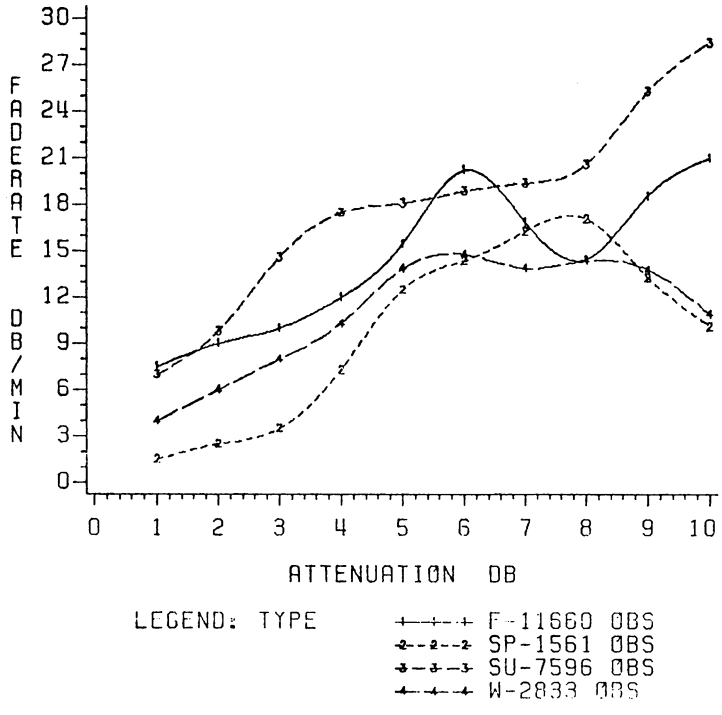

Figure 5.7. Quarterly faderate vs. attenuation, 19 GHz input, June 1978- May 1979; 23,839 observations.

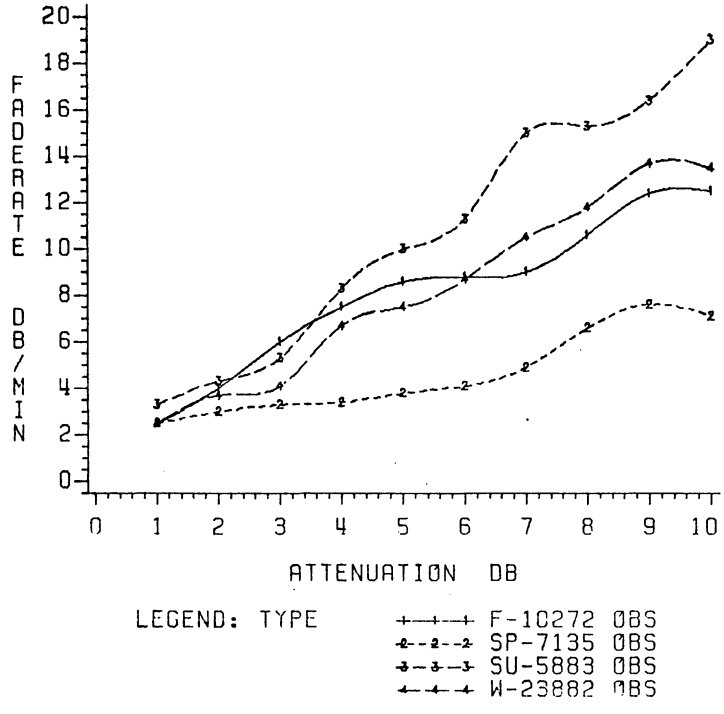

Figure 5.8. Quarterly faderate vs. attenuation, 28 GHz input, June 1977- May 1978. 47,174 obs.

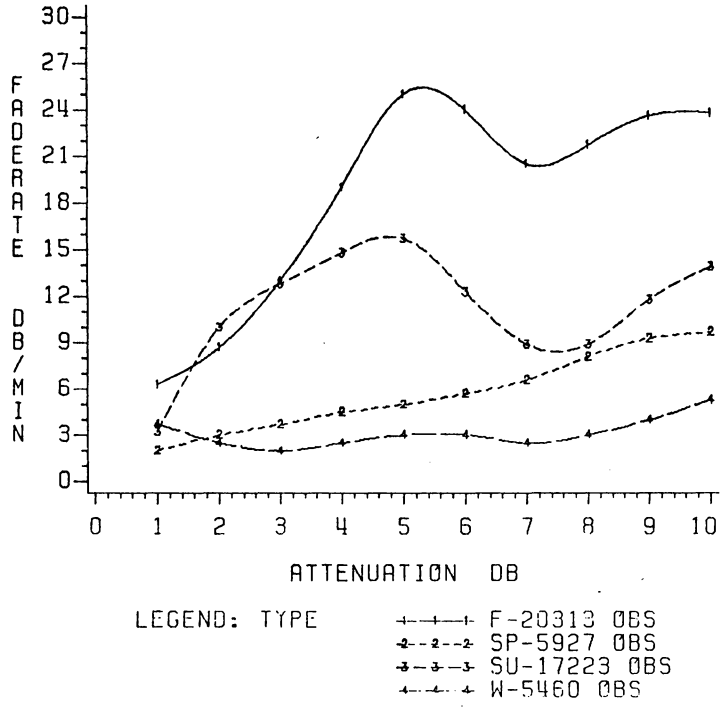

Figure 5.9. Quarterly faderate vs. attenuation, 28 GHz input, June 1978- May 1979. 48,924 obs.

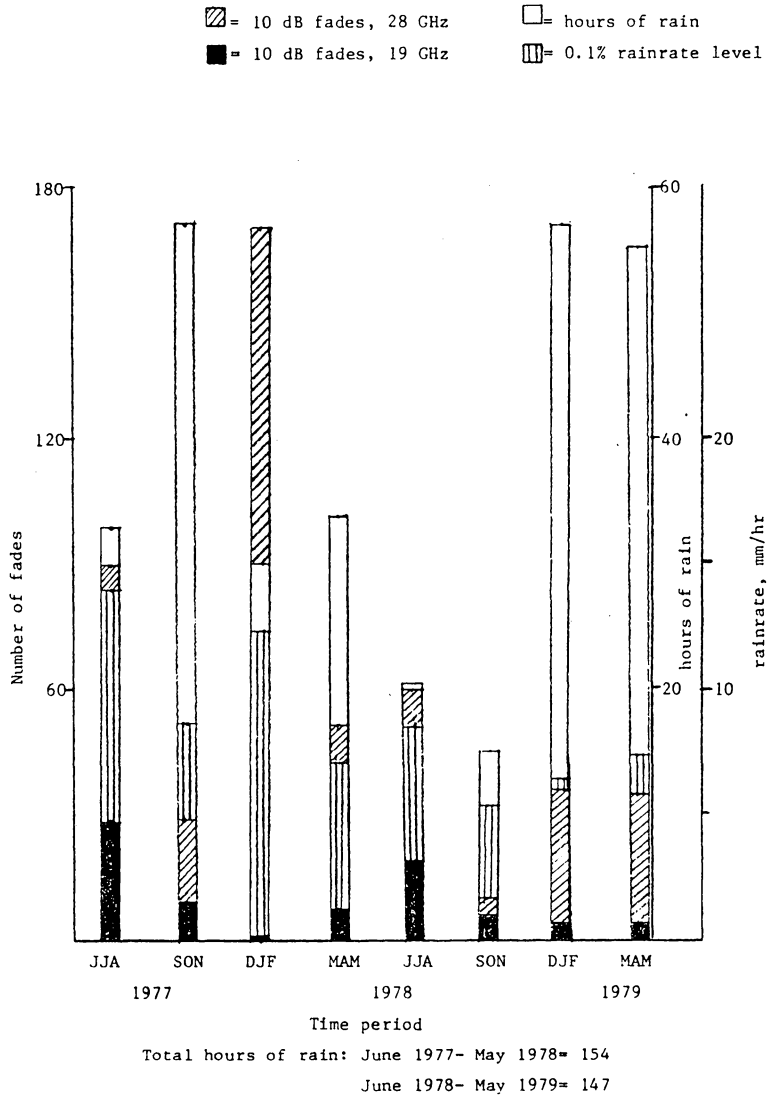

Figure 5.10. Quarterly incidence of 10 dB fades, rainrate, and rain time, June 1977- May 1979.

5.2 PERCENTILE DISTRIBUTIONS OF FADERATE DATA

Another aspect of the statistics which must be addressed is the nature of the distribution of faderate values associated with a given attenuation threshold. Figures 5.11 through 5.14 show the 10th, median, and 90th percentiles of faderates for a given value of attenuation. These figures show that the spread in values is quite large, but that the medians are considerably lower than the mean values. Furthermore, the spread tends to grow larger with increasing attenuation. Figures 5.13 and 5.14 show the amplitude probability distributions of faderates without attenuation as a parameter for several different time periods. These distributions are nearly symmetrical and Gaussian, and 90% of the values have magnitudes of less than 10.0 dB per minute. The large spread in faderate values at all attenuation thresholds suggests that measured attenuation per se may not be a suitable parameter to use in the prediction of faderate.

5.3 FADERATE MODELLING CONSIDERATIONS

As an alternative, a stochastic dynamic model suggested by Maseng, et. al. [9], could be used. This method models attenuation as a first-order Markov process and does not rely soley on the statistics of mean faderate to predict future values of attenuation. Instead, the value of attenua-

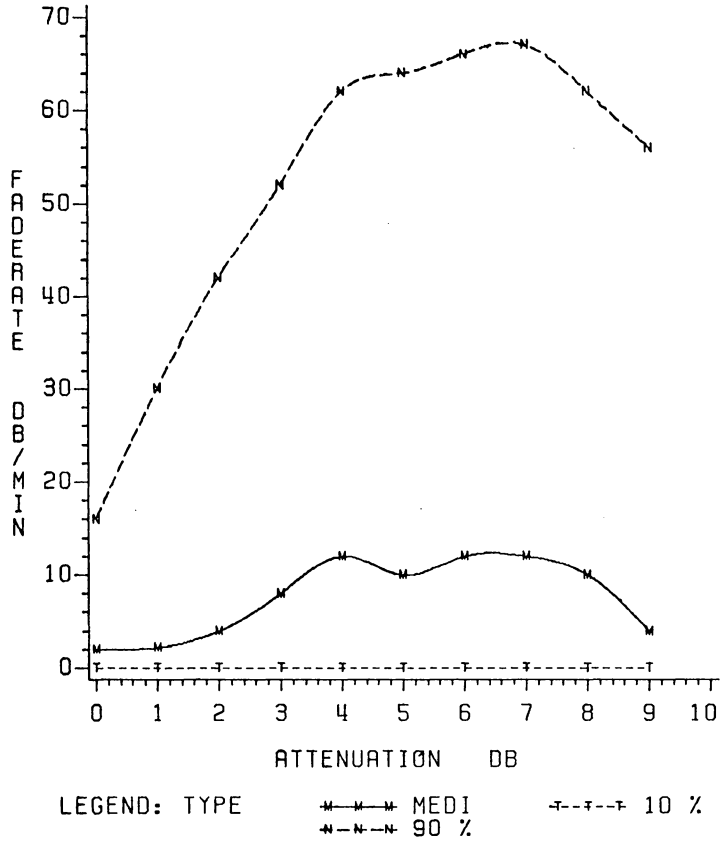

Figure 5.11. Faderate vs. Attenuation, 10th, median, and 90th percentiles; 19 GHz input, June 1977- May 1978.

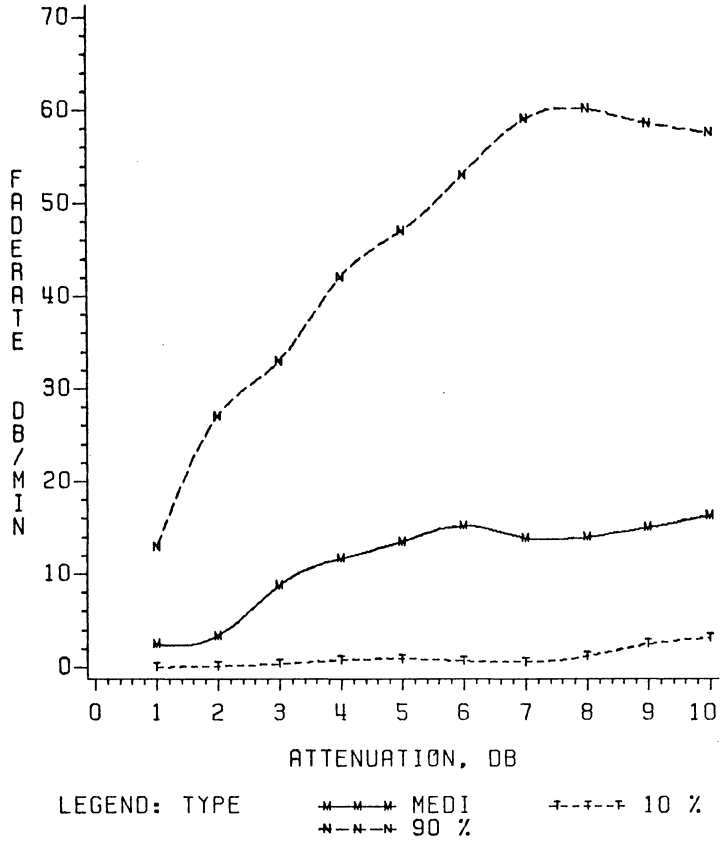

Figure 5.12. Faderate vs. attenuation, 10th, median, and 90th percentiles, 19 GHz input, June 1978- May 1979.

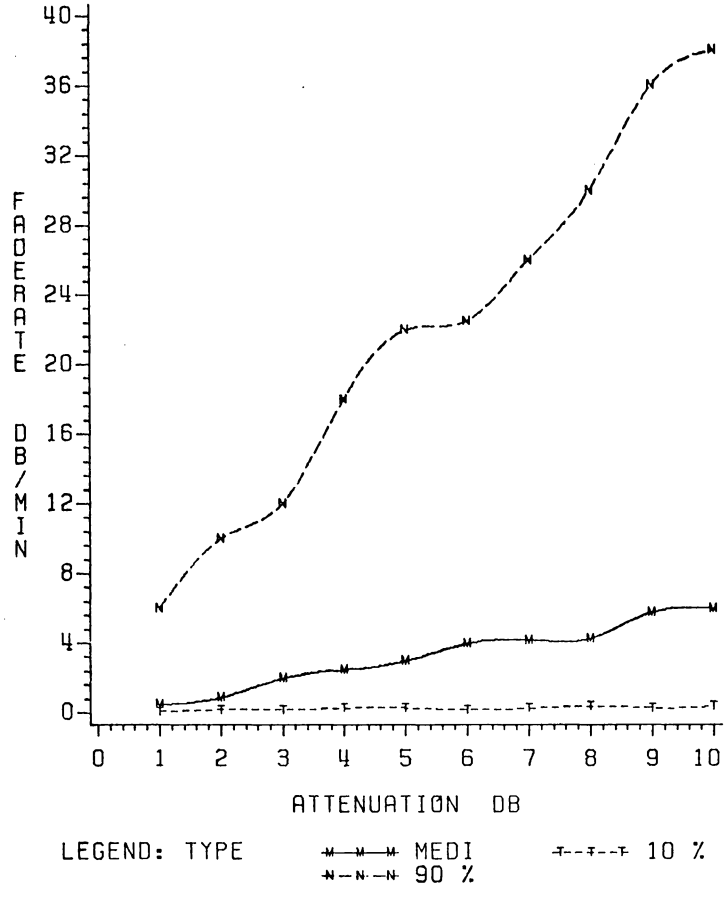

Figure 5.13. Faderate vs. attenuation, 10th, median. and 90th percentiles, 28 GHz input, June 1977- May 1979

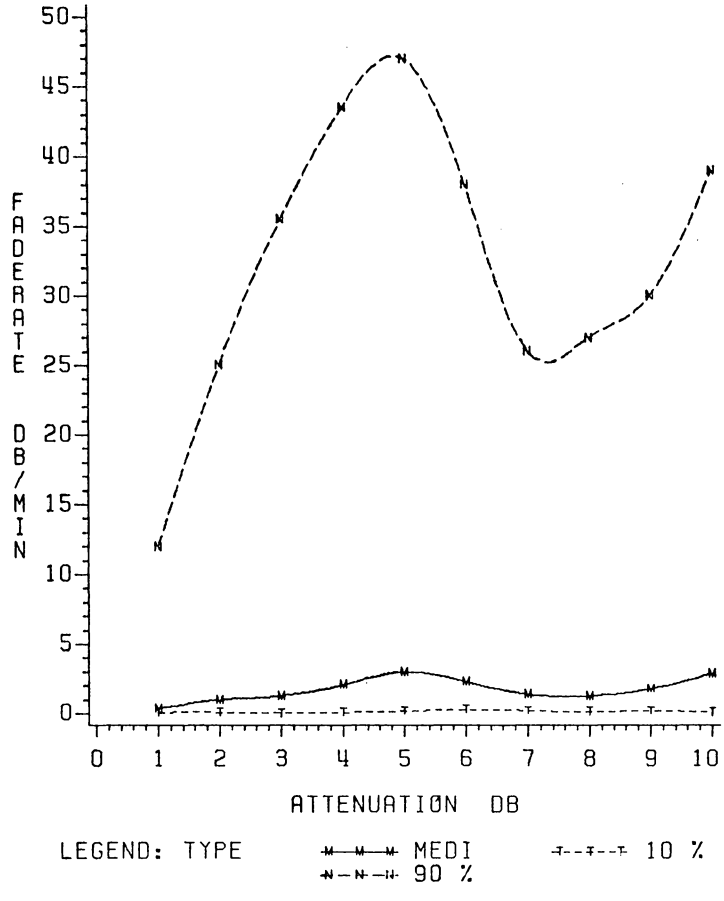

Figure 5.14. Faderate vs. attenuation, 10th, median, and 90th percentiles, 28 GHz input, June 1978- May 1979.

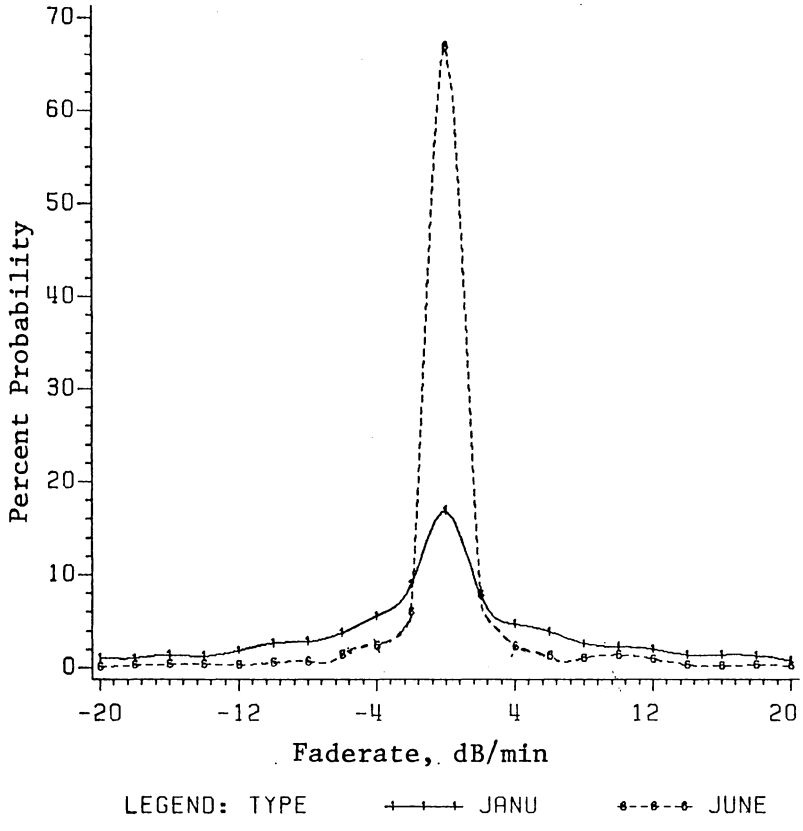

Figure 5.15. Percentage of faderates with given magnitude, 19 GHz input, January 1978 and June 1978.

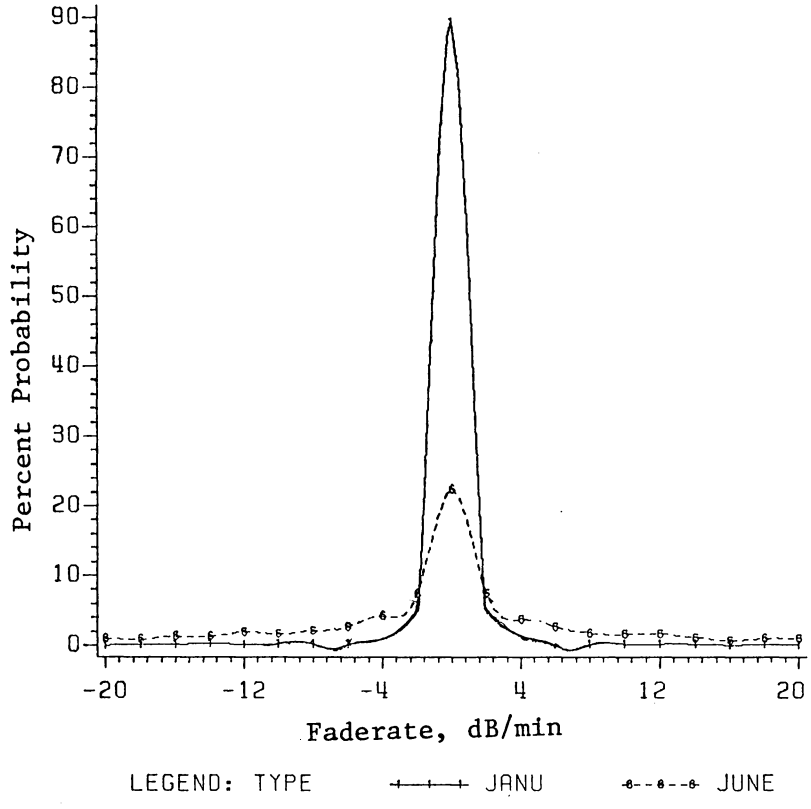

Figure 5.16. Percentage of faderates with given magnitude, 28 GHz input, January 1978 and June 1978.

tion immmediately preceeding the current sample, together with the current sample, are used to predict the next sample value. Any error in this predicted value is incorporated into the next predicted value. Faderate statistics could be used in the prediction process, however, an in-depth study of this method is beyond the scope of this thesis.

Another parameter which is strongly correlated with attenuation is rainrate. Theoretically, if a suitable attenuation model based on rainrate were developed, the time derivative of this model could give an accurate prediction of faderate and attenuation using a predictor-corrector type of operation. However, this approach has some practical contraints which tend to limit its effectiveness. The most accurate attenuation models which have been developed thus far (See [10] for a review of attenuation modelling.) are essentially statistical artifices with only secondary physical significance. There is little reason to expect the time derivative of such a model to have any real meaning. Another problem with this approach is the difficulty involved in obtaining an accurate measurement of the effective path rainfall rate. This can be done quickly and accurately using a meteorological radar, but this technique is not usually feasible. An attempt was made during the researching of this thesis to determine faderates using the time derivative

of the attenuation model given by Stutzman and Dishman (see [10]) with rainfall data collected at Blacksburg. This method gave poor results and is not presented here. The predictor-corrector stochastic model discussed previously appears to be the most promising method for modelling faderate.

5.4 EXPLANATION OF RESULTS

As stated previously, the relationship between mean faderate and attenuation is essentially lognormal up to about 10 dB of attenuation, beyond which it weakens considerably (particularly at 19 GHz). This behavior can be explained by examining the physical processes involved. As the fade depth exceeds 10 dB, the signal begins to fluctuate more rapidly, producing higher faderates. However, as the fade approaches its maximum depth, the faderate must decrease and eventually equal zero before fade recovery begins (This must always occur when a continuous function passes through a minimum or maximum.). Since fades have a strong tendency to reach their maximum depth at 10 dB or greater, the data at these thresholds are rather unstable, consisting of an almost random scattering of high and low faderate values. These factors combine to weaken any functional relationship between faderate and attenuation above 10 dB. For shorter

time periods (one month or less), the data set is actually more stable beyond 10 dB, with the mean faderate values tending to decrease in magnitude above this threshold. This is to be expected since all fades during a short time span will tend to reach approximately the same maximum depth, and near maximum depth the faderate values tend to lie near zero. When several events of similar depth and duration are analyzed, the resulting faderate versus attenuation curve resembles the derivative versus function value curve for a Gaussian distribution. This suggests that, with respect to time, a rain attenuation event can be modelled with reasonable accuracy by a Gaussian time distribution (or an amplitude weighted and time shifted sum of several Gaussians). This property will be taken advantage of later in the analysis of the effects of noise on faderate measurement.

5.5 FREQUENCY DEPENDENCE OF FADERATE DATA

Since rain attenuation is frequency dependent, one should also expect faderates to be frequency dependent. At a given instant during an event, the 28 GHz attenuation and faderate will be about twice the attenuation and faderate on the 19 GHz link (for equal path lengths and elevation angles). However, for equal values of attenuation, the faderates will be nearly equal, since a higher rainrate is needed on the 19

GHz link to produce the same amount of attenuation. The faderate versus attenuation curves for the two frequencies are similar, as can be seen in figures 5.1 and 5.3.

Chapter VI

EFFECTS OF SAMPLING RATE ON FADERATE STATISTICS

6.1 FACTORS AFFECTING SAMPLING RATE

According to the Nyquist sampling theorem, in order to reconstruct a bandlimited signal from its samples, the signal must first be sampled at a minimum rate of twice the highest information frequency contained in the signal. However, in order to reconstruct the derivative of a signal using a piecewise linear approximation, sampling must be done at several times the Nyquist rate. No formal criteria exist for determining this rate other than the specification of some desired error bound on the derivative measurement. For deterministic signals, this is a straightforward procedure, but for random signals such as fade events, one has no prior knowledge about the instantaneous behavior of the signal. If preexisting propagation data from the link are available, the signal can be described probabilistically, and a "worst case" design approach can be taken.

In reality, signals are never exactly bandlimited, since some noise will always be present. An accurate statistical description of this noise may be quite difficult to obtain, and derivative evaluation from samples is extremely sensitive to the presence of noise. As a noisy signal is sampled

faster, more noise power is aliased back into the information band. If consecutive samples are corrupted by noise, then the error in the derivative measurement will decrease as the sampling rate increases (the denominator of the $\Delta s/\Delta t$ term increases). The sampling rate which must be used is then a tradeoff between one which minimizes the derivative error caused by noise, and one which gives adequate resolution of the higher frequency components of the signal. This frequency is linked to the Nyquist frequency.

This presents a much simpler approach to determining the appropriate sampling rate than performing a probabilistic error analysis. The Nyquist frequency can be determined by performing a spectral analysis on uniformly sampled event data, and the sampling rate for derivative measurements can be set somewhat arbitrarily at several times the Nyquist rate. A factor of four was found to give good resolution in simulations using deterministic signals.

6.2 SPECTRAL ESTIMATION AND SAMPLING RATE LOWER BOUNDS

In order to perform a spectral estimate on discrete data, the samples must be available at uniform intervals. The Virginia Tech data were not collected in this manner, but a reasonably accurate spectral estimate can still be obtained by interpolating between samples to obtain an effective uni-

form sampling rate. This is justified for the following reason: to reduce the size of the data base, a uniform signal change interval of 0.7 dB was used rather than a uniform sampling rate. This means that the amount of uncertainty in the signal amplitude between samples is bounded by $2\Delta S=1.4$ dB. Since the fundamental sampling rate for the Virginia Tech data is 1 sec., it is desireable to have samples available every second. This algorithm is illustrated in figure 6.1. The sample error using this method will be plus or minus 0.7 dB, giving a maximum faderate error of 1.4 dB per second, or 84 dB per minute. While this amount of error appears to be large, an amplitude probability distribution for June 1978 showed that faderates of this magnitude account for less than 1.2% of the event time samples at 19 GHz, and less than 0.3% of the samples at 28 GHz (see figures 5.15 and 5.16). This particular month contains some of the most severe attenuation events of the entire two year period under consideration, so the above percentages probably represent a worst case scenario. During this same month, nearly 60% of all faderate samples had magnitudes of 10 dB per minute or less. This suggests that the amount of error introduced by using linear interpolation to replace missing samples is negligible with the type of data acquisition employed at Virginia Tech. The net effect is that small-am-

plitude, high frequency noise is filtered out of the signal, and unrealistically large values of faderate are eliminated from the data set.

This algorithm was applied to the reconstructed receiver input for several severe fade events, and a spectral estimator was then applied to the data. The estimator which was used is available as a library routine from the SAS Institute [12], and uses a variation of Singleton's method of averaged periodograms.

A brief discussion of digital spectrum estimation will now be given. For a more detailed analysis of the subject, the interested reader should see [13] and the references cited there.

The periodogram of a sequence of data is defined as

$$I_N(w) = \sum_{m=-(N-1)}^{N-1} c_{xx}(m)\, e^{-jwm}$$

where $c_{xx}(m)$ is the biased autocorrelation estimate, given by

$$c_{xx}(m) = \frac{1}{N} \sum_{n=0}^{N-|m|-1} x(n)x(n+m)$$

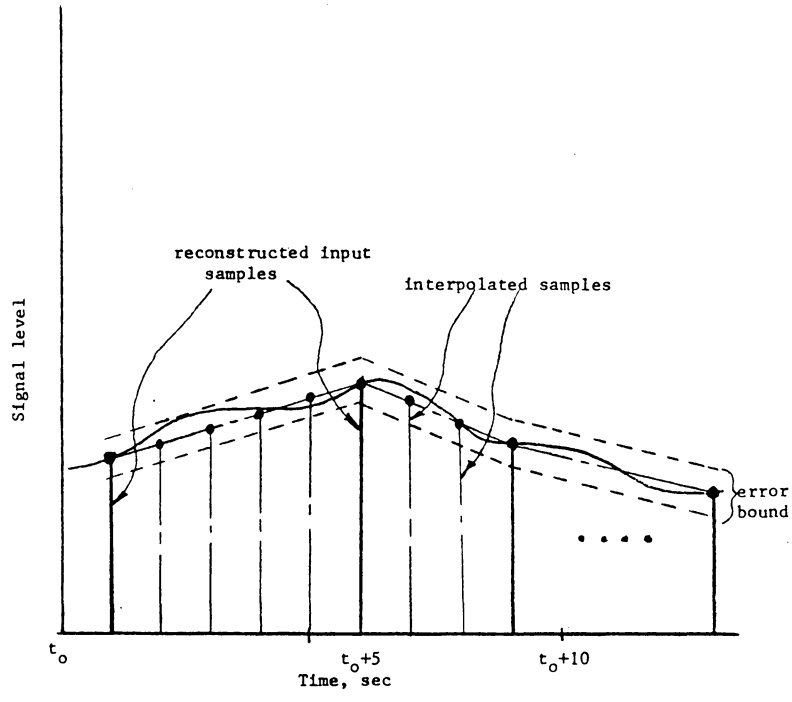

Figure 6.1. Illustration of the sample interpolation algorithm.

The autocorrelation sequence thus indicates the amount of variation between samples in the sequence x(n).

Writing the discrete Fourier transform of X(n) as

$$X(e^{jw}) = \sum_{n=0}^{N-1} x(n)e^{-jwn}$$

the periodogram can be written as

$$I_N(w) = \frac{1}{N} \sum_{m=-(N-1)}^{N-1} \sum_{n=0}^{N-m-1} x(n)x(n+m)e^{-jwm}$$

$$= \frac{1}{N} \left| X(e^{jw}) \right|^2$$

Hence $I_N(w)$ represents the power spectrum estimate of the random sequence x(n).

Two important indicators of the accuracy of a spectral estimate are its bias and its variance. The bias is the difference between the actual value of the spectral density component, and the mean value given by the estimator. The variance is defined as the mean of the square error of the estimator.

The drawback to using $I_N(w)$ as the spectral estimate of x(n) is that it is an inconsistent estimator; that is, the bias and the variance do not approach zero as the number of observations in the data set becomes large (The derivation of this property involves some advanced concepts in digital signal processing and will not be presented here. See [13].).

In order to reduce the variance of the estimator, the data sequence x(n) can be divided into a number of segments, the estimate for each segment can be computed, and several independent estimates can then be averaged together. The averaging is accomplished by convolving the periodograms with an appropriate window function. The choice of window shape and width is somewhat arbitrary: it must be narrow enough so that true variations in the spectrum can be adequately resolved, but wide enough so that the variance of the estimate is acceptable.

For the purposes of this study, it is desireable to have good resolution rather than minimal variance, since we are not interested in the spectral density per se, but rather in determining at what frequency the signal can be considered band limited. For this reason, the width of the weighting function was chosen as 1% of the length of the data sequence. Since the data sequences generally consisted of

over 1000 samples, this width should still yield an acceptable variance. The results were not particularly sensitive to the shape of the window; triangular and rectangular windows were used with little difference in the results.

Figures 6.2 and 6.3 show the results obtained for two severe fade events. As can be seen, the spectrum is essentially bandlimited to a period of 130 sec. This corresponds to a Nyquist sampling rate of approximately 65 sec. This is the minimum sampling rate which would permit reconstruction of the original waveform. The spectrum cutoff was chosen as -40 dB because this is the signal-to-noise ratio of the Virginia Tech receiver, and because the resolution of the estimator is rather poor below this level. However, to accurately approximate the derivative, sampling must be done at several times the Nyquist rate. Simulations using periodic signals have shown that the sampling rate should be at least three times the Nyquist rate, but this is a somewhat arbitrary function of how much resolution is desired.

From the foregoing discussion, we now have a practical lower bound on the sampling rate which should be used in the measurement of faderate data. The results suggest that this lower limit should be in the vicinity of 15 to 20 sec. This may vary with the climate at the earth terminal. In areas experiencing less intense rainfall, longer sampling inter-

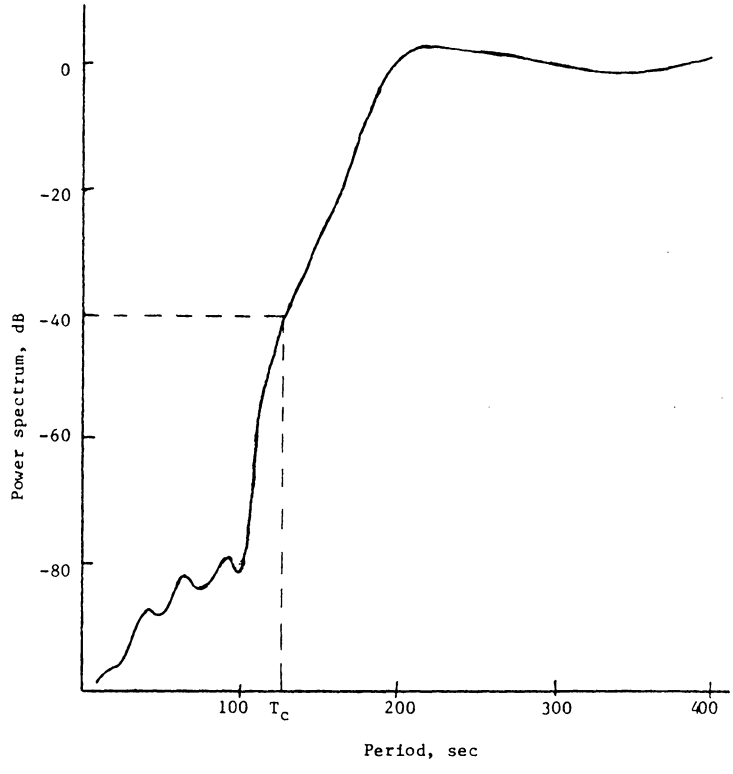

Figure 6.2. Spectral estimate of event of June 19, 1977.

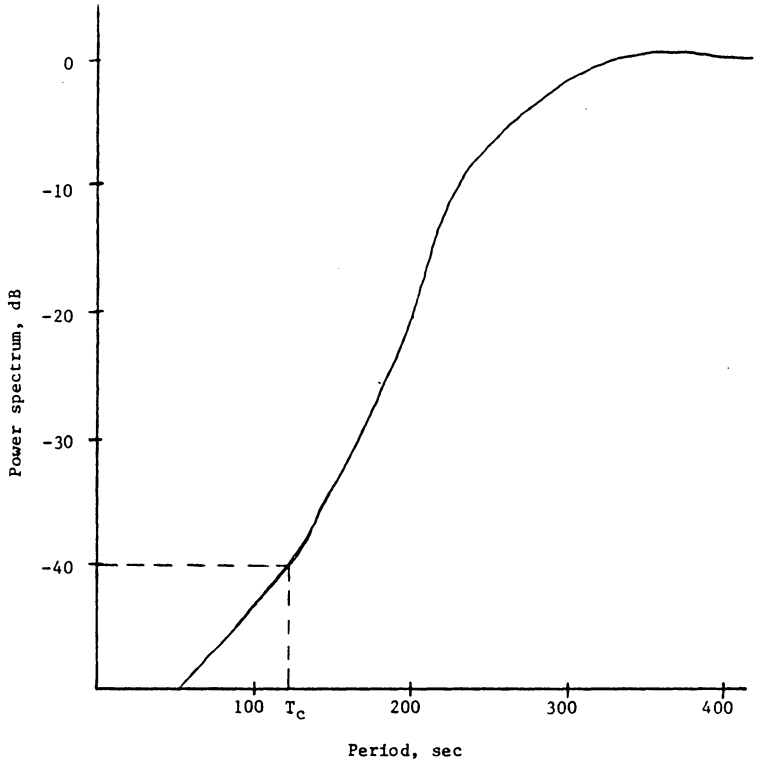

Figure 6.3. Spectral estimate of event of June 1, 1977.

vals could be used. Sampling could theoretically be done at an arbitrarily high rate, yielding better resolution of the derivative, but the data base would soon grow to unmanageable proportions, and the previously stated problems with noise would arise. Therefore, in order to determine the upper limit on the sampling rate, the effects of noise must be examined.

Chapter VII

THE EFFECTS OF NOISE ON FADERATE MEASUREMENT

7.1 TIME MODELLING OF FADE EVENTS

We will now examine the effects of noise on the measurement of the derivative of a signal, and will use the results to determine the upper bounds on the sampling rate needed for accurate faderate measurement.

A rigorous analytical approach to this problem would involve describing the received signal, with its additive noise, in an accurate, probabilistic sense. This is a complex problem in stochastic signal processing, which is further complicated by the nonstationary behavior of rain attenuation. That is, the statistical properties of attenuation vary with time in a very complicated manner. Even if this were done, one would have no information about the instantaneous behavior of the signal, thus it would not be possible to obtain accurate statistics on the instantaneous value of the derivative, or on the effects of different sampling rates.

A much simpler approach is to model a fade event using some deterministic signal. This signal can be sampled at different rates with various amounts of noise power added. The faderate statistics for this signal can then be computed

in a manner similar to that used for actual data. This method has the additional advantage that statistics can be computed for the noise-free case, assuming that the effects of finite word length in the computer are negligible. The effects of sampling rate and noise can then be accurately quantified by comparison with the ideal case. This cannot be done with actual data, since no noise-free analogy exists.

One approach to modelling the time history of a fade event is to curve fit actual data using numerical techniques. However, the essentially random behavior of the signal during a fade event makes this method rather complicated. Also, the interest is in the effects of sampling rate and noise, not in the accuracy of the curve fit. A simpler alternative is to model the fade with an amplitude weighted and time shifted sum of Gaussian time distributions. Other distributions which resemble fade events could also be used, but these time distributions should not be confused with the density functions of probability theory. Using the Gaussian time distributions, we can write the attenuation as

$$S(t) = S_{ref} - \sum_{n=1}^{N} A_n e^{-\gamma_n (t-t_n)^2}$$

where S_{ref} is the clear weather signal level. The selection of the constants A_n, η_n, N, and t_n is somewhat arbitrary, but can be done so that the depth and duration of the hypothetical fade closely match those of an actual fade. The signal S(t) can then be sampled every W seconds, generating the discrete sequence s(k) given by

$$S(k) = S_{ref} - \sum_{k=0}^{T} \sum_{n=1}^{N} A_n e^{-\eta_n (Wk - t_n)^2}$$

where T equals the fade duration in seconds, assuming that the fade begins at time k=0. The derivatives are then approximated by

$$\frac{dS}{dt} = \frac{\Delta S}{\Delta t} = \frac{S(i) - S(i-1)}{t_i - t_{i-1}}$$

with corresponding attenuation value

$$A = S_{ref} - \frac{1}{2}(S(i) - S(i-1))$$

The faderate statistics are then computed in the manner described previously.

7.2 MODELLING WITH NOISY SIGNALS

The next step in this procedure is to add Gaussian noise to the time sequence s(k) using a random number generator:

$$S_n(k) = S_{ref} - \sum_{k=0}^{T} \left\{ \sum_{j=1}^{N} A_j e^{-\gamma_j (Wk-t_j)^2} + V_n (R_k - \tfrac{1}{2}) \right\}$$

where R_k is a psuedorandom number with values between 0 and 1, with a Gaussian probability density. V_n is the RMS noise voltage, thus the clear weather signal-to-noise ratio (SNR) is given by

$$SNR = \frac{S_{ref}}{V_n}$$

The faderate statistics are computed in the usual manner for the noisy signal $s_n(k)$.

It is usually more convenient to express the above quantities in terms of decibels; for ease of computation, the attenuation can be referenced to a clear weather level of unity (0 dB). Assuming the A_j's are now in terms of decibels, $s_n(k)$ becomes

$$S_n(k) = -20\log_{10}\left[10^{\left\{ \sum_{k=0}^{T} \sum_{j=1}^{N} A_j e^{-\gamma_j (Wk - t_j)^2} \right\}/20} + \sum_{k=0}^{T} V_n (R_k - \tfrac{1}{2}) \right]$$

and the SNR in clear weather is simply

$$SNR = -20\log_{10}V_n$$

This will yield faderate statistics in terms of dB per second.

7.3 SIMULATION RESULTS

As a simple example, let N=1, A_1=20, η_1= , and t_1=2000. For a 30 dB SNR,

$$V_n = 10^{-SNR/20} = 0.0316$$

The results for the noise-free case are shown in figures 7.1 and 7.2 for 1, 5, and 30 sec sampling rates; note that there is no sensitivity to the sampling rate for the noiseless derivative. Figures 7.3 and 7.4 show the results for the same signal, but with the noise added. There is a distinct dependence on sampling rate for this case, particularly at the higher attenuation values where the SNR is poorest.

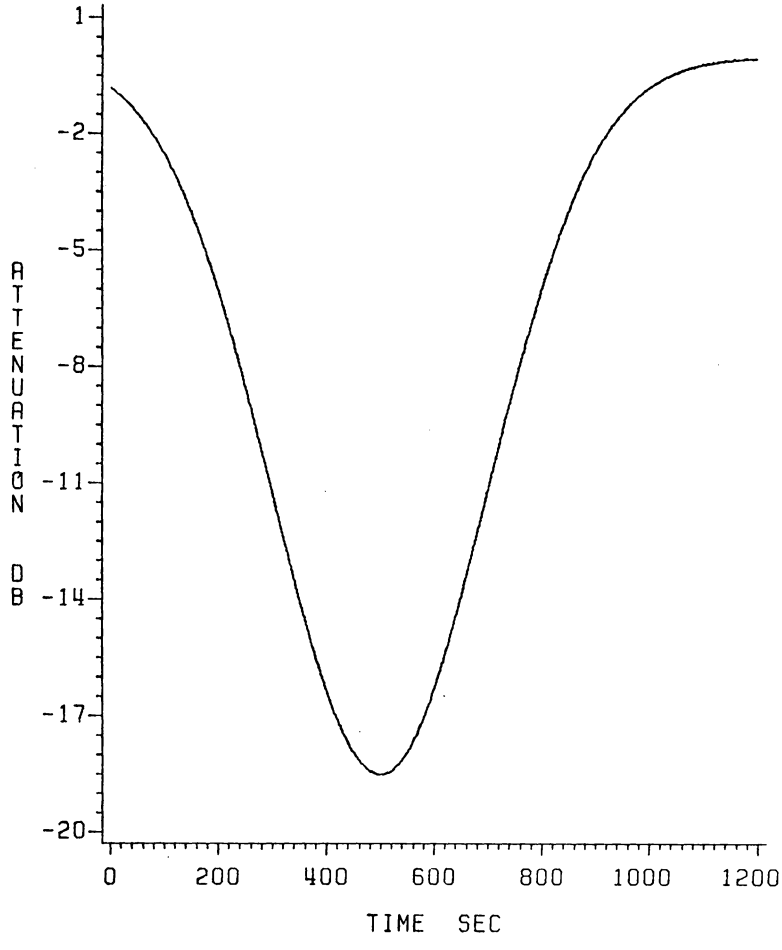

Figure 7.1. Signal level vs. time, noiseless Gaussian.

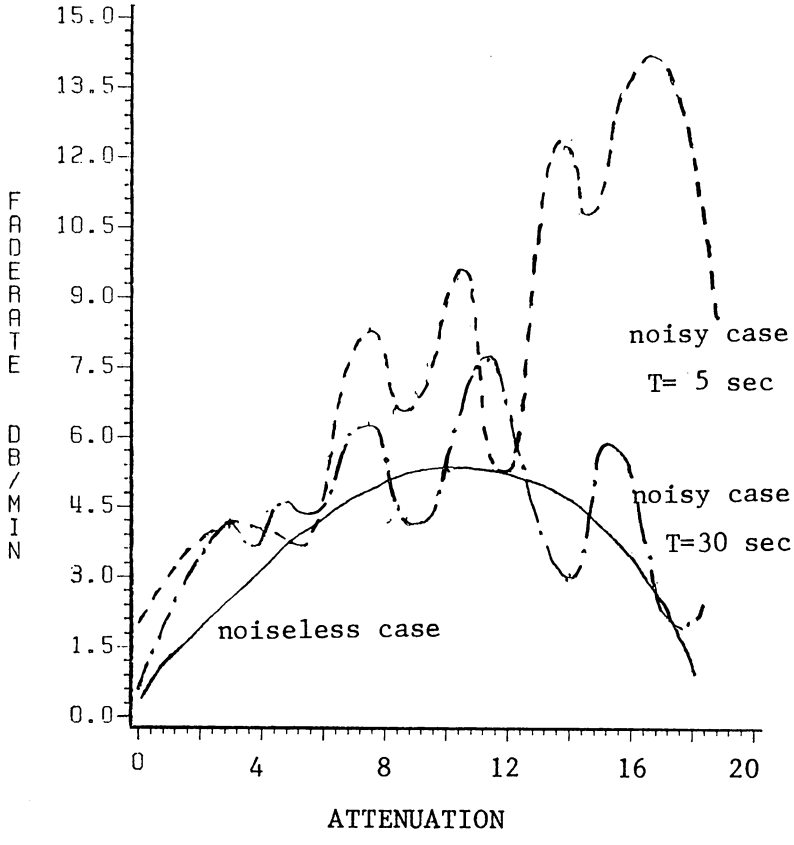

Figure 7.2. Faderate vs. attenuation statistics for figure 7.1; results for the noisy case approach those for the noise-free case as the sampling interval increases.

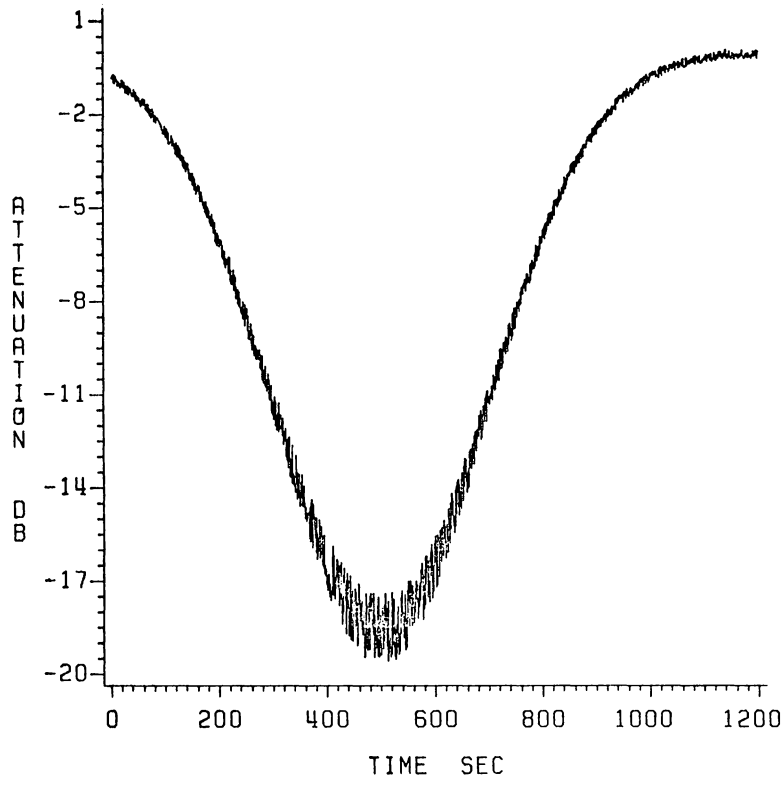

Figure 7.3. Signal level vs. time, noisy Gaussian; SNR=30 dB.

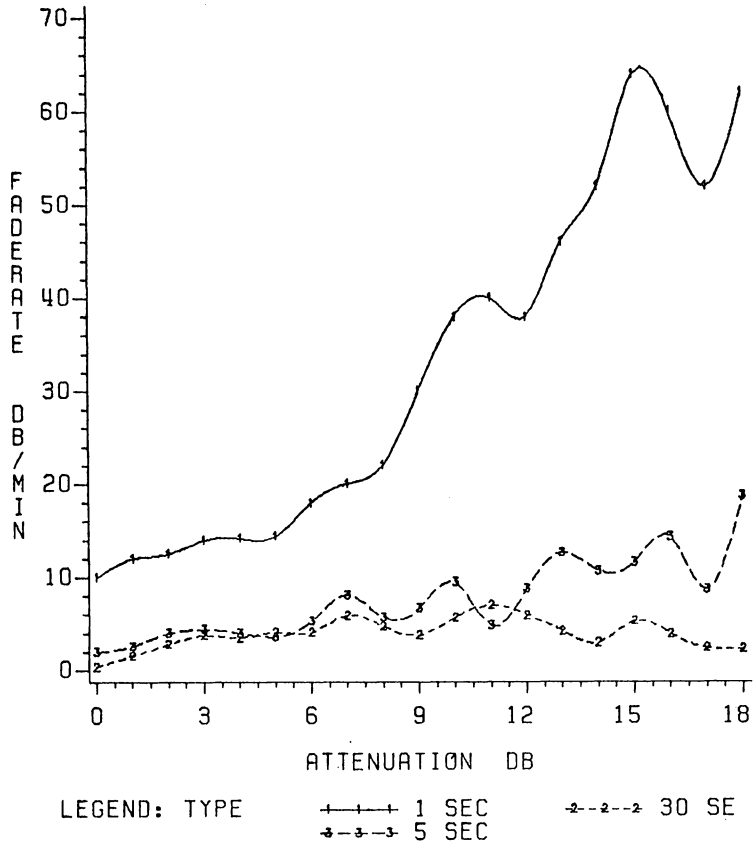

Figure 7.4. Faderate vs. attenuation statistics for figure 7.3; note that sensitivity to sampling rate decreases as the sampling interval increases.

These figures also illustrate the behavior of the statistics near maximum fade depth. The mean values of faderate tend to decrease due to the presence of a number of zero and near-zero values of the derivative as the signal passes through a minima. However, the combination of high sampling rate and poor SNR weaken the statistical relationship between faderate and attenuation near maximum fade depth. Up to this threshold, the relationship is nearly lognormal, as it was with actual data. This provides some justification for using the simulation, and demonstrates the sensitivity of faderate statistics to sampling rate and noise.

These results also seem to suggest that the physical process of rain attenuation is Gaussian (or some similar distribution) in time and is corrupted by Gaussian noise. This noise may be thermal or quantization noise contributed by the demodulating and data acquisition equipment, or it may be psuedonoise. That is, the randomness of the signal fluctuation during a fade due to actual variations in rainrate may simply look like Gaussian noise. Dynamic modelling of attenuation is beyond the scope of this thesis, but further investigation is warranted. The interested reader may consult [14] for more information.

Before investigating noise and sampling rate effects in actual data, it may be useful to examine a somewhat more complicated deterministic model. For this example, let N=9, SNR=40 dB, with the constants η_j, t_j, and A_j as given in table 7-1. The spectral estimate of this signal, shown in figure 7.5, indicates a Nyquist sampling interval of 200 sec. Hence, a sampling interval of 50 sec would be required for reasonably accurate measurements of the derivative. Figure 7.8 shows the faderate vs. attenuation statistics for this signal at 1, 5, and 30 sec sampling rates.

The behavior of these curves is very similar to the previous example, the dependence on sampling rate being almost linear, and the mean faderate decreasing in magnitude near maximum fade depth. At the 30 sec sampling rate, the results are close to the noiseless case shown in figure 7.9. These curves show that there is a range of sampling rates over which the measured value of the derivative of a noisy signal is dependent on the sampling rate. As the sampling rate decreases or the SNR increases, the amount of error in the derivative measurement decreases. The sampling rate at which the error reaches an acceptable level will be several times the Nyquist rate.

The error in the derivative can be quantified as follows (see figure 7.10). Let the faderate of a noiseless signal be given by

$$FR_o = \frac{S_2 - S_1}{t_2 - t_1}$$

Table 7-1. List of constants used for the signal shown in figure 7.6.

j	A_j	η_j	t_j
1	18.5	-1.25×10^{-5}	500
2	-11.0	-6.0×10^{-6}	575
3	17.0	-8.0×10^{-6}	750
4	15.0	-1.1×10^{-5}	1150
5	13.5	-6.0×10^{-6}	1750
6	12.0	-1.25×10^{-5}	2500
7	10.0	-1.0×10^{-5}	3075
8	-6.0	-4.0×10^{-6}	3400
9	15.0	-7.0×10^{-6}	3900

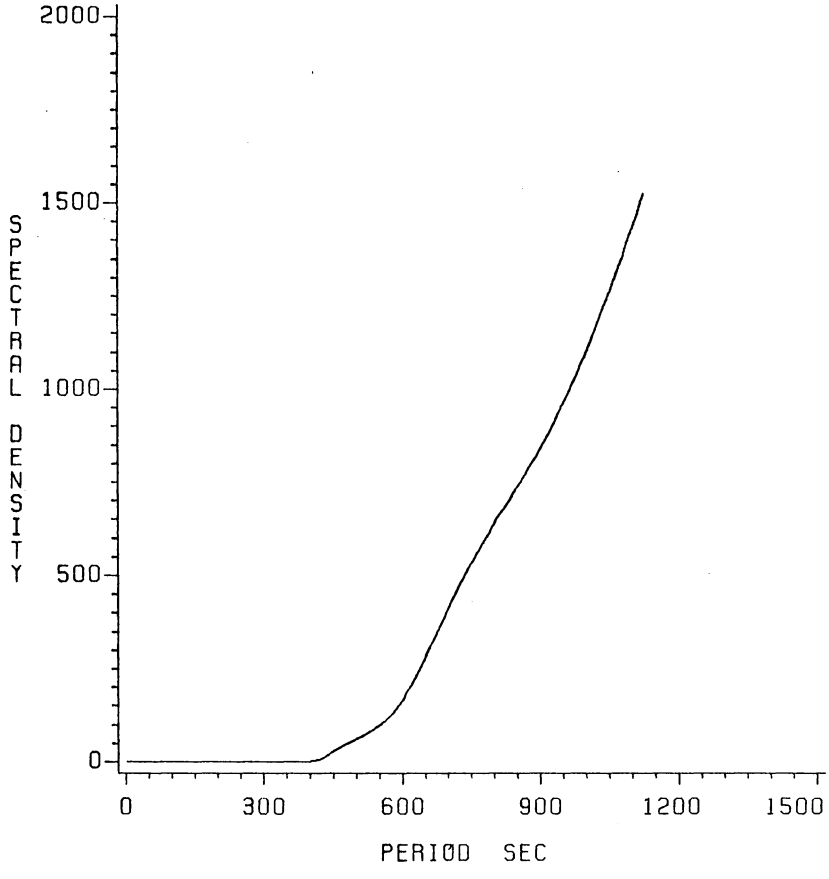

Figure 7.5. Spectral estimate of noisy signal shown in figure 7.7.

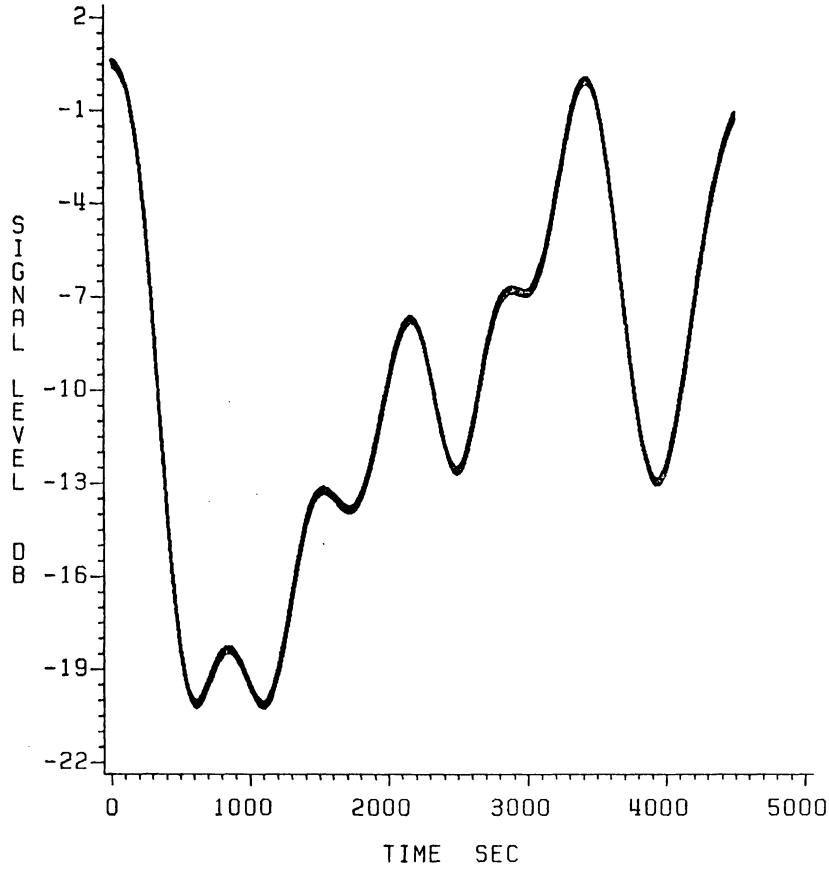

Figure 7.6. Signal level vs. time for noiseless Gaussians.

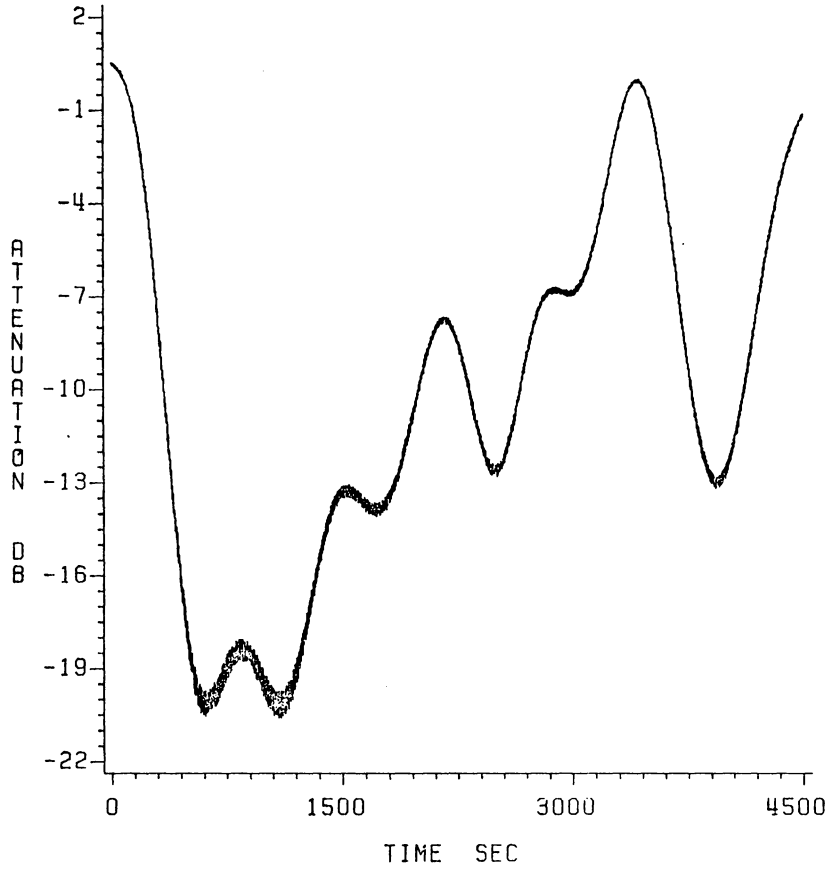

Figure 7.7. Signal level vs. time for noisy Gaussians; SNR=40 dB.

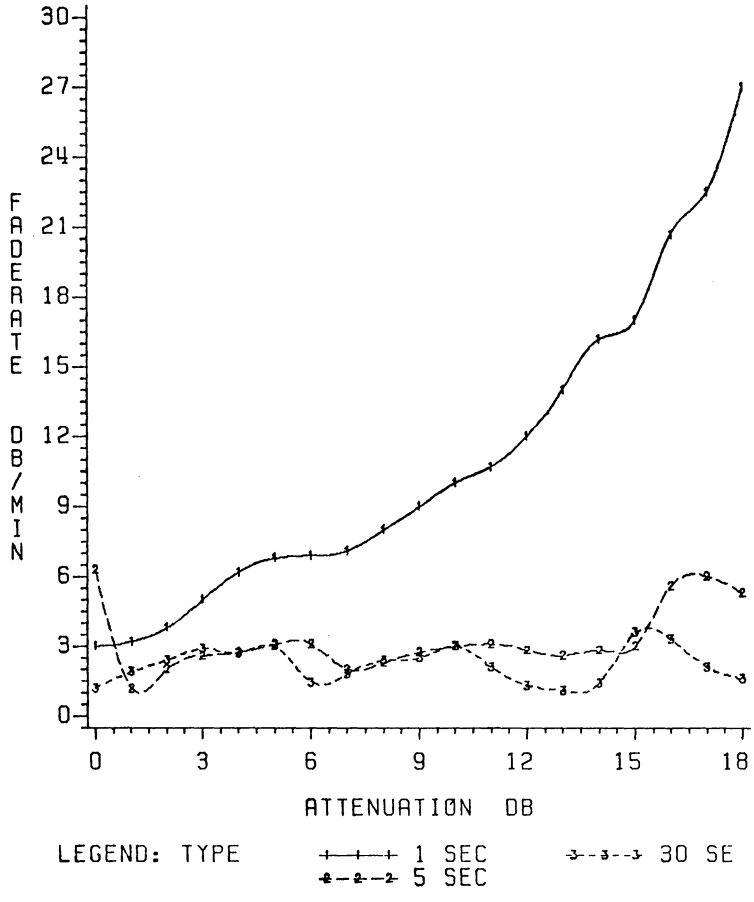

Figure 7.8. Faderate vs. attenuation statistics for noisy signal of figure 7.7; 1, 5, and 30 sec sampling rates. SNR=40 dB.

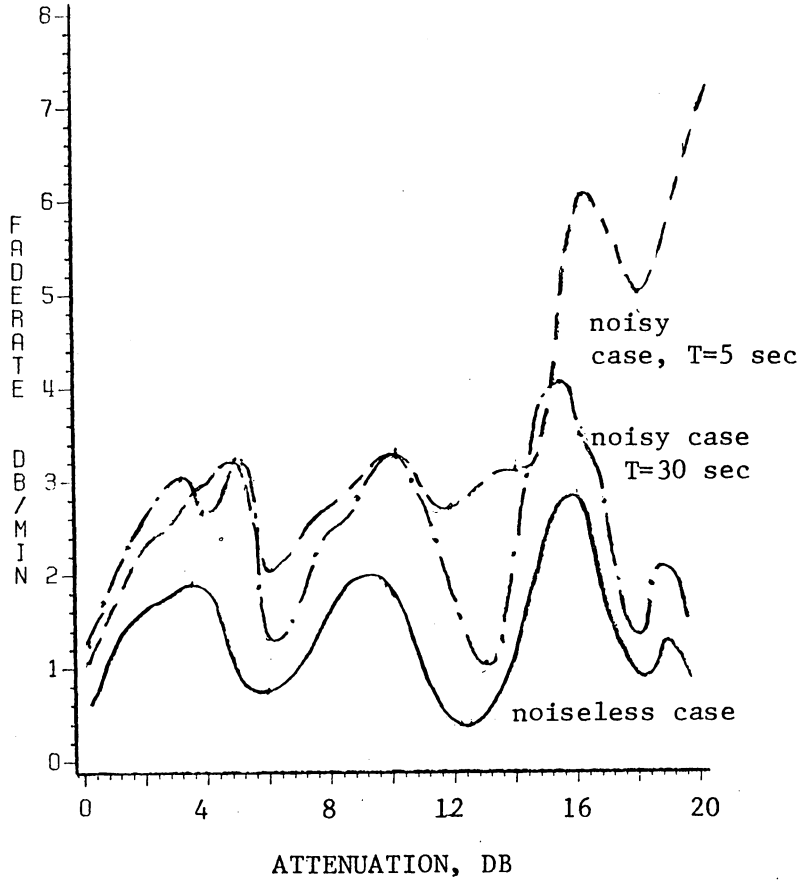

Figure 7.9. Faderate vs. attenuation statistics for the noiseless signal of figure 7.6 compared to the results for the noisy signal. Note improvement with longer sampling intervals.

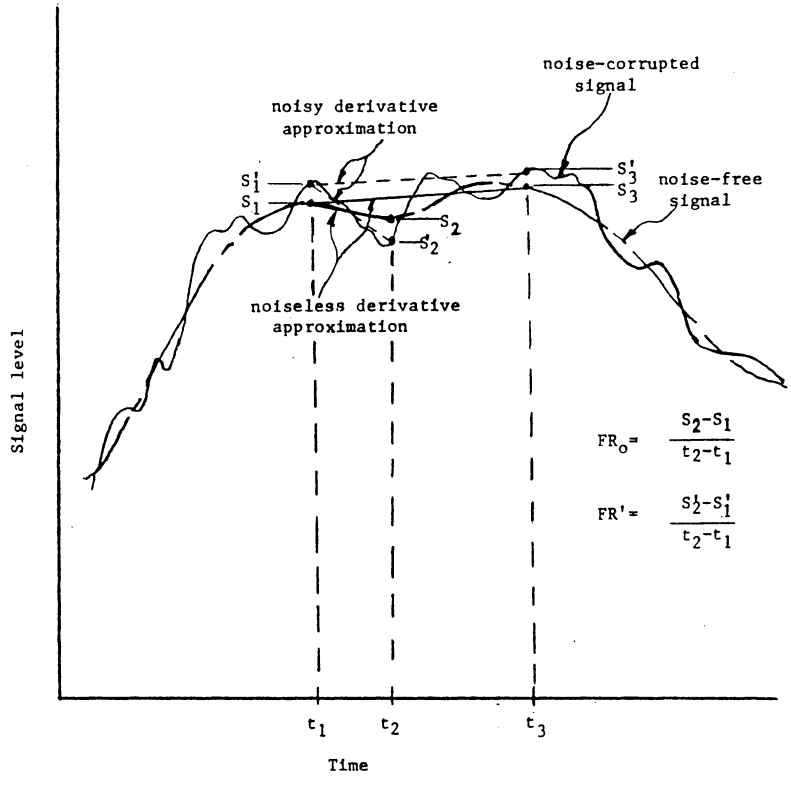

Figure 7.10. Illustration of the derivative error caused by noise-corrupted samples. Note improvement with longer sampling intervals.

If noise is added to this signal, the faderate will then be given by

$$FR' = \frac{S_2' - S_1'}{t_2 - t_1}$$

where the prime notation indicates a noisy sample of the signal. The worst case error occurs when

$$S_1' = S_1 \pm n'$$

$$S_2' = S_2 \mp n'$$

where

$$n' = \max |V_n (R - 1/2)|$$

Here, V_n is the RMS noise voltage, and R is a psuedorandom number on the interval (0,1), with a mean of 0.5. The maximum value of n' is

$$n_m' = V_n/2$$

The error in the derivative measurement is then given by

$$e = FR_o - FR'$$

$$= \frac{S_2 - S_1}{t_2 - t_1} - \left\{ \frac{(S_2' \pm n')}{t_2 - t_1} - \frac{(S_1' + n')}{t_2 - t_1} \right\}$$

$$= \frac{\pm n' \pm n'}{t_2 - t_1}$$

The maximum error is given by

$$e_{max} = \left| \frac{\pm n' \pm n'}{t_2 - t_1} \right|$$

$$= 2n'/(t_2 - t_1)$$

Defining the signal-to-noise ratio as

$$SNR = S_{ref}/V_n$$

where S_{ref} is again the clear weather signal level, we can write

$$n' = V_n/2 = S_{ref}/2SNR \qquad \text{or}$$

$$e_{max} = \frac{S_{ref}}{SNR}\left(\frac{1}{t_2 - t_1}\right)$$

If the signal levels are expressed in dB, then

$$e_{max_{dB}} = (S_{ref} - SNR)\left(\frac{1}{t_2 - t_1}\right)$$

From this, we can see that the error in the derivative measurement can be reduced by improving the SNR, or by effectively increasing the sampling interval.

Chapter VIII

THE EFFECTS OF SAMPLING RATE ON FADERATE STATISTICS

8.1 SAMPLING RATE CONVERSION

Using the reconstruction and interpolation algorithms described previously, samples of the receiver input signal can be obtained at 1 sec intervals. The effective sampling rate can then be changed by "combing" the discrete signal in time, that is, by retaining every nth sample, where n is the new sampling interval in seconds. Using the same procedure as before, the faderate statistics for the resampled signal are then computed.

Figure 8.1 shows the results of this procedure applied to the 19 GHz data for June, 1977, at several different sampling rates. Note that the data are sensitive to the sampling rate, but the dependence is not linear. Furthermore, this dependence nearly disappears for sampling intervals exceeding 5 sec. This suggests that the fading signal is being corrupted by broadband noise whose amplitude is quite small compared to the signal amplitude.

Since the statistics stabilize for for sampling intervals greater than 5 sec, the fading signal itself does not strongly resemble white noise. If this were the case, the

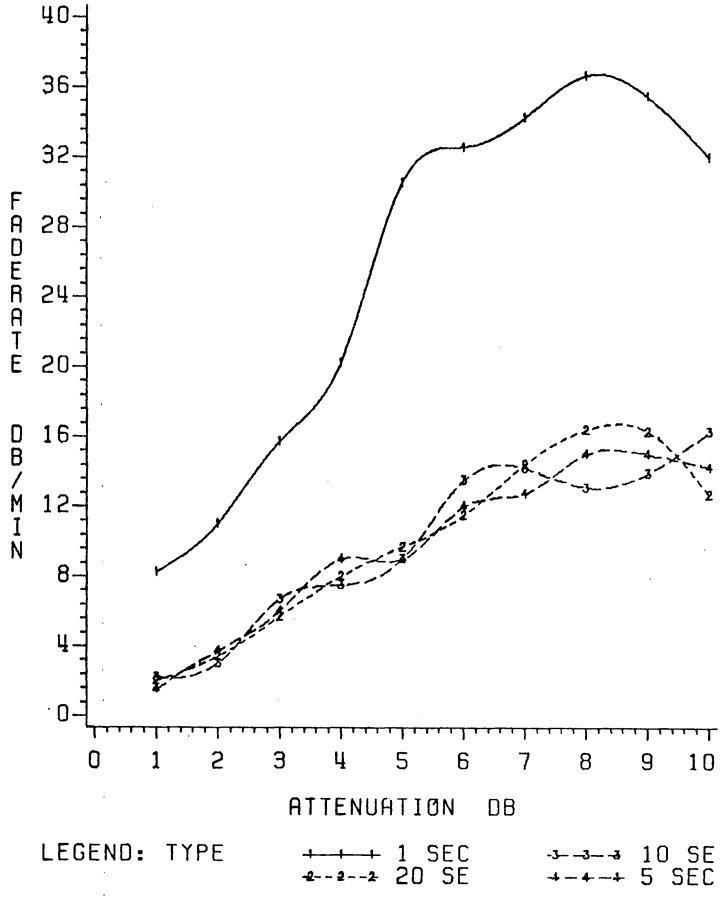

Figure 8.1. Faderate vs. attenuation, 19 GHz input, June 1977; 1, 5, 10, and 20 sec sampling rates.

faderate statistics would have a linear dependence on sampling rate, with no bounds on this behavior. This effect can be seen in figure 8.2, in which pure white noise has been sampled at several different rates. In this situation, the mean values of the piecewise linear derivative approximations depend linearly on sampling rate. Some of the white noise present in the signal may arise from scintillations; this effect is discussed briefly in [3].

Research indicates that this noise has three possible origins: 1) thermal noise introduced by the receiving equipment; 2) quantization noise introduced by the digitization and storage process; and 3) random but naturally occurring fluctuations in signal strength due to the physical structure of rain cells.

8.2 OVERCOMING THE EFFECTS OF NOISE

Sources 1) and 2) can be quantified with good accuracy. The Virginia Tech receivers were designed with clear weather SNR's of 40 dB, and measurements have confirmed this figure. In the simulation discussed previously, it was shown that for SNR's of this size, 1 sec sampling rates did not yield accurate faderate statistics. System thermal noise may therefore be a serious concern in determining the rate of change of attenuation. This difficulty could be overcome by

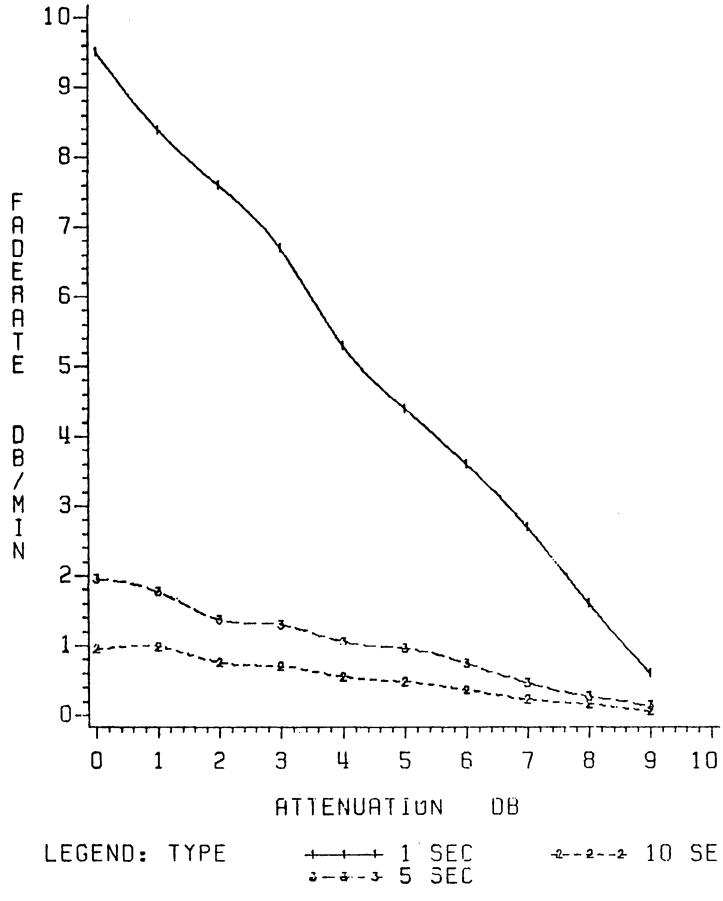

Figure 8.2. Faderate vs. attenuation, white noise at three different sampling rates.

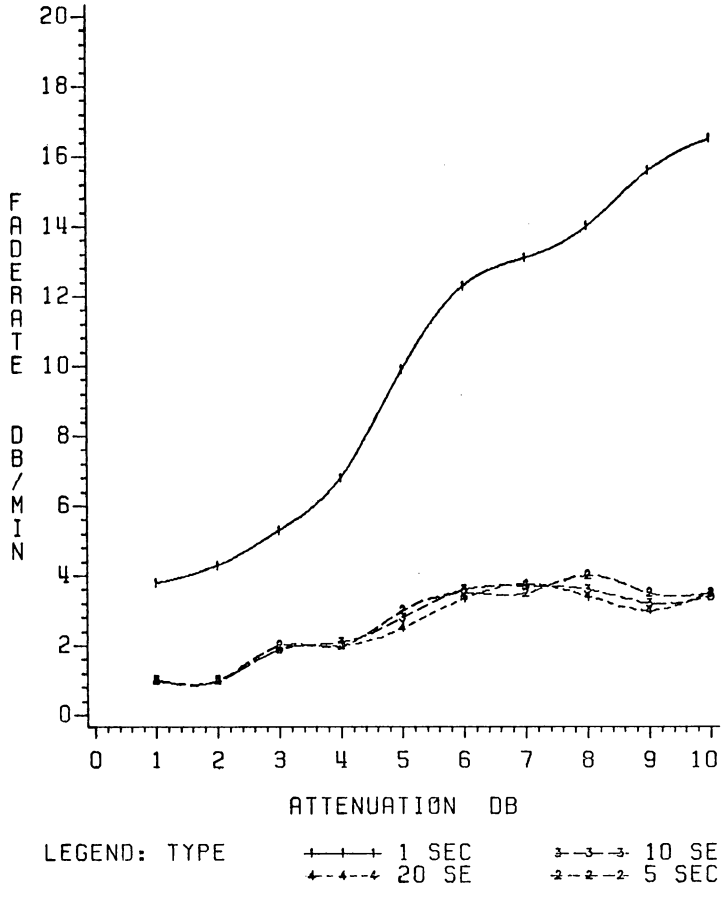

Figure 8.3. Fadrate vs. attenuation, 28 GHz input, June 1977; 1, 5, 10, and 20 sec sampling rates.

digitally filtering the signal, by using longer sampling intervals (5 to 20 sec), or by using a sample averaging (decimation) algorithm.

Digital filtering can be done in software, but may introduce more complication into the data acquisition system than is desirable. This is particularly true for systems in which many different parameters are monitored (such as at Virginia Tech). Also, since one has little a priori knowledge about the spectral content of the signal, selection of the filter cutoff frequency would be somewhat arbitrary. The filter passband must be narrow enough to filter out the noise, but wide enough so that information in the signal is not lost.

Use of longer sampling intervals is probably the simplest solution, although arriving at a suitable sampling rate would require some experimentation so that the desired amount of signal resolution is achieved. This also presents practical system design problems; in order to optimize the design of the downlink receiver and data acquisition system, the designer must have some information about the signal which is to be processed. It is difficult to design for a randomly fluctuating signal, particularly one which is significantly corrupted by white noise. In this situation, the goal of designing a system which will not bias the informa-

tion which it is intended to measure is difficult to achieve.

Sample averaging, or decimation, could be implemented in software with little difficulty, and it has the additional advantage that all forms of noise (including quantization noise) would tend to be averaged out of the data. Figure 8.4 shows faderate statistics for June 1977 at 19 GHz using 10 sample averaging of data which were sampled at a one sec rate. These results are similar to those obtained using longer sampling intervals. Also shown are statistics for 5 and 20 sec averaging, which are also in good agreement with the sampling rate conversion results.

It was stated previously that much of the noise present in the signal may simply be a natural consequence of the physical structure of rain, rather than system thermal noise. Even if this were the case, it would still be desireable to filter out these small amplitude, rapid fluctuations, since such fine control of transmitted power levels is neither practical or necessary.

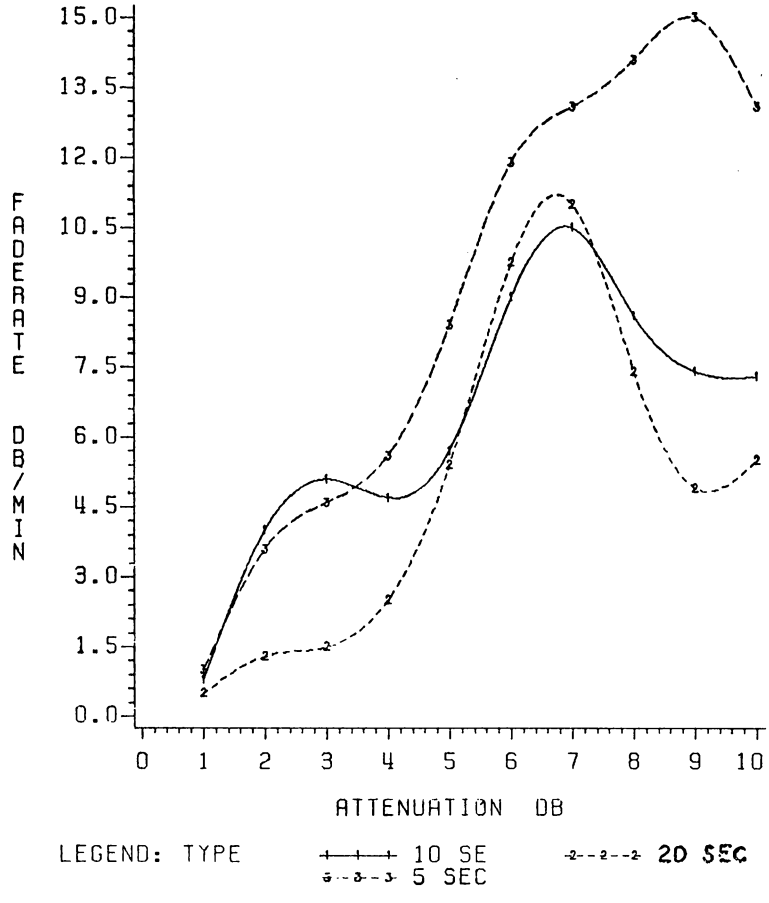

Figure 8.4. Faderate vs. attenuation, 19 GHz input, June 1977 using sample averaging.

8.3 ANALYSIS OF QUANTIZATION NOISE

The role of data acquisition system quantization noise will now be examined.

When an analog signal is input to a digital system, the process of quantizing the signal into discrete levels introduces white noise. If the quantization is coarse (the levels widely separated), this noise can become quite severe.

If the quantization levels are uniformly spaced, the signal-to -quantization noise ratio (SQNR) can be obtained straightforwardly. The final signal processing stage prior to digitization in the Virginia Tech receivers is a logarithmic amplifier whose output voltage (the control voltage of the pase-locked loop) varies from 0 to 5 volts. The characteristic equation of this amplifier is

$$P_{in}(\text{dBm}) = -0.904V^2 + 18.9V - 153.49$$

In clear weather, V=5 volts, and P_{in}=-81.54 dBm. The 5 volt spread is uniformly quantized into 255 levels, each level spanning 0.0197 volts. The SQNR is given by equation 3.1.2-3 (p. 89) of [15] as

$$\text{SQNR} = \frac{X_{rms}^2}{(\Delta^2/12)}$$

where X_{rms} is the RMS voltage of the signal being quantized. In clear weather,

$$SQNR = \frac{25}{(0.0197^2/12)} = 58.9 \text{ dB}$$

During a severe event, the PLL control voltage may go as low as 3 volts before lock is lost, so

$$SQNR \cong 55 \text{ dB}$$

This shows that the quantization noise is always considerably less than the system thermal noise (which is nominally 40 dB in clear weather), and therefore does not contribute significantly to the white noise problem.

Based on the foregoing discussion, we can conclude that in order to measure accurately the rate of change of attenuation on earth to space communication links, the signal should be sampled at intervals ranging from 5 to 15 sec. At intervals faster than 5 sec, system noise begins to bias the measurements. At intervals longer than 25 sec, resolution in the piecewise linear derivative approximation is lost.

The upper sampling rate bound will depend on the SNR of receiver being used.

When applied to actual adaptive power control systems, these bounds also lie within a practical range. In a computer simulation of the NATO satellite communication system, Ince, et al. (8), showed that a total loop delay of 10 sec could be expected in a typical earth terminal network. This loop delay includes time for measurement of signal parameters, path propagation delays, implementation of the control action, and verification of the control action.

Chapter IX

FADE DURATION AND INTERFADE INTERVAL STATISTICS

This chapter will present the statistics of fade event durations, and the duration of the time intervals between successive events. The same data base which was used previously will be examined.

9.1 DATA REDUCTION

In this thesis, a fade will be defined as the time that the received signal power stays below a given threshold. Using this definition, several deep fades can occur during the course of one long fade of shallow depth, and several fades may occur during a single storm (see figure 9.1). An interfade interval is defined as the time that the received signal power is above the threshold, before the onset of the next fade of the same depth. Data sets of one month were analyzed.

In addition to the above procedure, the data were processed using 1 dB of hysteresis. In other words, a fade was not terminated until the signal power had increased to 1 dB above the fade threshold. This procedure is probably more representative of actual system performance, since the pull-in range of phase- locked loops is generally less than

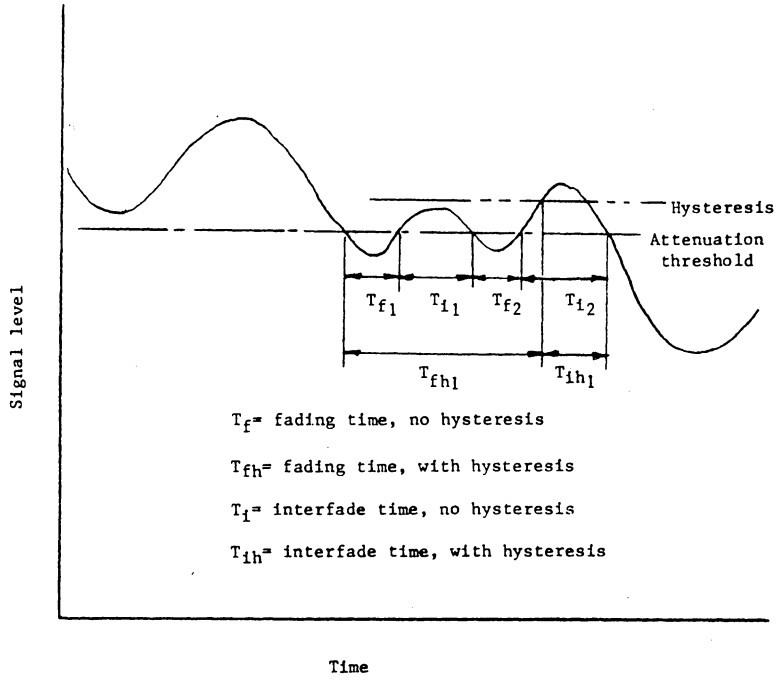

Figure 9.1. Illustration of the method for determining fade durations and interfade intervals.

the hold-in range. To reacquire the signal after loss of lock, the signal must be stronger than it was at the time lock was lost. Also, the accuracy with which the receiver can be calibrated and data samples measured and stored is several tenths of a dB.

In the analysis program (see appendices), data were first sorted into 1 dB bins over the attenuation interval 1 to 35 dB, in time-sequential order. Rather than having samples available for every 0.7 dB change in signal level, the data were processed so that samples were available every 30 sec. When the attenuation reached a given threshold, counters for that threshold were switched on. Each 30 sec interval that the signal remained below that threshold was then counted. When the signal rose above the threshold (1 dB above the threshold for the hysteresis case), the fade duration counters were switched off, and the interfade interval counters switched on. Interfade intervals ranging from 3 to 360 minutes (in 3 minute increments) were counted in the same manner as the fade duration intervals.

9.2 RESULTS OF THE STUDY

Statistics were compiled for two 12 month periods, June 1977 through May 1978, and June 1978 through May 1979. The yearly statistics were then combined together to produce the yearly average plots shown in figures 9.2 through 9.5.

The receiver time constants were not found to affect the fade duration statistics significantly. Since, in effect, we are trying to reconstruct the signal, not its derivative, the sampling rate need only satisfy the Nyquist criterion. The 30 sec sampling rate used in this phase of the study was found to satisfy the Nyquist criterion, yet yield receiver output samples which nearly equaled the true values. This can be seen from the reconstruction algorithm, using a 14 sec time constant (typical of the Virginia Tech receivers). Since $\Delta t = 30$ sec and $R/R_i = 1$, we have

$$v_i(t_1 + \frac{\Delta t}{2}) = \frac{-R}{R_i}\left(\frac{v_o(t_2) + v_o(t_1)}{2} + \frac{RC(v_o(t_2) - v_o(t_1)}{\Delta t}\right.$$

$$= -\left(\frac{v_o(t_2) + v_o(t_1)}{2} + \frac{14}{30}(v_o(t_2) - v_o(t_1))\right.$$

$$\cong -\frac{1}{2}(v_o(t_2) + v_o(t_1) + v_o(t_2) - v_o(t_1))$$

$$= -v_o(t_2)$$

$$\therefore \quad \left|v_i(t_1 + \frac{\Delta t}{2})\right| \cong \left|v_o(t_2)\right|$$

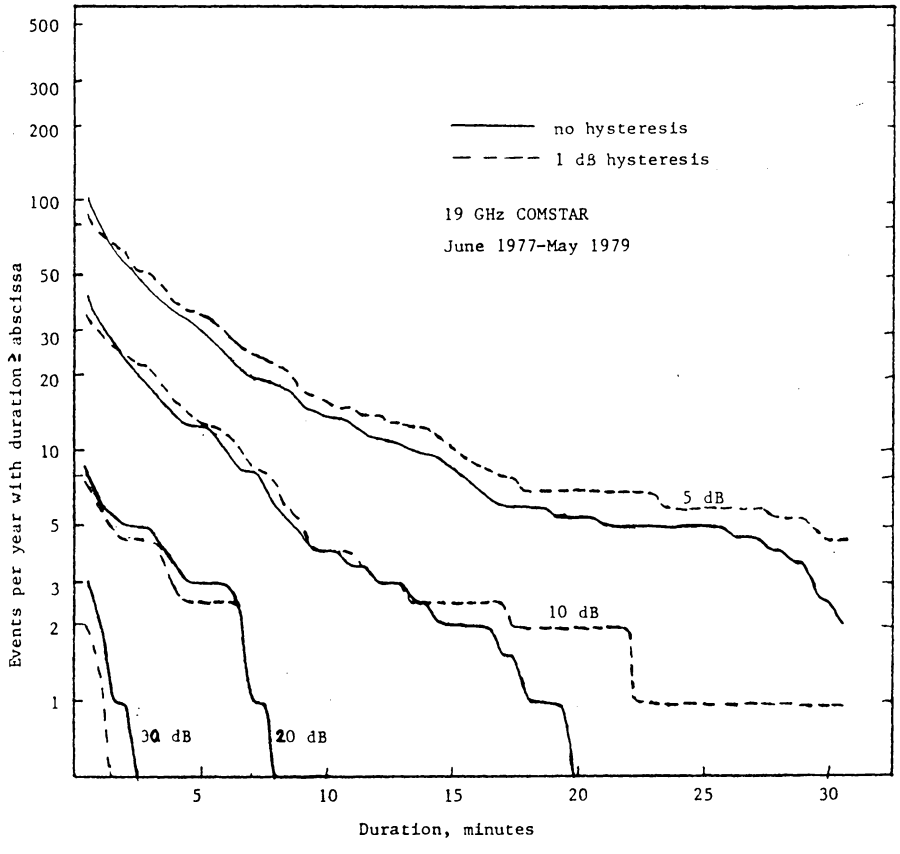

Figure 9.2. Events per year with given duration, 19 GHz, June 1977- May 1979.

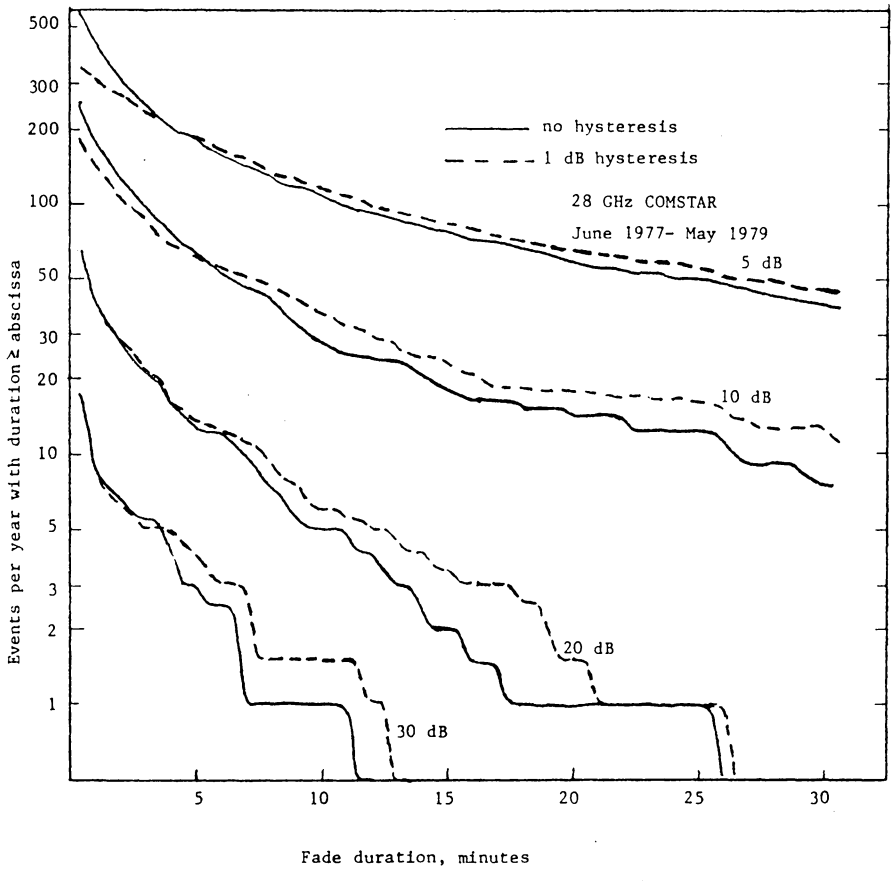

Figure 9.3. Events per year with given duration, 28 GHz, June 1977- May 1979.

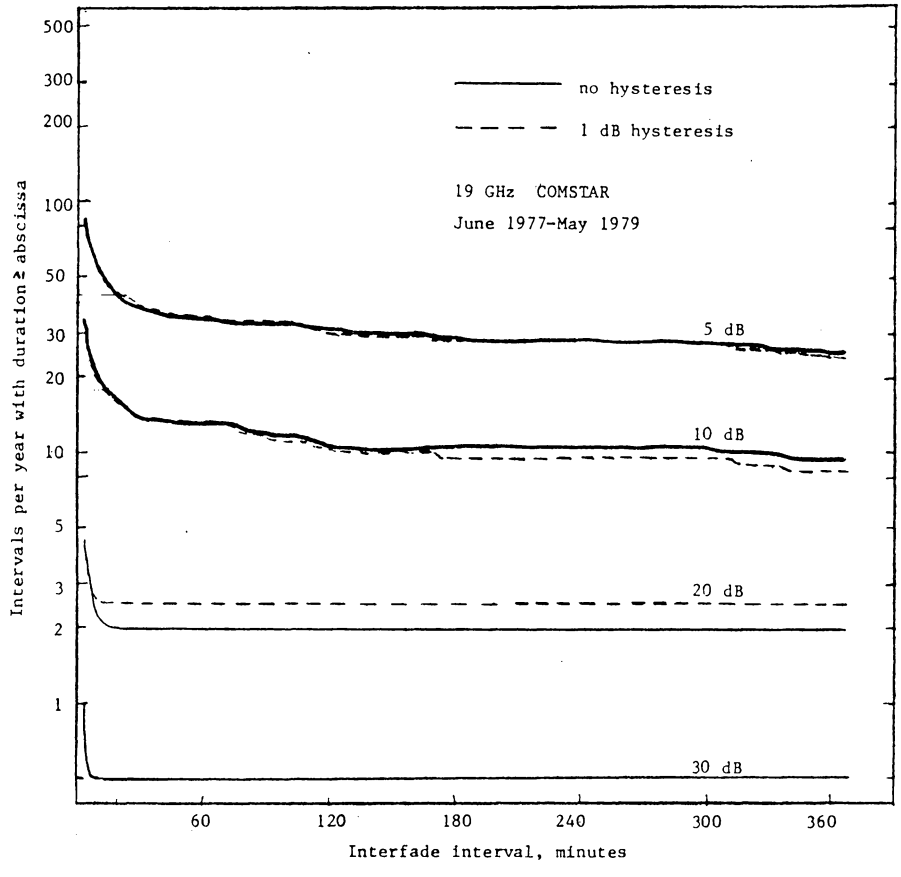

Figure 9.4. Interfade intervals per year with given duration, 19 GHz, June 1977- May 1979.

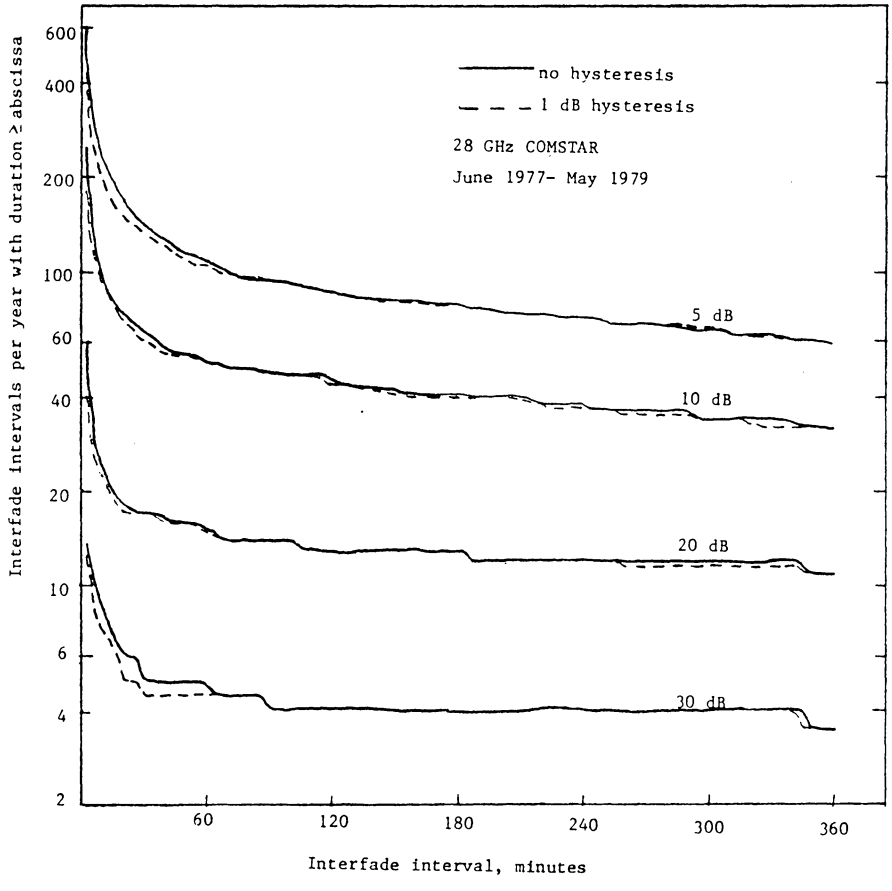

Figure 9.5. Interfade intervals per year with given duration, 28 GHz, June 1977- May 1979.

Hence the fade duration statistics are not significantly affected by the receiver time constants.

The results show the average number of events per year whose duration equaled or exceeded the corresponding time value shown on the abscissa. The leftmost points on the graphs thus represent the total number of events per year observed at the given threshold.

As should be expected, long duration fades occur less frequently than short fades, and deep fades occur less frequently than shallow fades. These effects become less pronounced as event duration increases. The interfade interval curves show the same basic characteristics.

With 1 dB of hysteresis added to the data, the number of short duration events decreases slightly, while the number of long duration events increases slightly. An alternative interpretation of this is that many of the rapidly varying, shallow fades are masked by the hysteresis, which in turn causes the longer, deeper fades to appear slightly longer. This is probably a more accurate description of the signal behavior which would be seen on an actual communication link.

Tables 9-1 and 9-2 show the median values of fade durations and interfade intervals at 19 and 28 GHz. The median fade durations are on the order of a few minutes at shallow-

er fade depths, and tend to increase with fade depth. The median interfade intervals are somewhat longer than the median fade durations, but show the same behavior with fade depth. These reults are consistent with [3]. However, the Bell Laboratories study showed a substantially larger number of fades at all thresholds. Comparisons with this study, which was performed at an elevation angle of 18 degrees, suggest that the number of fades seen on a link depends strongly on the elevation angle, but the fade durations do not. The exact reasons for this behavior are not clear.

9.3 DISCUSSION OF RESULTS

9.3.1 Elevation Angle Dependence

The percentage of time that a given attenuation threshold is exceeded on a link varies as the inverse ratio of the sines of the elevation angles. This ratio is 2.3 for the Virginia Tech and Bell Labs links, and would account for most of the discrepancy. The climates at the two sites are nearly identical, and should not cause a noticeable difference in the results. Why elevation angle should influence the results so strongly is not obvious, but a lower elevation link would intercept more rain cells over a given time period. This could cause more fade events to be seen.

Table 9-1

Median fade durations and interfade intervals, 19 GHz.

Fade Durations, min.		Fade Depth (dB) 5	10	20	30	Elevation Angle
No Hysteresis	Bell Labs	2.7	2.8	2.8	3.5	18.5
	VPI&SU	2.5	2.3	3.3	1.3	45
1 dB Hysteresis	Bell Labs	7.5	4.3	3.5	3.7	18.5
	VPI&SU	3.2	3.3	4.0	1.0	45

Interfade Intervals, min.		Fade Depth (dB) 5	10	20	30	Elevation Angle
No Hysteresis	Bell Labs	7.4	14.5	125	360	18.5
	VPI&SU	20	15	9	360	45
1 dB Hysteresis	Bell Labs	32	45	360	360	18.5
	VPI&SU	21	14.5	360	360	45

Table 9-2

Median fade duration and interfade intervals, 28 GHz. (minutes)

Fade Durations, min.	Fade Depth (dB) 5	10	20	30
No Hysteresis	2.3	2.2	1.9	1.2
1 dB Hysteresis	3.4	2.3	1.5	1.0

Interfade Intervals	Fade Depth (dB) 5	10	20	30
No Hysteresis	6.7	6.0	5.9	16.5
1 dB Hysteresis	9.7	8.1	6.6	16.5

9.3.2 Rainfall Dependence

Another factor which appears to influence the number of fades seen on a link is the year-to-year variations in the distribution of rainfall. In the Virginia Tech study, the period June 1977 through May 1978 had approximately 20% more fades than the June 1978 through May 1979 time period at 19 GHz. At 28 GHz, the difference was more than 50% (see figures 9.6 through 9.9). Although the net amount of rainfall for the two years was nearly identical, the seasonal distributions of the rainfall differed markedly. Since, for equal path lengths, it is rainrate, not the total amount of rainfall per se, which determines attenuation, seasonal anomalies in rainfall could cause significant differences in the number of events observed.

For example, a large amount of rain which fell at a slow rate would produce a low number of long, shallow fades. If this same amount of rain fell at an intense rate, such as during a thunderstorm, shorter and deeper fades would result. If one year had a preponderance of storms having long duration, low intensity rain (such as the 1978-1979 time period), fewer events would be seen. Conversely, a year having an unusually large number of intense thunderstorms (such as the 1977-1978 time frame) would yield a larger number of deeper fades. Additionally, the statistics for unu-

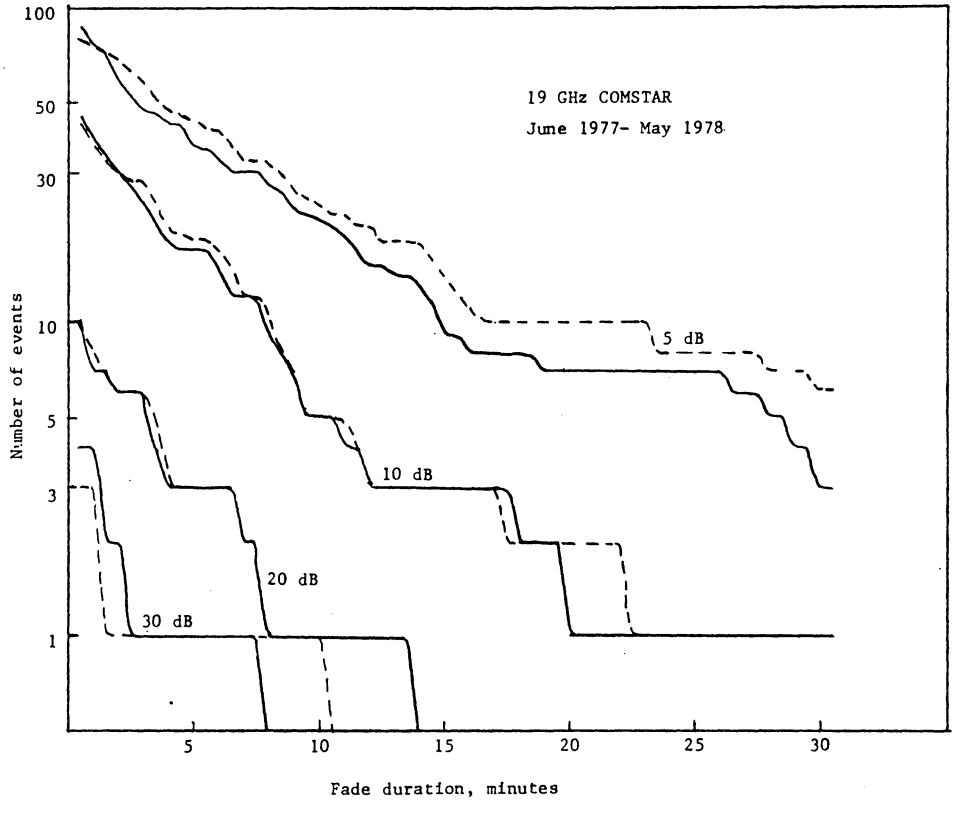

Figure 9.6. Number of events with given duration, 19 GHz, June 1977- May 1978.

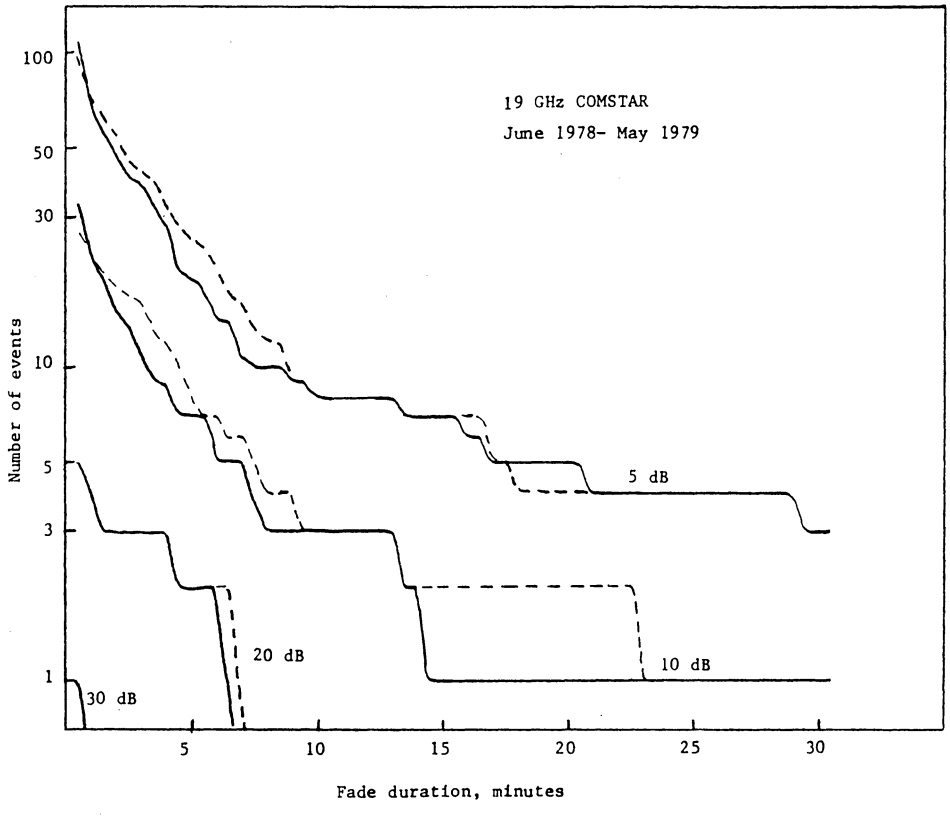

Figure 9.7. Number of events with given duration, 19 GHz, June 1978- May 1979.

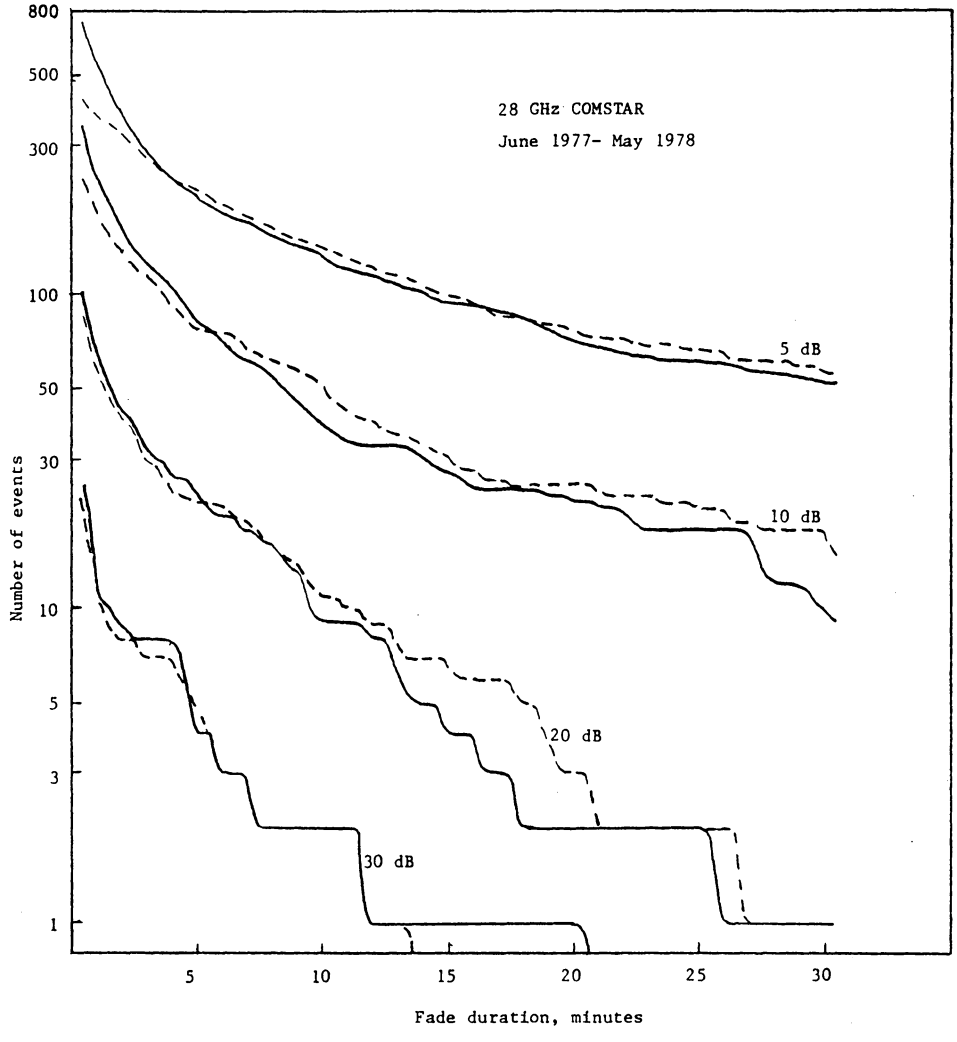

Figure 9.8. Number of events with given duration, 28 GHz, June 1977- May 1978.

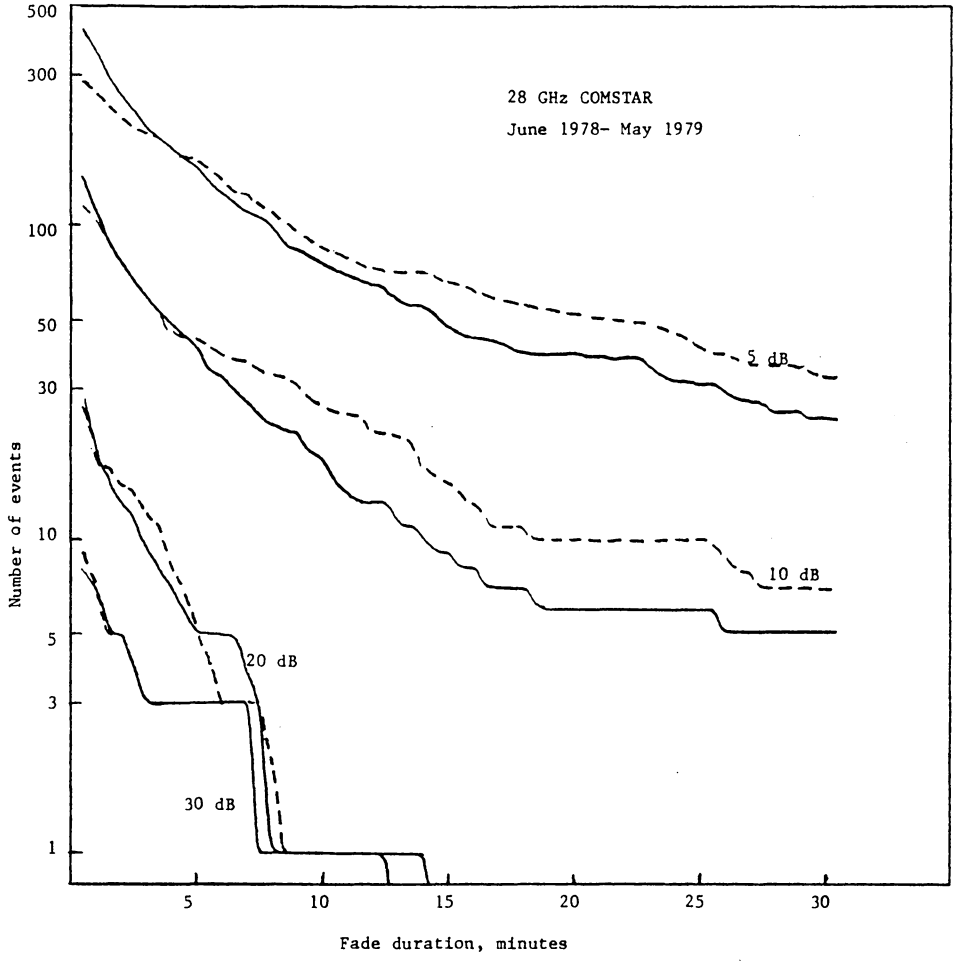

Figure 9.9. Number of events with given duration, 28 GHz, June 1978- May 1979.

sually dry years would differ markedly from the statistics for wetter years.

Figures 9.10 through 9.15 show the quarterly and yearly distribution of fades for 1977 through 1979, along with the 0.1% and 0.01% rainrate levels. From these figures and figure 5.11, the variation of the statistics with rainrate can be seen to follow the behavior explained above. Note the much higher incidence of fades during high rainrate months.

9.3.3 Frequency Dependence

The frequency scaling properties of attenuation might suggest that the number of events seen on a link can also be frequency scaled. However, the results shown indicate that, in general, this is not the case. In the results presented by Khumar [4], scaling by the square of the frequency ratios is also an inaccurate predictor of the actual number of events (see tables 9-3 and 9-4). The scaled values for Kumar's 28 GHz results are reasonably accurate, but the 19 GHz scaled values are not. For the Virginia Tech data, the scaled values differ markedly from the actual values. More extensive research is needed in this area before any conclusive results can be drawn about frequency scaling.

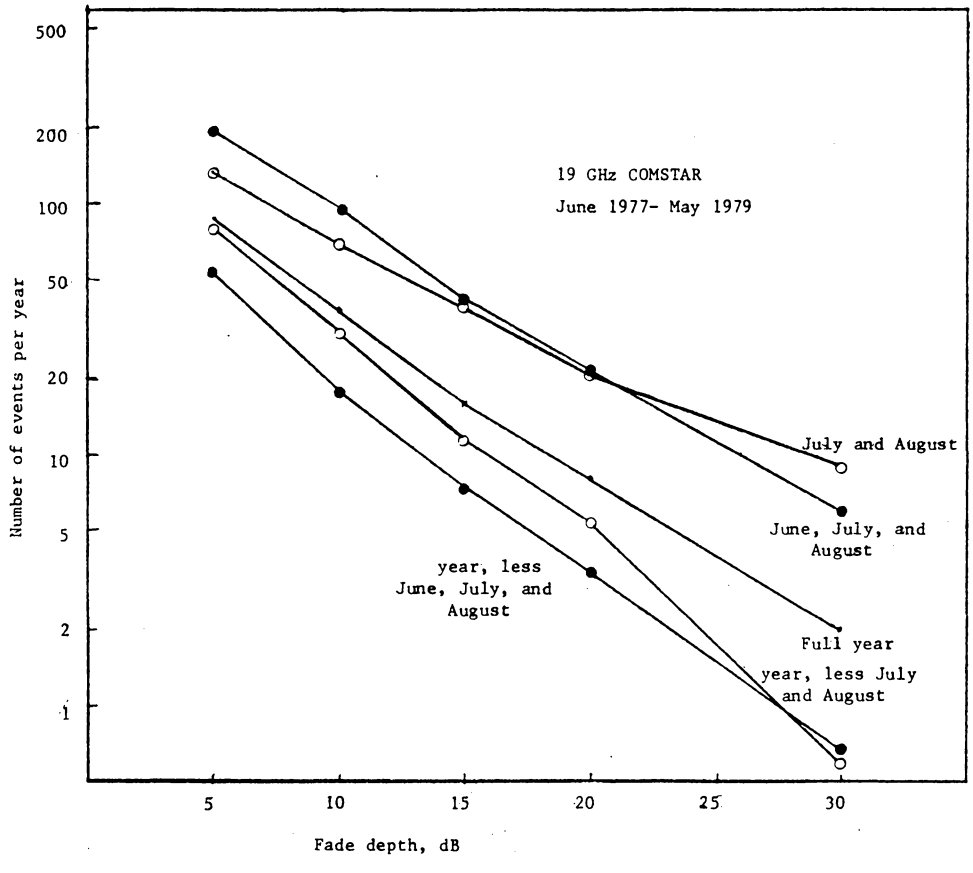

Figure 9.10. Yearly and seasonal distributions of fades, 19 GHz, June 1977- May 1979.

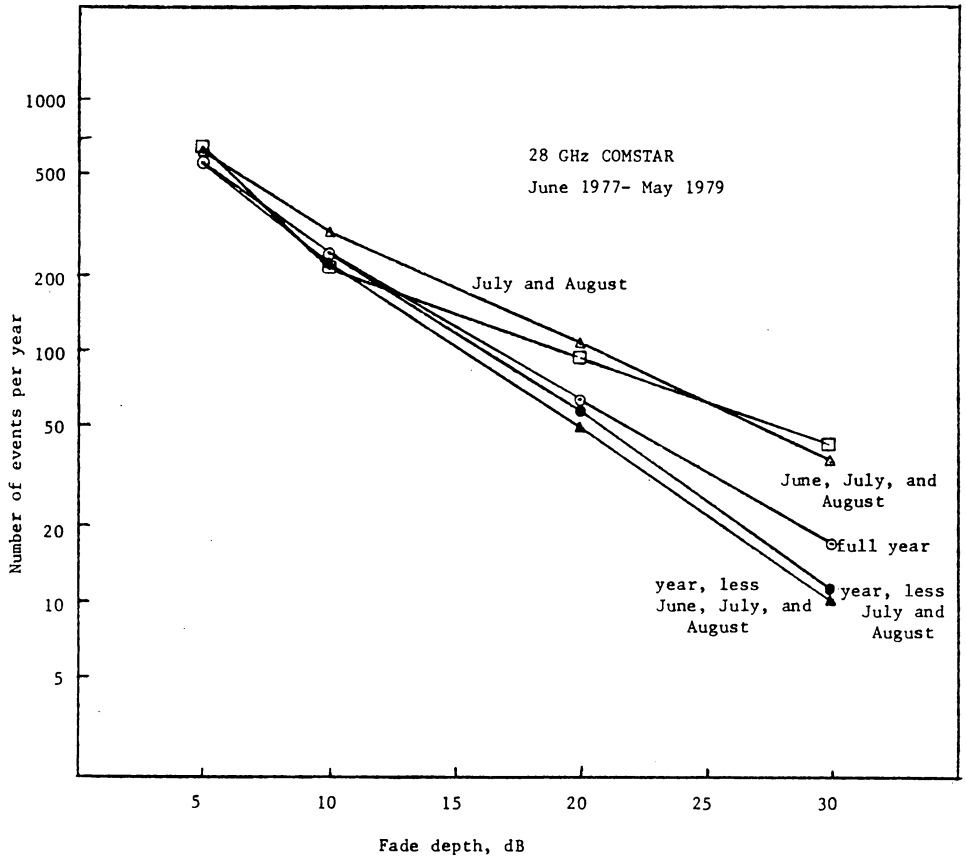

Figure 9.11. Yearly and seasonal distributions of fades, 28 GHz, June 1977- May 1979.

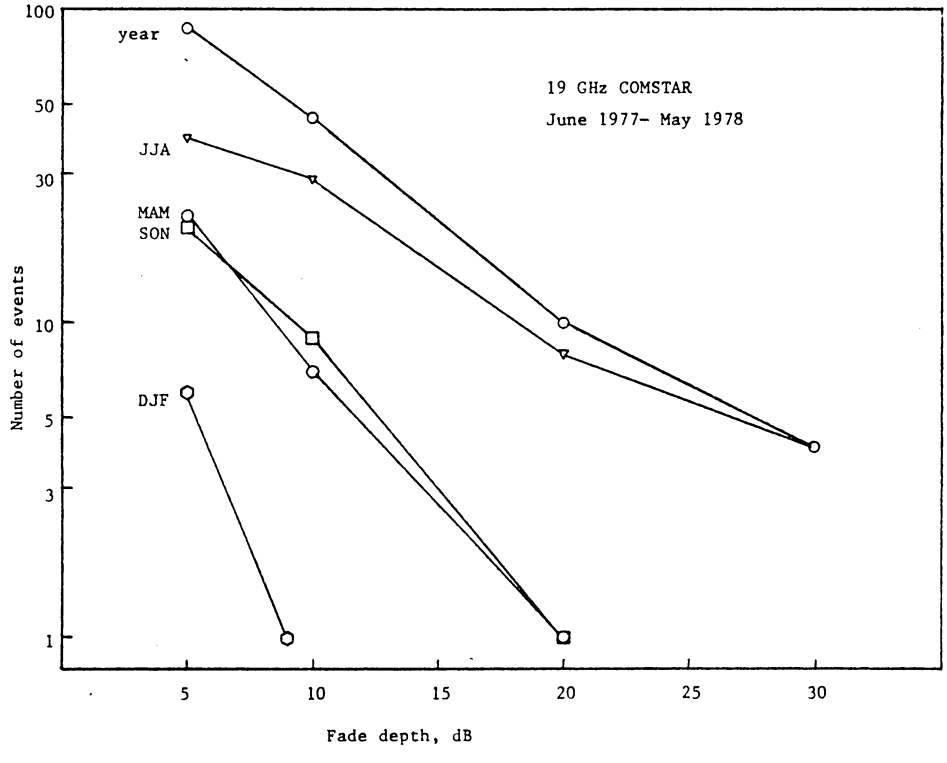

Figure 9.12. Seasonal distribution of fades at 19 GHz, June 1977- May 1978.

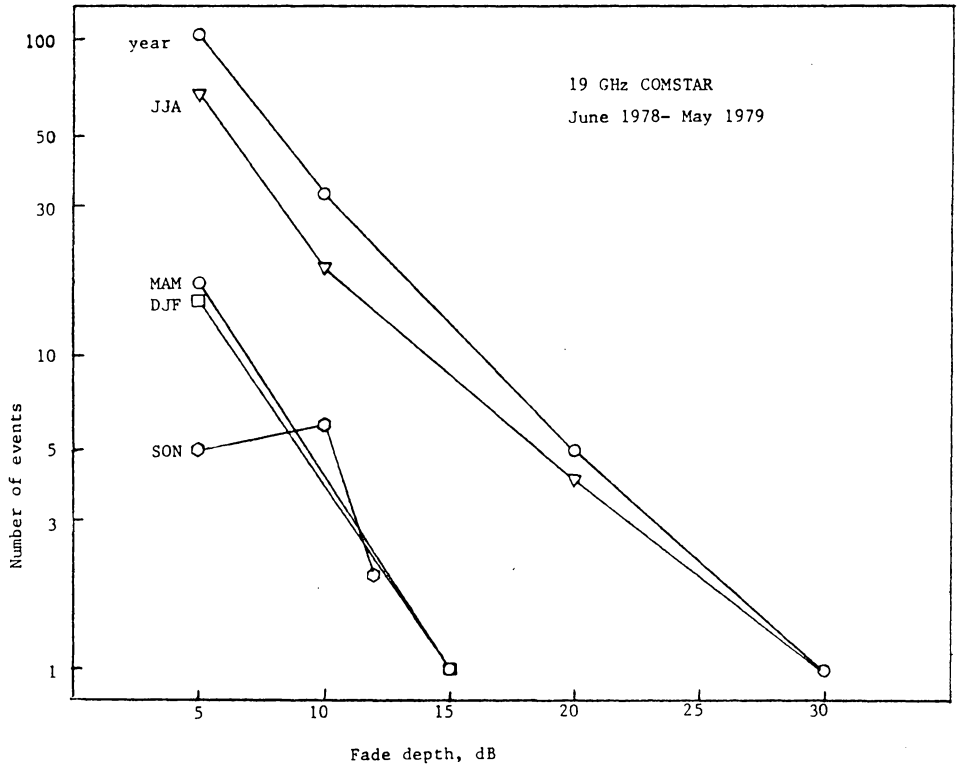

Figure 9.13. Seasonal distribution of fades at 19 GHz, June 1978- May 1979.

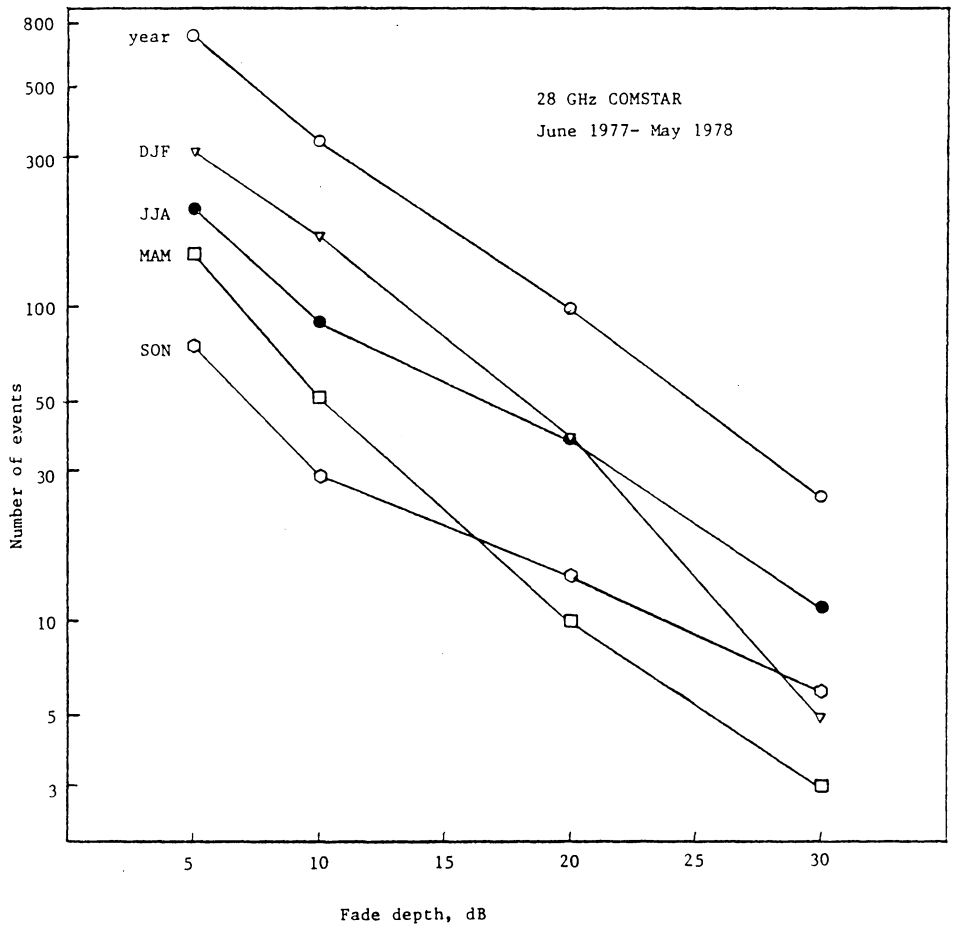

Figure 9.14. Seasonal distribution of fades at 28 GHz, June 1977- May 1978.

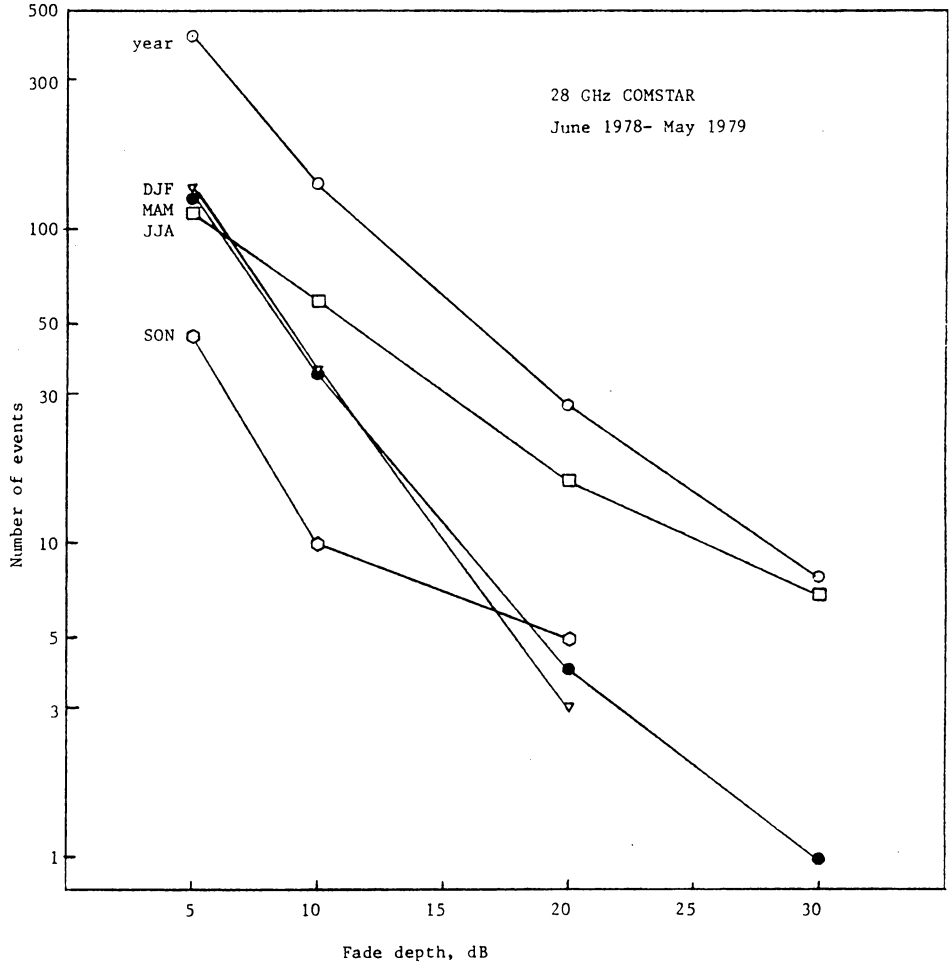

Figure 9.15 Seasonal distribution of fades at 28 GHz, June 1978- May 1979.

Table 9-3. Frequency scaling of the number of fade events (after Khumar).

	Fade Depth (dB)		
	4	6	12
12 GHz Events (unscaled)	35	11	0
19v GHz Events (scaled)	87	27	0
19v GHz Events (unscaled)	125	98	41
29 GHz Events (scaled)	291	228	95
29 GHz Events (unscaled)	315	219	118

Table 9-4. Frequency scaling of the number of fade events, VPI&SU data.

	Fade Depth (dB)			
	5	10	20	30
19v GHz Events	101	39	8	3
28 GHz Events (scaled)	219	84	17	7
28 GHz Events (unscaled)	577	241	64	17

Chapter X

CONCLUSIONS

This thesis has presented the statistics of faderate, fade duration, and interfade intervals on a 45 degree elevation angle satellite communication link. The statistics span the time period June 1977 through May 1979, at frequencies 19 and 28 GHz. Included in this analysis are the effects of long receiver time constants, noise, and sampling rate on the measurement of faderate.

When extremely narrowband filters are used in the signal demodulation process, the resulting long time constants may severely bias the data. For first order filters, the true sample values can be reconstructed from the biased values in an accurate and straightforward manner using the techniques discussed in chapter III. This method also requires that sampling be done at a rate which is high enough to preserve adequate resolution in the piece-wise linear derivative approximation. This rate should be several times the Nyquist rate; a discrete spectral estimate can be performed on the data to determine the Nyquist sampling rate.

The faderate statistics were also found to depend somewhat on the sampling rate, and this sensitivity was shown to be related to the white noise present in the signal. More

accurate statistics can be obtained by using somewhat longer sampling intervals, by increasing the signal to noise ratio, or by using a sample averaging algorithm (decimation). The sampling interval must be short enough so that the sampling rate is several times the Nyquist rate. This will preserve adequate resolution in the derivative approximation, as well as the accurracy of the reconstruction algorithm.

Sampling rate conversions performed on actual data showed that the sensitivity to sampling rate begins to dissappear for sampling intervals longer than 5 sec. Spectral analyses of data indicate a Nyquist sampling interval of about 40 sec for more severe events. These factors suggest that a sampling interval in the range of 5 to 15 sec would yield accurate faderate statistics. This rate would work well with adaptive transponder power control systems which have been proposed in [8].

Fade duration and interfade interval statistics were found to depend heavily on frequency, rainrate, elevation angle, and time of year. The statistics can also vary widely from one year to the next, by as much as a 2 to 1 margin. Frequency scaling was not found to be an accurate predictor of the number of events. Several mechanisms might cause these variations, but their exact nature will be difficult to determine until more research is done in this area.

The basic trends are that the number of fade events seen on a link increases with the frequency of the signal, and decreases with the path elevation angle. Months having higher rainfall rates also had more events; these were usually the summer months of June, July, and August. Events exceeding 10 dB in depth were rare outside the summer months at 19 GHz. The number of events seen does not appear to depend on the amount of rainfall per se, but rather on the rate at which it fell. As would be expected, deeper fades occur much less frequently than shallow fades, and tend to have shorter durations. The addition of hysteresis to the data reduction program slightly reduced the number of short duration fades, and slightly increased the number of long duration fades. The interfade interval results showed this same basic behavior.

REFERENCES

Matricciani, E. "Rate of Change of Signal Attenuation from SIRIO at 11.6 GHz," Eletronics Letters, 1982, 18, pp. 253-255.

Matricciani, E. "Effects of Filtering on the Rate of Change of Rain Induced Attenuation," private communication with author, February, 1982.

Lin, S.H., Bergman, H.J., and Pursley, M.V. "Rain Attenuation on Earth-Satellite paths- Summary of 10-year Experiments and Studies," The Bell System Technical Journal, February, 1980, pp. 183-228.

Dintelman, F. "Analysis of 11 GHz Slant Path Fade Duration and Fade Slope," Electronics Letters, 1981, 17, pp. 660-669.

Arnold, H.W., Cox, D.C., and Hoffman, H.H. "Fade Duration and Interfade Interval Statistics Measured on a 19 GHz Earth-Space Path," IEEE Trans. Comm., vol. COM-30, no. 1, January 1982.

Matricciani, E. "Effects of Filtering on Statistics of Rain Induced Fade Durations," Electronics Letters, 1982, 18, pp. 253-255.

Kumar, P.N. "Precipitation Fade Statistics for 19/29 GHz COMSTAR Beacon Signals and 12 GHz Radiometric Measurements," COMSAT Technical Review, vol. 12, no. 1, Spring 1982, pp. 1-27.

Vogel, W.J. "Measurements of Satellite Beacon Attenuation at 11.7, 19.04, and 28.56 GHz and Radiometric Site Diversity at 13.6 GHz," Radio Science, vol. 17, no. 6, November-December 1982, pp. 1511-1520.

Ince, A.N., Brown, D.W., and Midgley, J.A. "Power Control Algorithms for Satellite Communication Systems," IEEE Trans. Comm., February 1976, pp. 267-275.

Maseng, T., and Bakken, P.M. "A Stochastic Dynamic Model of Rain Attenuation," IEEE Trans. Comm., vol. COM-29, no. 5, May 1981, pp. 660-669.

Van Trees, H.L., ed. Satellite Communications, New York: IEEE Press, 1979.

Ince, A.N., and Wallrabe, A. "Ground Terminal Measurement Requirements with Respect to Satellite Communication Link Availability," Conf. Proc. Aerosp. Telecomm. Sys., AGARD-CPP-103, 1972.

Oppenheim, A.V., and Schafer, R.W. Digital Signal Processing. Englewood Cliffs, N.J.: Prentice-Hall, Inc., 1975.

SAS Institute Inc. SAS User's Guide, 1979 Edition. Cary, North Carolina: SAS Institute, 1979.

Bostian, C.W., et al. "Final Report for Third Year of Work on a Depolarization and Attenuation Experiment Using the COMSTAR and CTS Satellites," Contract NAS5-22577, February 9, 1979.

Bostian, C.W., et al. "Final Report for Fourth Year of Work on a Depolarization and Attenuation Experiment Using the COMSTAR and CTS Satellites," Contract NAS5-22577, March 25, 1980.

Arnold, H.W., Cox, D.C., and Rustako, A.J. "Rain Attenuation at 10-30 GHz Along Earth-Space Paths: Elevation Angle, Frequency, Seasonal, and Diurnal Effects," IEEE Trans. Comm., vol. COM-29, no. 5, May, 1981, pp. 716-721.

Brussaard, G. "Prediction of Attenuation Due to Rainfall on Earth-Space Links," Radio Science, vol. 16, no. 5, Sept-Oct. 1981, pp. 745-760.

Brussaard, G. "Attenuation Due to Rain on a Slant Path," Alta Frequenza, vol. 48, no. 4, pp. 104-109.

Ippolito, L.J. "Radio Propagation for Space Communication Systems," Proc. IEEE, vol. 69, no. 6, June 1981, pp. 697-727.

Wilson, R.W., and Mammel, W.L. "Results From a Three Radiometer Path Diversity Experiment," Proc. IEE Conf. Prop. Radio Waves at Freq. Above 10 GHz, London, England, April 10-13, 1973, pp. 23-27.

Schafer, R., and Rabiner, L. "A Digital Signal Processing Approach to Interpolation," Proc IEEE, vol. 61, no. 6, June 1973, pp. 692-702.

Crochiere, R.E., and Rabiner L. R. "Interpolation and Decimation of Digital Signals- A Tutorial Review," Proc. IEEE, vol.69, no. 3, March 1981, pp. 300-331.

Ricardi, L.J. "Research and Development Efforts Necessary to Evolving Satellite Communication Systems," IEEE Trans. Ant. Prop. Newsletter, August, 1981, pp. 8-11.

Lin, S.H. "Statistical Behavior of Rain Attenuation," Bell System Tech. J., vol. 52, no. 4, April, 1973, pp. 557-581.

Hogg, D.C., and Chu, T.S. "The Role of Rain in Satellite Communications," Proc. IEEE, vol. 63, Sept. 1975, pp. 1308-1331.

Galante, F.M. "Statistical Evaluation of Rain Fades and Fade Durations at 11 GHz in the European Region," Proc. 1975 Int. Conf. Sat. Comm. Sys. Tech., IEE Conf. Pub. 126, London, England, April 7-10, 1975, pp. 302-307.

Carassa, F. "Technical Aspects in the Future Development of Satellite Communication Systems with Particular Reference to the use of Frequencies Above 10 GHz," 19th Conv. Int. Scien. Sullo Spazio, Rome, March, 1979.

Crane, R.K. "Prediction of Attenuation by Rain," IEEE Trans. Comm., vol. 28, no. 9, pp. 1717-1733.

Arnold, H.W., et al. "Rain Attenuation Statistics From a 19 and 28 GHz COMSTAR Beacon Propagation Experiment: One Year Cumulative Distributions and Relationships Between the Two Frequencies," IEEE Trans. Comm., vol. COM-27, no. 11, Nov. 1979, pp. 1725-1728.

Tseng, F., and Hyde, G. "Frequency Scaling of Attenuation Above 10 GHz," EASCON 1978 Record, Sept. 1978, pp. 396-403.

CCIR. "Propagation Data Required for Space Telecommunications Systems," Report 564-1, Documents of the XIV Plenary Assembly, Kyoto, 1978, vol. V.

Goldhirsh, J. "Prediction Methods for Rain Attenuation Statistics at Variable Path Angles and Carrier Frequencies Between 13 and 100 GHz," IEEE Trans. Ant. Prop., vol. AP-23, no. 6, Nov. 1975, pp. 786-791.

Arnold, H.W., et al. "Rain Attenuation Statistics from a 19 and 28 GHz COMSTAR Propagation Experiment: One Year Cumulative Distributions and Relationships Between the Two Frequencies," IEEE Trans. Comm., vol. COM-27, Nov. 1979, pp. 1725-1728.

Alta Frequenza, Special issue on SIRIO results in the first year of experiments, Alta Frequenza, vol. 48, no. 6.

Davidson, C. "Comparison between attenuations measured by means of a radiometer an d a satellite signal receiver, Rep. RL 36/79, Radio Dept., Swed. Telecom. Adm., Stockholm, 1979.

Drufca, G. "Rain attenuation statistics for frequencies above 10 GHz from raingauge observations," Journ. Atmos. Res., vol. 8, nos. 1-2, pp. 399-411.

Appendix A

RECEIVER EFFECTS ON FADERATE DATA

A.1 RECEIVER EFFECTS

In order to determine faderates and fade durations the received signal amplitude as a function of time must be available. If the instantaneous output signal of a receiver is not directly proportional to the instantaneous input signal, then faderates and fade durations cannot be determined directly from the receiver output signal. This problem arises in receivers with narrow bandwidths, and especially in receivers employing phase-locked loops with synchronous detection and post-detection filtering.

For simplicity we will assume that the receiver in question can be described approximately by a single time constant model, which is usually the case in receivers with post-detection filtering. A typical low-pass filter which is often used as a post-detection filter in satellite receivers is shown in schematic form in Figure 1. The differential equation describing the relationship between the instantaneous input signal, v_i, and the instantaneous output signal, v_o, can be obtained from elementary operational am-

plifier theory. Assuming a virtual ground at the negative input, the input current i_i is v_i/R_i. With no current flowing into the negative input the sum of the currents through the resistor, R, and the capacitor, C, must equal the input current, i_i, or

$$i_i = v_i/R_i = i_R + i_c$$

But $i_R = -v_o/R$ and $i_c = -C\, dv_o/dt$. Then

$$\frac{dv_o}{dt} + \frac{1}{RC}v_o = -\frac{1}{R_iC}v_i \qquad (1)$$

If the input signal is assumed to fade linearly in dB then the input voltage, v_i, will be of the form

$$v_i = K\, e^{-\beta t} \qquad t \geq 0$$

where K is the amplitude of v_i at the beginning of the fade and $1/\beta$ is the time constant of the fade. The time constant, $1/\beta$, is related to the faderate in dB per second by

$$FR_{dB} = 20 \log_{10} e^{-\beta} \qquad \text{dB/s}$$

Substituting for v_i in eq. 1 we obtain

$$\frac{dv_o}{dt} + \frac{1}{RC}v_o + \frac{K}{R_iC}\, e^{-t} = 0 \qquad (2)$$

The solution to eq. 2 represents the response of the receiver to a signal which decreases linearly in dB. The solution can be obtained by assuming a solution of the form

$$v_o = c_1\, e^{-\alpha t} + c_2\, e^{-\beta t}$$

$$+ c_3 e^{+\alpha t} + c_4 e^{+\beta t}$$

The constants c_3 and c_4 are zero by inspection. The constant c_2 is obtained immediately by substituting the assumed solution into eq. 2. The result is

$$C_2 = -\frac{K}{(\alpha-\beta)R_i C} \qquad \text{with } \alpha = \frac{1}{RC}$$

Assuming that the receiver has reached the steady state before the fade begins, then at t = 0, the output signal must be K multiplied by $-R/R_i$ Applying this as an initial condition results in

$$C_1 = \frac{K}{(\alpha-\beta)R_i C} = -\beta C_2$$

Then the output voltage, v_o, is

$$v_o = \frac{K}{R_i C(\alpha-\beta)}\left(\frac{\beta}{\alpha}e^{-\alpha t} - e^{-\beta t}\right)$$

Multiplying numerator and denominator by R, and noting that $1/RC = \alpha$, results in

$$v_o = K\frac{R}{R_i}\left(\frac{\alpha}{\alpha-\beta}\right)\left(\frac{\beta}{\alpha}e^{-\alpha t} - e^{-\beta t}\right) \qquad (3)$$

The effect of the receiver time constant on the time variation of the output voltage may be most easily assessed by an example. Without loss of generality let K = 1 and $R/R_i = 1$ in eq. 3. Also let $\alpha = 0.1$ which represents a 10 second receiver time constant. We then assume various faderates for the input signal and calculate the corresponding faderate which one would observe at the receiver output. The results

of such an analysis are shown in Table 1. Column 1 shows the assumed faderates of the input signal, and the corresponding faderates of the output signal are shown in the last column. As can be seen, the output signal changes so much more slowly than the input signal, that the faderates calculated from the output voltages provide no direct indication of how the input signal is changing. It is only for an elapsed time of 100 seconds (or 10 receiver time constants) that the output faderates even approach those of the input signal.

The conclusion which must be drawn is that the output signal of a receiver provides no direct indication of the faderate of the input signal unless the observation time is more than 10 receiver time constants. This indicates that a receiver with a 10 second time constant cannot be used to directly measure <u>any</u> fade occuring in less than about 100 seconds, and this is <u>independent</u> of the faderate. Even extremely small faderates cannot be determined directly in less than 100 seconds, and no faderate greater than 0.87 dB/s can be directly determined (assuming a 10 s receiver time constant).

A.2 CORRECTING FOR RECEIVER EFFECTS

In spite of the fact that, as pointed out in the previous section, the output of a receiver may not change at the same rate as the input signal, the necessary information for calculating the actual faderate is contained in the output signal. The requirement for extracting it is to solve differential equation 1 for v_i rather than for v_o. Although an analytic solution might be feasible for a single time constant exponential input signal, it would have little practical value. This is because the time variation of an actual input signal cannot be described by any simple analytic function. However, since the receiver output voltage is usually sampled at discrete times, and stored in a computer, a numerical solution is suggested. Beginning with eq. 1

$$\frac{dv_o}{dt} + \frac{1}{RC}v_o = -\frac{1}{R_iC}v_i$$

Solving for v_i

$$v_i = \frac{R_i}{R}(v_o + RC\frac{dv_o}{dt})$$

Now if the time interval between samples of v_o is sufficiently small (Δt), we may approximate the derivative in the above equation by a finite difference divided by Δt, and replace v_o by its average value during Δt. We may then calculate the average value of v_i for the interval Δt (which is assumed to be the value of v_i at the midpoint of the inter-

val Δt). With capital letters denoting discrete values of the variables the resulting solution is

$$v_i(t_1 + \frac{\Delta t}{2}) = -\frac{R}{R_i}\left(\frac{v_o(t_2) + v_o(t_1)}{2} + RC\frac{v_o(t_2) - v_o(t_1)}{\Delta t}\right) \tag{4}$$

This equation allows a time history of the input signal to be developed as a set of discrete points correspnding to the samples of the output signal. The only requirement is that the interval Δt be sufficienty small so that enough points result to provide the desired detail in v_i

In order to prove the ability of eq. 4 to faithfully reproduce an input signal from the discrete samples of the output signal, a test was performed using exponential input signals whose time constants were greater than, equal to, and less than the receiver time constant. The method employed was to assume the input signal time constant and then to calculate the output signal at discrete times using the analytic solution for v_o (eq. 3). Then the input signal values were calculated from the discrete values of v_o using eq. 4, and compared to the original input signal. The results appear in Table 2. As before, the assumptions were K = 1, R/R_i = 1, and α = 0.1. For each value of time, the actual value of v_i was calculated half-way between that time and the previous time.

A comparison of the actual v_i and the calculated v_i reveals excellent agreement. Even when $\beta = 1$, which represents a faderate of 8.7 dB/s, and with a relatively large time increment of 0.5 second, the agreement is still very good. The maximum error occurs for a time of 2.5 seconds and is 1.9% or 0.16 dB. Therefore it may be concluded that a receiver with a relatively long time constant of 10 seconds may be used to obtain accurate faderate data for faderates from 0 dB/s to over 10 dB/s.

A.3 CHARACTERIZATION OF THE VPI&SU COMSTAR RECEIVER

In order to apply the previously described method to the data obtained from the COMSTAR receivers it was necessary to make a measurement of the time constant of each of the receiver channels. This was done by removing the input signal and allowing the computer to sample the receiver output. The decay of each of the channel output voltages was expressed in dB/s and the corresponding time constants were calculated. The results were

		dB/s	α
19 GHz	VCO	0.63	0.073
	VX	0.58	0.067
	HCO	0.58	0.067
	HX	0.56	0.064
28 GHz	Co	0.65	0.075
	X	0.55	0.063

These values of α correspond to receiver time constants of about 15 seconds. With this information and the method previously described, faderate and fade duration information can be extracted from VPI&SU COMSTAR data.

A.4 RECEIVER RESPONSE MEASUREMENTS

In order to test the validity of the theoretical results presented in this report, tests were conducted on the vertical co-polarized channel of the COMSTAR 28 receiver. The procedure was to insert a step attenuator in series with the 1.05 GHz IF input signal, and then to increase the attenuator setting by 1 dB every second, beginning with zero attenuation at t = 0. This procedure provides a step approximation to a 1 dB/s fade. The receiver signal level in dBm was recorded every three seconds and the faderate was determined by subtracting the signal at time t from the signal at time t = 0 and dividing by the elapsed time. Then eq. 3 was used to calculate the predicted faderate observed for an input faderate of 1 dB/s. The results, as shown in Table 3, show excellent agreement. As before $K = 1$ and $R/R_i = 1$. For the COMSTAR 28 vertical co-polarized channel $\alpha = 0.075$.

Table A1. Faderate comparison of input and output signals.

Input					Output			
Faderate dB/s	β	v_i	Fade dB	time sec	α	$-v_o$	Fade dB	Faderate dB/s
0.1	0.0115	0.9886	0.1	1	0.1	0.9994	0.0048	0.0048
0.1	0.0115	0.8914	1.0	10	0.1	0.9594	0.3600	0.0360
0.1	0.0115	0.3166	10.0	100	0.1	0.3578	8.9278	0.0893
0.5	0.0575	0.9441	0.5	1	0.1	0.9973	0.0237	0.0237
0.5	0.0575	0.5627	5.0	10	0.1	0.8263	1.6573	0.1657
0.5	0.0575	0.0032	50.0	100	0.1	0.0074	42.58	0.4258
1.0	0.115	0.8914	1.0	1	0.1	0.9946	0.0466	0.0466
1.0	0.115	0.3166	10.0	10	0.1	0.7095	2.981	0.2981
5.0	0.575	0.5627	5.0	1	0.1	0.9769	0.2033	0.2033
5.0	0.575	0.0032	50.0	10	0.1	0.4447	7.039	0.7039
10.0	1.15	0.3166	10.0	1	0.1	0.9609	0.3468	0.3468
10.0	1.15	----	100.0	10	0.1	0.4029	7.896	0.7896

Table A2. Results of input signal calculation.

Faderate dB/s	β	time, s	actual v_i	v_o	Calculated v_i
0.087	0.01	0	1	-1	----
↓	↓	2	0.9900	-0.9981	0.9896
		4	0.9704	-0.9931	0.9706
		6	0.9512	-0.9854	0.9508
		8	0.9324	-0.9758	0.9326
		10	0.9139	-0.9645	0.9137
0.87	0.10	0	1	-1	----
↓	↓	2	0.9048	-0.9825	0.9038
		4	0.7408	-0.9384	0.7400
		6	0.6065	-0.8781	0.6068
		8	0.4966	-0.8088	0.4970
		10	0.4066	-0.7356	0.4062
8.7	1.0	0	1	-1	----
↓	↓	0.5	0.7788	-0.9895	0.7848
		1.0	0.4724	-0.9645	0.4770
		1.5	0.2865	-0.9315	0.2880
		2.0	0.1738	-0.8947	0.1771
		2.5	0.1054	-0.8563	0.1075

Table A3. Receiver response; measured vs. calculated for an input faderate of 1 dB/sec.

time, s	signal level dBm	measured faderate dB/s	calculated faderate dB/s
0	-79.41	--	--
3	-79.65	0.08	0.09
6	-80.30	0.15	0.16
9	-81.26	0.21	0.22
12	-82.57	0.26	0.26
15	-83.95	0.30	0.30
18	-85.33	0.33	0.33
21	-87.05	0.36	0.35

$\alpha = 0.075$

$\beta = 0.115$

Appendix B

PROGRAM FOR CALCULATING INPUT FADERATE AND ATTENUATION

```
*
*   Programmer:  David Lee
*   Latest revision:  April 10, 1983
*
*   This program computes the statistics of mean faderate with
*   respect to attenuation, and plots the results on a line
*   printer.  The faderates are binned according to their
*   corresponding attenuation values, into bins 1 dB wide.  All
*   faderates (positive and negative) in each bin are averaged
*   together to yield the mean values.
*
*   The raw data are read from a SAS data set tape, unformatted.
*   The tape must also contain the SAS variable 'TIME' for each
*   value of attenuation.  The tape used in this example has the
*   signal levels for the 19 GHz and 28 GHz COMSTAR beacons as
*   AV19 and AV28, for June 1977 through May 1979.
*   They are then screened for drop-lock, test mode, and out of
*   range values.  The receiver input values are reconstructed
*   using the algorithm discussed in chapter III of the thesis.
*   The mean faderates are computed using these reconstructed
*   samples.
*
 DATA RD1; SET INTAPE.JUN78; REF=-84.79;
 DATA RD2; SET INTAPE.JUL78; REF=-81.80;
 DATA RD3; SET INTAPE.AUG78; REF=-82.35;
 DATA RD4; SET INTAPE.SEP78; REF=-82.95;
 DATA RD5; SET INTAPE.OCT78; REF=-84.84;
 DATA RD6; SET INTAPE.NOV78; REF=-83.45;
 DATA RD7; SET INTAPE.DEC78; REF=-83.93;
 DATA RD8; SET INTAPE.JAN79; REF=-82.81;
 DATA RD9; SET INTAPE.FEB79; REF=-82.88;
 DATA RD10; SET INTAPE.MAR79; REF=-81.22;
 DATA RD11; SET INTAPE.APR79; REF=-81.19;
 DATA RD12; SET INTAPE.MAY79; REF=-81.23;
DATA RAWDATA; SET RD1 RD2 RD3 RD4 RD5 RD6 RD7 RD8 RD9 RD10 RD11 RD12;
IF V28 NOT=.;
IF -81.4>V28>-101.0;
LD=DAY-1;
TI=TIME+LD*86400.0;
LT=LAG(TI);
DELT=TI-LT;
IF 0<DELT<300;
RC=13.33;
L28=LAG(V28);
X=V28/20.0;
VOUT=-(10.0**X);
LVO=LAG(VOUT);
TAV=LT+0.5*DELT;
LTA=LAG(TAV);
DELTI=TAV-LTA;
IF 300>DELTI>0;
VIN=-((VOUT+LVO)/2.0+RC*(VOUT-LVO)/DELT);
IF VIN>0 THEN VI28=20.0*LOG10(VIN);
   ELSE VI28=.;
LVI=LAG(VI28);
```

```
SIG=0.5*(V28+L28);
SIGI=0.5*(VI28+LVI);
IF SIG<REF THEN A28=REF-SIG;
   ELSE A28=0;
IF SIGI<REF THEN A28I=REF-SIGI;
   ELSE A28I=0;
IF 1.0<A28<18.5;
IF 1.0<A28I<18.5;
R28=((V28-L28)/DELT)*60.0;
R28I=((VI28-LVI)/DELTI)*60.0;
AR28=ABS(R28);
AR28I=ABS(R28I);
IF AR28<100.0;
IF AR28I<100.0;
IN28=INT(A28);
IN28I=INT(A28I);
KEEP AR28 AR28I IN28 IN28I;
DATA RWDO;  SET RAWDATA;
KEEP IN28 AR28;
PROC SORT DATA=RWDO;
   BY IN28;
PROC UNIVARIATE DATA=RWDO NOPRINT;
 VAR AR28;   BY IN28;
 OUTPUT OUT=VAROUT MEDIAN=MED280 P10=O2810 P90=O2890;
 TITLE 28 GHZ OUTPUT FR VS. A WITH MEDIANS, 10TH AND 90TH PERCENTILES;
 PROC PLOT DATA=VAROUT;
 PLOT MED280*IN28='O' O2810*IN28='-' O2890*IN28='+' / HPOS=60
   VPOS=60 OVERLAY;
PROC MEANS DATA=RWDO NOPRINT;
  BY IN28;
  OUTPUT OUT=OUTFAD MEAN=MR;
PROC PLOT DATA=OUTFAD;
  PLOT MR*IN28='O'/HPOS=60 VPOS=60;
TITLE 28 GHZ OUTPUT FR VS. A -- MEAN VALUES;
DATA RWDI;  SET RAWDATA;
KEEP IN28I AR28I;
PROC SORT DATA=RWDI;
   BY IN28I;
PROC UNIVARIATE DATA=RWDI NOPRINT;
 VAR AR28I;   BY IN28I;
 OUTPUT OUT=VARIN MEDIAN=MED28I P10=I2810 P90=I2890;
 TITLE 28 GHZ INPUT FR VS. A WITH MEDIANS, 10TH AND 90TH PERCENTILES;
 PROC PLOT DATA=VARIN;
 PLOT MED28I*IN28I='I' I2810*IN28I='-' I2890*IN28I='+' / HPOS=60
   VPOS=60 OVERLAY;
PROC MEANS DATA=RWDI NOPRINT;
  BY IN28I;
   OUTPUT OUT=INFAD MEAN=MRI;
PROC PLOT DATA=INFAD;
   PLOT MRI*IN28I='I'/HPOS=60 VPOS=60;
TITLE 28 GHZ INPUT FR VS. A -- MEAN VALUES;
```

Appendix C

PROGRAM FOR MODELLING FADES WITH NOISY GAUSSIANS

```
*
*   Programmer: David Lee
*   Latest revision: May 11, 1983
*
*   This program models attenuation events using amplitude
*   weighted and time shifted sums of Gaussian functions.  The
*   user may specify the weights (A), time shifts (alpha),
*   standard deviations (eta), the signal to noise ratio
*   (SNR), and the sampling intervals.
*   The program also produces SAS Versatec plots of the results.
*
*   For this example, the sampling interval is 1, 5, and 10 sec.
*   The fade is modelled by a sum of Gaussian curves with
*   40 dB SNR. Fade duration is 4400 sec.
*   The signal level is normalized to a maximum of 0 dB.
*                                                                ;
DATA GAUSS;
A1=18.5;
A2=-11.0;
A3=17.0;
A4=15.0;
A5=13.5;
A6=12.0;
A7=10.0;
A8=-6.0;
A9=15.0;
ALPHA1=-1.25E-5;
ALPHA2=-6.0E-6;
ALPHA3=-8.0E-6;
ALPHA4=-1.1E-5;
ALPHA5=-6.0E-6;
ALPHA6=-1.25E-5;
ALPHA7=-1.0E-5;
ALPHA8=-4.0E-6;
ALPHA9=-7.0E-6;
ETA1=500;
ETA2=575;
ETA3=750;
ETA4=1150;
ETA5=1750;
ETA6=2500;
ETA7=3075;
ETA8=3400;
ETA9=3900;
SNR=40.0;
V=10.0**(-SNR/20.0);
*DO I=1 TO 1200 BY 1;
DO I=1 TO 4500 BY 1 ;
R=UNIFORM(0);
A= -A1*EXP(ALPHA1*(I-ETA1)**2)-A2*EXP(ALPHA2*(I-ETA2)**2)
   -A3*EXP(ALPHA3*(I-ETA3)**2)-A4*EXP(ALPHA4*(I-ETA4)**2)
   -A5*EXP(ALPHA5*(I-ETA5)**2)-A6*EXP(ALPHA6*(I-ETA6)**2)
   -A7*EXP(ALPHA7*(I-ETA7)**2)-A8*EXP(ALPHA8*(I-ETA8)**2)
   -A9*EXP(ALPHA9*(I-ETA9)**2);
X=10.0**(A/20.0)+V*(R-0.5);
```

```
*X=10.0**(A/20.0);
ATTEN=20.0*LOG10(X);
*ATTEN=A;
OUTPUT;
END;
KEEP ATTEN I;
TITLE ATTENUATION VS TIME FOR NOISY GAUSSIANS;
PROC SPECTRA DATA=GAUSS OUT=FFT S WHITETEST ADJMEAN;
  VAR ATTEN;
WEIGHTS  1 2 3 4 3 2 1;
PROC PLOT DATA=FFT;
  PLOT S_01*PERIOD/HAXIS=0 TO 1000 BY 50;
PROC PLOT DATA=FFT;
  PLOT S_01*FREQ/HAXIS=0 TO 0.2 BY 0.02;
DATA FADE ;
SET GAUSS;
LI=LAG(I);
DELT=I-LI;
LAT=LAG(ATTEN);
FD=0.5*(ATTEN+LAT);
A=INT(FD);
ATT=ABS(A);
*ATT=FD;
FR=(ATTEN-LAT)/DELT;
AFR=ABS(FR);
KEEP ATT AFR;
PROC SORT DATA=FADE;
   BY ATT;
PROC MEANS DATA=FADE NOPRINT;
  BY ATT;
  OUTPUT OUT=MEANFR MEAN=MFR;
PROC PLOT DATA=MEANFR;
   PLOT MFR*ATT='+'/HPOS=60 VPOS=60;
PROC PLOT DATA=FADE;
   PLOT AFR*ATT='+'/HPOS=60 VPOS=60;
TITLE MEAN FR VS. A FOR NOISY GAUSSIANS. T=1 SEC;
DATA SAMP1;
SET GAUSS;
IF MOD(_N_,5)=0;
LI=LAG(I);
DELT=I-LI;
LAT=LAG(ATTEN);
FD=0.5*(ATTEN+LAT);
A=INT(FD);
*A=FD;
ATT=ABS(A);
FR=(ATTEN-LAT)/DELT;
AFR=ABS(FR);
KEEP ATT AFR;
PROC PLOT DATA=SAMP1;
   PLOT ATT*I='+';
   TITLE ATTEN VS TIME FOR NOISY GAUSSIAN. T=5 SEC;
PROC SORT DATA=SAMP1;
   BY ATT;
PROC MEANS DATA=SAMP1 NOPRINT;
```

```
   BY ATT;
   OUTPUT OUT=MEAN1 MEAN=MFR1;
PROC PLOT DATA=MEAN1;
   PLOT MFR1*ATT='+'/HPOS=60 VPOS=60;
PROC PLOT DATA=SAMP1;
   PLOT AFR*ATT='+'/HPOS=60 VPOS=60;
TITLE MEAN FR VS A FOR NOISY GAUSSIANS. T=5 SEC;
DATA SAMP2;
SET GAUSS;
IF MOD(_N_,30)<0.02;
LI=LAG(I);
DELT=I-LI;
LAT=LAG(ATTEN);
FD=0.5*(ATTEN+LAT);
A=INT(FD);
*A=FD;
ATT=ABS(A);
FR=(ATTEN-LAT)/DELT;
AFR=ABS(FR);
KEEP ATT AFR;
PROC PLOT DATA=SAMP2;
   PLOT ATT*I='+';
   TITLE ATTEN VS TIME FOR NOISY GAUSSIAN. T=30 SEC;
PROC SORT DATA=SAMP2;
   BY ATT;
PROC MEANS DATA=SAMP2 NOPRINT;
   BY ATT;
   OUTPUT OUT=MEAN2 MEAN=MFR2;
PROC PLOT DATA=MEAN2;
   PLOT MFR2*ATT='+'/HPOS=60 VPOS=60;
PROC PLOT DATA=SAMP2;
   PLOT AFR*ATT='+'/HPOS=60 VPOS=60;
TITLE MEAN FR VS A FOR NOISY GAUSSIANS. T=30 SEC;
DATA TEMP; SET MEANFR MEAN1 MEAN2;
RATE=60*MFR;  TYPE='1 SEC';  OUTPUT;
RATE=60*MFR1;  TYPE='5 SEC';  OUTPUT;
RATE=60*MFR2;  TYPE='30 SEC';  OUTPUT;
PROC GPLOT DATA=TEMP GOUT=PLOT1 ;
PLOT RATE*ATT=TYPE/VAXIS=0 TO 3 BY .3 HAXIS=0 TO 20 BY 4;
LABEL ATT=ATTENUATION  DB;
LABEL RATE=FADERATE  DB/MIN  SEC;
TITLE1 FIGURE 7.9. FADERATE VS. ATTENUATION;
TITLE2 NOISELESS GAUSSIANS   (SEE FIG. 7.6);
TITLE3 1, 5, AND 30 SEC SAMPLING RATES;
TITLE4  ;
SYMBOL1 V=1 I=SPLINE C=BLACK L=1;
SYMBOL2 V=3 I=SPLINE C=BLACK L=2;
SYMBOL3 V=2 I=SPLINE C=BLACK L=3;
PROC GPLOT DATA=GAUSS GOUT=PLOT2 ;
PLOT ATTEN*I/HAXIS=0 TO 5000 BY 1000 VAXIS=-22 TO 2 BY 3;
LABEL ATTEN=SIGNAL LEVEL  DB;
LABEL I=TIME  SEC;
TITLE1 FIGURE 7.6. ATTENUATION VS. TIME;
TITLE2 NOISELESS GAUSSIANS;
TITLE3  ;
SYMBOL I=SPLINE C=BLACK L=1;
DATA ALL;
SET PLOT1 PLOT2 ;
PROC GREPLAY DATA=ALL;
/*
//
```

Appendix D

PROGRAM FOR PERFORMING SAMPLING RATE CONVERSIONS

```
*
*   THIS PROGRAM READS THE OUTPUT SIGNAL LEVELS OF THE COMSTAR
*   19 AND 28 GHZ BEACONS FROM SAS DATA SET MAG TAPES.  IT THEN
*   RECONSTRUCTS THE RECEIVER INPUTS, PERFORMS SAMPLING RATE
*   CONVERSIONS USING THE IF MOD(_N_) STATEMENTS, AND CALCULATES
*   THE FADERATE VS. ATTENUATION STATISTICS FOR THIS DATA.
*                                                                    ;
DATA RD1; SET INTAPE.JUN77 ; REF=-81.45;
TITLE FR DATA FOR 1,5,10 SEC SAMPLING (A,B,C);
DATA RAWDATA;   SET RD1;
LD=DAY-1;
TI=TIME+LD*86400.0;
LT=LAG(TI);
DELT=TI-LT;
IF 0<DELT;
RC=13.69;
L28=LAG(V28);
X=V28/20.0;
VOUT=-(10.0**X);
LVO=LAG(VOUT);
TAV=LT+0.5*DELT;
VIN=-((VOUT+LVO)/2.0+RC*(VOUT-LVO)/DELT);
IF VIN>0 THEN VI28=20.0*LOG10(VIN);
   ELSE VI28=.;
IF VI28>-103.0;
LVI=LAG(VI28);
LTA=LAG(TAV);
DELTI=TAV-LTA;
DATA INTPA;  SET RAWDATA;
BT=LTA+1;
DO I=BT TO TAV;
N+1;
DELT2=I-LTA;
SAMP=DELT2/DELTI*(VI28-LVI)+LVI;
IF SAMP NE.;
*IF MOD(N,1)=0 THEN OUTPUT;
LSAMP=LAG(SAMP);
LI=LAG(I);
DELTS=I-LI;
ISIG=0.5*(SAMP+LSAMP);
IF ISIG<REF THEN A28I=REF-ISIG;
 ELSE A28I=0.0;
IF 1.0<A28I<19.0;
R28I=(SAMP-LSAMP)/DELTS*60.0;
AR28I=ABS(R28I);
IF 0.1<AR28I<110.0;
IF DELTS<300;
IN28I=INT(A28I);
END;
KEEP IN28I AR28I;
PROC SORT DATA=INTPA;
 BY IN28I;
PROC MEANS DATA=INTPA NOPRINT;
 BY IN28I;
 OUTPUT OUT=ISAMA MEAN=MIA;
```

```
DATA INTPB;  SET RAWDATA;
BT=LTA+1;
DO I=BT TO TAV;
N+1;
DELT2=I-LTA;
SAMP=DELT2/DELTI*(VI28-LVI)+LVI;
IF SAMP NE.;
IF MOD(N,5)=0 THEN OUTPUT;
LSAMP=LAG(SAMP);
LI=LAG(I);
DELTS=I-LI;
ISIG=0.5*(SAMP+LSAMP);
IF ISIG<REF THEN A28I=REF-ISIG;
 ELSE A28I=0.0;
IF 1.0<A28I<19.0;
R28I=(SAMP-LSAMP)/DELTS*60.0;
AR28I=ABS(R28I);
IF 0.1<AR28I<110.0;
IF DELTS<300;
IN28I=INT(A28I);
END;
KEEP IN28I AR28I;
PROC SORT DATA=INTPB;
 BY IN28I;
PROC MEANS DATA=INTPB NOPRINT;
 BY IN28I;
 OUTPUT OUT=ISAMB MEAN=MIB;
DATA INTPC;  SET RAWDATA;
BT=LTA+1;
DO I=BT TO TAV;
N+1;
DELT2=I-LTA;
SAMP=DELT2/DELTI*(VI28-LVI)+LVI;
IF SAMP NE.;
IF MOD(N,10)=0 THEN OUTPUT;
LSAMP=LAG(SAMP);
LI=LAG(I);
DELTS=I-LI;
ISIG=0.5*(SAMP+LSAMP);
IF ISIG<REF THEN A28I=REF-ISIG;
   ELSE A28I=0.0;
IF 1.0<A28I<19.0;
R28I=(SAMP-LSAMP)/DELTS*60.0;
AR28I=ABS(R28I);
IF 0.1<AR28I<110.0;
IF DELTS<300;
IN28I=INT(A28I);
END;
KEEP IN28I AR28I;
PROC SORT DATA=INTPC;
   BY IN28I;
PROC MEANS DATA=INTPC NOPRINT;
 BY IN28I;
 OUTPUT OUT=ISAMC MEAN=MIC;
DATA SCATTER;   SET ISAMA ISAMB ISAMC;
PROC PLOT DATA=SCATTER;
 PLOT MIA*IN28I='A' MIB*IN28I='B' MIC*IN28I='C'/HPOS=60 VPOS=60 OVERLAY;
TITLE MEAN FR VS A JUNE77 SAMPLING RATE=1,5,10 SEC;
```

Appendix E

PROGRAM FOR PERFORMING SAMPLE AVERAGING

```
*
*    PROGRAMMER:  DAVID LEE
*    LATEST REVISION:  APRIL 23, 1983
*
*    THIS PROGRAM CALCULATES MEAN FADERATE VS ATTENUATION STATISTICS
*    BY AVERAGING A PREDETERMINED NUMBER OF CONSECUTIVE SAMPLES.  THE
*    NUMBER OF SAMPLES TO BE AVERAGED IS CONTROLLED BY THE IF MOD(_N_)
*    STATEMENT.  FIRST, THE RECEIVER INPUT SAMPLES ARE RECONSTRUCTED
*    USING THE METHOD OF CHAPTER III; THEN, SAMPLES ARE MADE AVAILABLE
*    EVERY 1 SEC USING LINEAR INTERPOLATION.  THIS SIGNAL IS THEN
*    RESAMPLED, AND THE MEAN FADERATE VALUES ARE COMPUTED FOR THIS
*    NEW SIGNAL.  THIS METHOD EFFECTIVELY AVERAGES OUT THE WHITE NOISE
*    IN THE SIGNAL, GIVING MORE ACCURATE RESULTS.
*
*    THE DATA ARE READ FROM SAS DATA SET TAPES UNFORMATTED, ALONG
*    WITH THE CORRESPONDING VALUES OF TIME, AS EITHER AV19 OR AV28,
*    THE 19 AND 29 GHZ COMSTAR BEACON SIGNAL LEVELS;
*                                                                    ;
DATA AVG; SET INTAPE.AUG77 END=LAST; REF=-85.74;
AV=10;
LD=DAY-1;
TI=TIME+LD*86400.0;
LT=LAG(TI);
DELT=TI-LT;
IF 0<DELT;
RC=13.69;
L28=LAG(V28);
X=V28/20.0;
VOUT=-(10.0**X);
LVO=LAG(VOUT);
TAV=LT+0.5*DELT;
VIN=-((VOUT+LVO)/2.0+RC*(VOUT-LVO)/DELT);
IF VIN>0 THEN VI28=20.0*LOG10(VIN);
   ELSE VI28=.;
LVI=LAG(VI28);
LTA=LAG(TAV);
DELTI=TAV-LTA;
BT=LTA+1;
DO I=BT TO TAV;
N+1;
DELT2=I-LTA;
SAMP=DELT2/DELTI*(VI28-LVI)+LVI;
IF SAMP NE.;
IF MOD(N,AV)=1 THEN LINK INIT;
TEMP=TEMP+SAMP;
IF MOD(N,AV)=0 THEN LINK OUT;
IF LAST=1 THEN AVE=.;
OUTPUT;
END;
RETURN;
INIT: TEMP=0.0;
RETAIN TEMP;
RETURN;
OUT: AVE=TEMP/AV;
LAV=LAG(AVE);
```

```
LI=LAG(I);
DELTS=I-LI;
ISIG=0.5*(AVE+LAV);
IF ISIG<REF THEN A28I=REF-ISIG;
   ELSE A28I=0.0;
IF 1.0<A28I<11.0;
R28I=(AVE-LAV)/DELTS*60.0;
AR28I=ABS(R28I);
IF 0.1<AR28I<110.0;
IF DELTS<300;
IN28I=INT(A28I);
RETAIN IN28I AR28I;
RETURN;
KEEP IN28I AR28I;
PROC SORT DATA=AVG;
   BY IN28I;
PROC MEANS DATA=AVG NOPRINT;
   BY IN28I;
   OUTPUT OUT=TSAV MEAN=MAV;
PROC PLOT DATA=TSAV;
   PLOT MAV*IN28I='A'/HPOS=60 VPOS=60;
TITLE MEAN FR VS. A  JUNE77 USING 10 AVERAGED 1-SEC SAMPLES;
PROC GLM DATA=TSAV;
   MODEL MAV=IN28I;
   OUTPUT OUT=LINAV PREDICTED=R28T;
PROC PLOT DATA=LINAV;
   PLOT R28T*IN28I='A'/HPOS=60 VPOS=60;
```

Appendix F

PROGRAM FOR FADE DURATIONS AND INTERFADE INTERVALS

```
C
C    THIS PROGRAM READS 30 SEC INTERVAL ATTENUATION LEVEL DATA
C    IN F7.2 FORMAT AND THEN COUNTS THE NUMBER OF FADE EVENTS
C    IN THE DATA SET HAVING A GIVEN DURATION.  IT ALSO COUNTS
C    THE NUMBER OF INTERFADE INTERVALS IN THE DATA SET.
C    THE RESULTS ARE THEN PRINTED IN TABULAR FORM
C
      INTEGER HFDC(35)
      INTEGER HFTBL(35,61)
      LOGICAL HFDR(35)
      REAL HYST(35)
      REAL HOLD
      DATA HOLD /0.0/
      DATA HYST /35*1.0/
      CALL STDUR(HFDR,HFDC,HFTBL)
   12 READ(1,*,END=30) ATTEN
    1 FORMAT(F7.2)
      IF(ATTEN.GT.35.0)ATTEN=35.0
        CALL PTDUR(ATTEN,HOLD,HFDR,HFDC,HFTBL,HYST)
        GO TO 12
   30 CONTINUE
      ATTEN=0.0
      CALL PTDUR(ATTEN,HOLD,HFDR,HFDC,HFTBL,HYST)
      WRITE(3,302)
  302 FORMAT('1'///' FADE DURATION WITH HYSTERESIS ')
      CALL EXDUR(HFTBL)
      STOP
      END
C
C  >     POINT-TO-POINT SIGNAL DURATION SUBPROGRAM: PTDUR
C  >
C  >     THIS PROGRAM WAS BASED ON AN ALGORITHM SUGGESTED IN:
C  >     'FADE DURATION AND INTERFADE INTERVAL STATISTICS MEASURED
C  >     ON A 19-GHZ EARTH-SPACE PATH', H.W. ARNOLD, D.C. COX, AND
C  >     H.H. HOFFMAN. IEEE TRANS. ON COMMUNICATIONS, JAN82
C  >
C  >     THIS PROGRAM WAS DEVELOPED FOR THE SATCOM GROUP BY BOB PORTER.
C
      SUBROUTINE PTDUR(SIGNAL,RLAST,SIGREG,SIGCNT,SIGTBL,HYST)
      REAL    SIGNAL,RLAST
      INTEGER SIGCNT(35)
      INTEGER SIGTBL(35,61)
      LOGICAL SIGREG(35)
      REAL    HYST(35)
C
C  >     WHEN SIGREQ(F) IS TRUE THEN WE ARE IN A REGION OF SIGNAL >= F
C  >     SIGTBL - TABLE OF SIGNAL (DB) VS DURATION (0.5 SEC STEPS)
C
      INTEGER LAST
      INTEGER F
      INTEGER BIN,SIGBIN
C
C  >     BINING STATEMENT FUNCTIONS
C
      SIGBIN(ICNT) = ICNT
```

```
      KSIG=SIGNAL
      LAST = RLAST
      IF (SIGNAL .GT. RLAST ) GO TO 20
      IF (SIGNAL .LT. RLAST ) GO TO 30
      IF (SIGNAL .NE. 0.0 ) GO TO 40
C
C  >     CLEAR WEATHER. SIGNAL IS UNCHANGED AND EQUAL TO 0.0
C
      RETURN
C
C  >     SIGNAL HAS INCREASED.
C  >      BEGIN NEW SIGNAL REGIONS
C
   20 CONTINUE
      IF (KSIG .EQ. LAST) GO TO 40
      K = LAST + 1
      DO 22 F = K,KSIG
      IF(SIGREG(F))GO TO 21
         SIGCNT(F) = 0
         SIGREG(F) = .TRUE.
   21    CONTINUE
   22 CONTINUE
      GO TO 40
C
C  >     SIGNAL DECREASE.
C  >      END SIGNAL REGIONS - ACCUMULATE SIGNAL DURATION
C
   30 CONTINUE
      K = KSIG + 1
      DO 32 F = K,35
         IF (.NOT. SIGREG(F) ) GO TO 33
         IF (SIGNAL.GT.F-HYST(F)) GO TO 32
         BIN = SIGBIN(SIGCNT(F))
         SIGTBL(F,BIN) = SIGTBL(F,BIN) + 1
         SIGREG(F) = .FALSE.
         SIGCNT(F) = 0
   32 CONTINUE
   33 CONTINUE
      GO TO 40
C
C  >     COME DIRECTLY TO HERE WHEN THERE HAS BEEN NO CHANGE IN SIGNAL AN
C  >     NOT CLEAR WEATHER.  ALSO COME HERE AFTER ALLOWING FOR CHANGES IN
C  >     SIGNAL.  HERE WE UPDATE ALL THE SIGNAL COUNTERS.
C
   40 CONTINUE
      DO 42 F = 1,35
         IF ( SIGREG(F) ) SIGCNT(F) = SIGCNT(F) + 1
         IF (SIGCNT(F) .GT. 61 ) SIGCNT(F) = 61
   42 CONTINUE
      RLAST = SIGNAL
      RETURN
      END
C
C  >     SIGNAL DURATION REPORT SUBPROGRAM: EXDUR
C
```

```
      SUBROUTINE EXDUR(SIGTBL)
      INTEGER SIGTBL(35,61)
C
C  >     PRINT THE SIGNAL FADE DURATION TABLE RESULTS.
C
      WRITE(3,30) (I,I=1,20)
   30 FORMAT(' ',/////,T35,' SIGNAL FADE DURATION TABLE '//
     *    ' THRESHOLD:',4(3X,5(1X,I3),3X)/' DURATION')
      DO 10 K = 1,61
         IF ((K-1)/5*5.EQ.K-1) WRITE(3,300)
  300    FORMAT(11X,4(3X,5('----'),3X))
         TIME = K/2.0
         WRITE(3,34) TIME,(SIGTBL(KSIG,K),KSIG=1,20)
   34    FORMAT(3X,F5.1,3X,4(3X,5I4,3X))
   10 CONTINUE
      WRITE(3,310)
  310 FORMAT ('+',7X,' PLUS ')
      WRITE(3,35) (I,I=21,35)
   35 FORMAT(' ',/////,T35,' SIGNAL FADE DURATION TABLE '//
     *    ' THRESHOLD:',3(3X,5(1X,I3),3X)/' DURATION')
      DO 110 K = 1,61
         IF ((K-1)/5*5.EQ.K-1) WRITE(3,300)
         TIME = K/2.0
         WRITE(3,34) TIME,(SIGTBL(KSIG,K),KSIG=21,35)
  110 CONTINUE
      WRITE(3,310)
      RETURN
      END
C
C  >     SIGNAL DURATION INITIALIZATION SUBPROGRAM: STDUR
C
      SUBROUTINE STDUR(SIGREG,SIGCNT,SIGTBL)
      INTEGER SIGCNT(35),SIGTBL(35,61)
      LOGICAL SIGREG(35)
      DO 12 K = 1,35
         DO 11 L = 1,61
              SIGTBL(K,L) = 0
   11    CONTINUE
   12 CONTINUE
C
C  >     ENTRY POINT TO CLEAR COUNTERS BETWEEN BLOCKED EVENTS
C
      ENTRY STDUR2(SIGREG,SIGCNT)
      DO 10 K = 1,35
         SIGCNT(K) = 0
         SIGREG(K) = .FALSE.
   10 CONTINUE
      RETURN
      END
```

The vita has been removed from the scanned document